ADDIS ABABA UNIVERSITY

ADDIS ABABA INSTITUTE OF TECHNOLOGY

AFRICAN RAILWAY CENTER OF EXCELLENCE

FATIGUE ANALYSIS OF THE RAILCAR WHEELSET UNDER DIFFERENT LOADING AND TRACTION CONDITIONS: THE CASE OF AALRTS

A Thesis in Master of Science In Railway Engineering (Rolling stock Stream)

By Sileamlak Ayenew

Augest 9, 2019

Addis Ababa

The undersigned have examined the thesis entitled '**Fatigue Analysis of the Railcar Wheelset Under Different Loading and Traction Condition: The Case of AALRTS** presented by **Sileamlak Ayenew**, a candidate for the degree of **Master of Science in Railway Engineering (Rolling stock Stream)** and hereby certify that it is worthy of acceptance.

Celestin Nkundineza (PhD)		
Advisor	Signature	Date
Dr. Samuel Tesfaye		
Internal Examiner	Signature	Date
Mr. Behailu Mamo		
External Examiner	Signature	Date
Chair person	Signature	Date

DECLARATION

I certify that research work titled "'Fatigue Analysis of AALRT Wheelset under Different Loading and traction conditions" is my own work. The work has not been presented elsewhere for assessment. Where material has been used from other sources it has been properly acknowledged / referred.

SILEAMLAK AYENEW

ACKNOWLEDGEMENT

At the head of my intentions to forward my acknowledgement to the ones that deserve it, my heartfelt thanks will be directed to the almighty God and St. virgin Merry who are the source of my success in my life.

I would also like to express my appreciation and thanking's to my advisor Dr. Celestin Nkundineza for his unreserved assistance and resource full advice that encouraged me to conduct my research successfully and courageously. I would like to thank AALRT staffs and workers for giving me the necessary technical data's and their collaborations.

Finally, I would like to thank all those who stand by my side and giving me their significant advice and motivation throughout the entire progress of my research undertakings.

ABSTRACT

Railcar wheelset is a type of wheelset specially designed for use on rail tracks to transmit the sprung and unsprung weight of the train to the rail and to give traction. However, since they are subjected to cyclic axial, lateral and horizontal loads fatigue failures are common. In addition, a railway companies like Addis Ababa light rail train (AALRT) Transport passengers and goods in most cases face overloading beyond the loading capacity. On the other hand, the speed has a direct effect on the fatigue of wheelset. By fundamental mechanics for a train moving at constant power, increase in speed causes the decrease in axle twisting moment leading to a decrease in torsional stresses; but, this effect is only significant at relatively low and medium speeds. Also, according to Hirakawa & Kubota (2001), increase in speed causes an increase in axle bending stresses; but, this effect is only significant at very high speeds and the effect is nonexistent for speeds less than 60 km/hr.

Therefore, the main objective of this paper is to perform stress and fatigue analysis of a wheelset under different loading and traction conditions on a straight railroad in case of AALRT.

This research uses both primary and secondary data sources for analysis. The researcher employs different analytical and numerical approaches, to determine induced stresses and loads that act on the wheelset. We use different mechanics theories (static and dynamic) and FEA analysis was carried out by ANSYS 15.0 for different loading (39158.25 N, 51571.36 N & 57307.88 N) and traction condition (V_{Avg}, 10 Km/hr to 70 Km/hr). On the bases of this analysis the results show that the fatigue life improves by 57 % if the trains carry passengers only by seat and by 16% if AALRT limits the passenger number to 317 passengers/train instead of 420 passengers per train. Also, the results show that the increased average speed up to 40 km/hr. contributes to the increase of fatigue life and factor of safety of the axle caused by a combination of twisting and bending moments by 3.1 % and 4%, respectively.

The results in this analysis provide a good start to be taken by an urban rail transit such as AALRT to determine optimum train loadings and travel speed range in combination of other detrimental factors that were out of scope of this research.

Key words: - AALRT, wheelset, Fatigue failures, FEA analysis, Overloading, fatigue of railway axle

TABLE OF CONTENTS

LIST OF TABLES

LIST OF FIGURES

NOMENCLATURES

ERC	Ethiopia Railway Corporation
AA LRT	Addis Ababa light rail transit
HCF	High cycle fatigue
LCF	Low cycle fatigue
A	Stress amplitude
σ_a	Alternating stress
σ_m	Mid-range or mean stress
σ_{max}	Maximum stress
σ_{min}	Minimum stress
R	Stress range
S_{ult}	Ultimate strength
S_y	Yield strength
v	Poisson's ratio
E	Young's Modulus
S_e	Endurance limit Actual component
$S_e{}'$	Endurance limit of test specimen.
K_a	Surface factor
K_b	Size factor
K_c	Load factor
K_d	Temperature factor
K_d	Miscellaneous-effects factor
F	Applied load
M	Moment Load
T	Torque
P	Power
N	Rotational speed (RPM)
ω	Angular speed
T_A	Axle torque
T_M	Motor output torque
I	Moment of inertia

J	Polar moment of inertia
τ_{Max}	Maximum shear stress induced
K_w	Constants that depend on the material properties of wheel.
K_r	Constants that depend on the material properties of rail.
R_1^w	The Principal Rolling Radii of the Wheel
R_2^w	The principal transverse radii of the wheel
R_1^r	The principal rolling radii of the rail
R_2^r	The principal transverse radii of the rail
Z	Contact Point Depth
a	Major Semi-axis
B	Minor Semi-axis
P	Contact Pressure
P_0	Maximum Contact Pressure
m and n	Hertz coefficients
φ	Yaw Rotation Angle

.

CHAPTER 1
INTRODUCTION

1.1 Background

Rolling stock wheelset is a type of wheelset specially designed for use on rail tracks. A rolling component is typically pressed onto an axle and mounted directly on a rail car or locomotive or indirectly on a bogie. The purpose of the wheel set is to give traction and transmit the weight of the vehicle and passengers to the rail and ground. Therefore, usually wheel sets are exposed to different types of loadings and stress.

Since the wheelset is subjected to this long repetitive alternating or cyclic loads, the issue of fatigue failure and damages always exists. Fatigue is an important characteristic of an engineering component and is measured by a number of cycles it can withstand before fatigue failure takes place. As a one-time occurrence, the load is not dangerous in itself. It is actually less than Yield Stress of the material, but over time the alternating load is able to break the component anyway. It is estimated that between 50 and 90 % of product failures is caused by fatigue [1].

Loads and stress that the wheel sets of a rolling stock are subjected can generally be classified into basic subdivisions: bending, torsional, lateral and axial. Bending stresses are stresses which can results from these types of bending loads: unidirectional (one-way), reversed (two-way), and rotating. In unidirectional bending, the stress at any point fluctuates. Fluctuating stress refers to a change in magnitude without changing algebraic sign. In reversed bending and rotating bending, the stress at any point alternates. Alternating stress refers to cycling between two stresses of opposite algebraic sign, that is, tension (+) to compression (-) or compression to tension. Also, torsional stresses can result from application of fluctuating or alternating twisting moments (torque) and also axial stresses can result from application of alternating (tension-and-compression) loading or fluctuating (tension-tension) loadings. [2]

As a result of these different types of repetitive alternating or cyclic loads and stresses fatigue on the wheelset will be generated and fatigue failure might happen. But the effect of the axial loading here has a limited effect therefore it is omitted in this research.

However, based on this fact, fatigue evaluation should be a part of all product development of rolling stock design and operations.

Fatigue theory is basically empirical. This means that the process of initiation of micro cracks that finally will form macroscopic cracks in the material is not accounted for in detail in the equations. Fatigue properties must be treated by statistical means due to large variation during testing. Virtually all mathematical equations dealing with fatigue are fitted to test results coming from material testing.

There are different types of fatigue in machine components and structures like mechanical fatigue, thermal fatigue, creep fatigue, thermo-mechanical fatigue, fretting fatigue and corrosion fatigue. Among these different types of fatigues, mechanical fatigue is the focus on this research. Mechanical fatigue mainly because of fluctuating stresses and strains on the component [2].

The damage done during the fatigue failure is cumulative and generally unrecoverable. It is nearly impossible to detect any progressive changes in material behavior during fatigue crack initiations and propagations and measurable healing or recovery isn't possible. Since failures often occur without warning unexpected accidents and fatalities might happen which has economic and social effects [3].

On this study the researcher mainly tries to study the effect of different loading and traction conditions basically three loading & fourteen traction conditions, on fatigue life of a wheelset as a case study for Addis Ababa light rail train (AALRT).

1.2 Problem Statement

Impact of loading and traction condition on rail traffic includes economic, social and environmental losses. Many countries are confronted with this problem. Overloaded rail traffic induces extreme harm to the economy of an entire country by increasing failure rate of mechanical components, increase spare part cost, maintenance cost and time also may lead to unexpected accident and train exposure to a dangerous conditions and its impact includes social and economic losses for the country.

In case of Addis Ababa light rail train (AALRT) Transport in most cases overloading of passenger and goods beyond the normal train carrying capacity is obvious, and also, they operate relatively at slow speed. ERC employees are interviewed and explained that the trains are operating slowly[1] and beyond their operating load limit which have on direct effect on axial, bending, torsional and other forms of load and stresses generated on the axle and wheel. Other previous researches also imply this overloading and traction condition problem on their study [4, 5, 6].

These overloading and traction conditions mainly affect the static and dynamic behavior of the wheelset and also have impact on fatigue life and might shorten the life span of the wheel set by increasing the stress induced and rate of fatigue failure [7].

1.3 Scope of the Research

The present work focuses on fatigue durability analysis for axle and wheel of AALRT considering different condition of traction and loading of passengers on a straight track. Only a straight track is considered, and curving effects are not included in this research. The paper mainly tries to analyse the fatigue failure of a wheelset which is one of the main and crucial component of a rolling stock. It predicts and compares fatigue life, safety factor, stresses generated by the different loadings and traction speed, deformation and damage results for wheel set by analyzing sensitivity factors in different loading and traction parameters using FEM software.

1. The rated traveling speed of the train is 37.5 km/hr. at a rated motor torque of 689.7 Nm and rotational speed of 1,800 RPM [8].

1.4 Objectives

1.4.1 General Objective

The general objective of this research is to study effect of different loading and traction conditions on fatigue life, factor of safety, stresses induced and deformation of a wheel set on a straight railroad in the case of Addis Ababa light rail service (AALRTS) trains.

1.4.2 Specific Objective

- Collecting and analyzing data of AALRT rolling stock wheel set, track line and passenger loading.
- Analyzing the loading & stresses induced on the axle and on the wheel using analytical techniques, with considering different loading and traction conditions.
- CAD modeling of the wheel and the axle of the AALRT Railcar based on the specifications and the measurements
- Performing finite element analysis (FEA) by applying appropriate boundary conditions and loading on the wheelset for different loading and traction conditions, and determining stresses and deformations generated by the loads.
- Estimating the fatigue life of the wheel-set under different loading and traction conditions, and analyzing the sensitivity of fatigue results and safety factors in different loading and traction parameters, using Finite Element Method (FEM) software, and comparing analytical and FEA results.

1.5 Limitations

This research project was intended to find effect of passenger weight and traction condition on Addis Ababa light rail train on the mechanical fatigue life of the wheel and the axle by under different loading conditions under different loading conditions. Only a straight track is considered, and curving effects are not included in this research. Also, this research intends to find those effects for only a urban light rail and AALRT is taken as a case study.

Also other than mechanical fatigue other forms of fatigue like thermal fatigue –, creep fatigue, rolling contact fatigue, corrosion fatigue, fretting fatigue are not part of this research.

For FEA analysis results, because the documents and standards of AALRT railcars are not available, the researcher uses other related previous works and commons standards for validation.

1.6 Outline of the Thesis

This thesis contains six chapters that address the research objectives. The content of each chapter is briefly outlined as follows: Chapter one briefs general information about the research conducted. Initially, the background of the research is discussed and presented. Following the back ground of the research, statement of the problem, general and specific objectives, scope and the limitations of this research are described. The second chapter presents an overview of the related literatures, describes about fatigue overviews, theoretical foundations and design approaches of fatigue analysis of wheel set. These literature reviews are basics for the present thesis. Chapter three describes the methods used on this research, that addresses all necessary steps of the research, the collected data of loadings, specifications of both the railcar and the wheel set, material properties etc… the fourth chapter is the main body of the thesis.it contains analysis of all loadings and forces acted on the Wheelset analytically to obtain the input loadings and boundary conditions for the FEA, Modeling and geometries from solid work, finite element modeling, boundary conditions, loadings etc…. for different loading and traction conditions. The next chapter presents result and discussions. In this chapter the simulated model gives results in counter plots and the obtained results are discussed one by one in tables and graphs form and the last chapter describes briefly the conclusion, recommendations, and future works of the thesis.

CHAPTER 2
LITRATURE REVIEW

2.1 Fatigue overview

A. Historical background of Fatigue

Among the many parts that make up a railway vehicle, Wheel and axles are considered the most important safety-related items because a broken axle or wheel can directly lead to derailment, with serious damage for the rolling stock and the infrastructure; it can cause injury to passengers and it can lead to casualties in the most serious cases. In addition, since railway wheelset are subjected to different types of loads and stress, issue of fatigue failure always exist.

The first study of metal fatigue is believed to have been conducted around 1829 by the German mining engineer W.AJ. Albert. He performed repeated load proof tests on mine-hoist chains made of iron. One end of the chain was loaded while the chain was supported on a 360-cm (12-ft) disc. The chain links were repeatedly subjected to bending, at a rate of 10 bends per minute up to 100000 bends, by a crank coupling which oscillated the disc through an arc [9].

Interest in the study of fatigue began to expand with the increasing use of ferrous structures, particularly bridges in railway systems. The first detailed research effort into metal fatigue was initiated in 1842 following the railway accident near Versailles in France which resulted in the loss of human lives. The cause of this accident was traced to fatigue failure originating in the locomotive front axle.

Wohler [9] conducted systematic investigations of fatigue failure during the period 1852-1869 in Berlin, where he established an experiment station. He observed that the strength of steel railway axles subjected to cyclic loads was appreciably lower than their static strength. Wohler's studies involving bending, torsion and axial loading included fatigue tests on full-scale railway axles for the Prussian Railway Service and on a variety of structural components used in small machines. His work (e.g., Wohler, 1860) also led to the characterization of fatigue behavior in terms of stress amplitude-life (S-N) curves and to the concept of fatigue 'endurance limit'.

In fig 2.1 a, the upper drawing shows Wohler's apparatus for the measurement of service strains on railway axles. The dashed line indicates the deflected position,

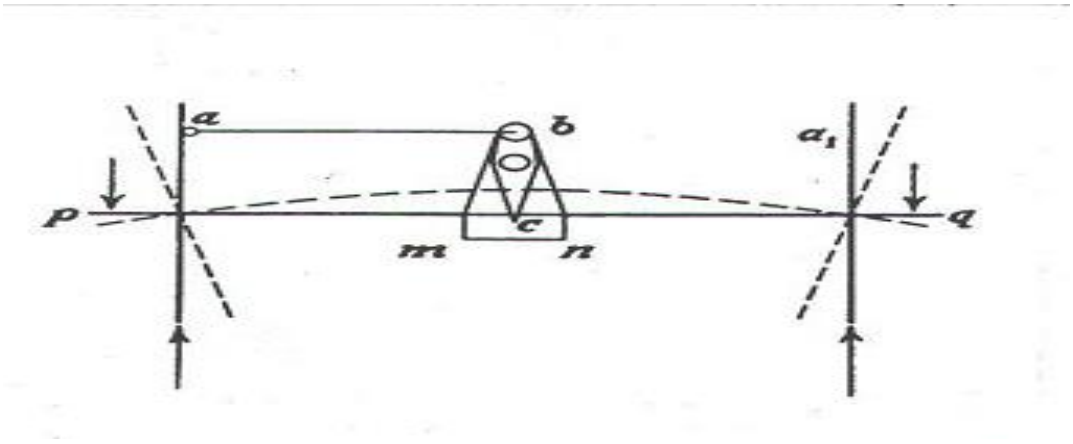

(a)

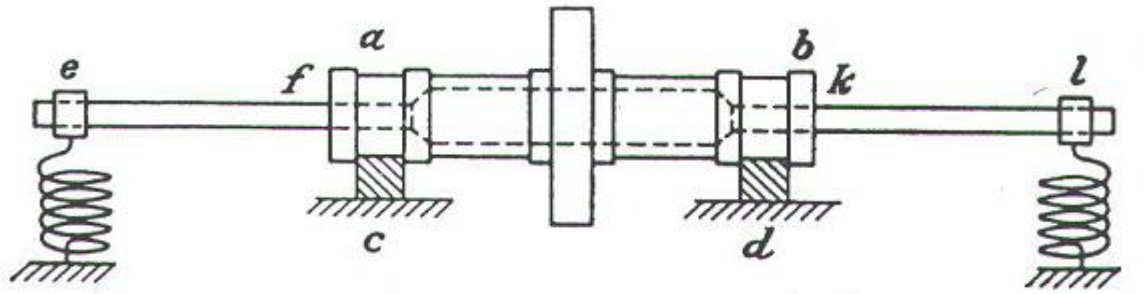

(b)

Fig 2.1 a & b: Wohler's apparatus fatigue testing machine [4]

In fig 2.1 b, shows Wohler's purpose to build fatigue testing machine to apply reserved bending to axle-like specimen. He conducted a systematic experiment to evaluate the fatigue of steam locomotive axles and studied the stress (S)-life (N) relationship, which is used even today as the most basic fatigue characteristic data. He established the foundation for the study of fatigue. The stress locally in the axle to initiate a fatigue crack. Wohler led to the identification of the fatigue limit for steels. Despite its long use, there is growing evidence that for lives longer than the conventional 10^6 to 10^7 cycles, at which the fatigue limit is determined, the safe stress range continues to be eroded down to 10^9 cycles and more, which is at the very long lives typical of that required of axles and wheels.

In 1874, the German engineer Gerber [9] began developing methods for fatigue design; his contribution included the development of methods for fatigue life calculations for different mean levels of cyclic stresses. Similar problems were also addressed by Goodman (1899).

In 1910, Basquin [9] proposed empirical laws to characterize the S-N curves of metals. He showed that a log-log plot of the stress versus the number of fatigue cycles resulted in a linear relationship over a large range of stresses. Other notable contributions of this time period included those of Smith (1910), Bach (1913), Haigh (1915), Moore & Seeley (1915), Smith & Wedgwood (1915), Ludwik (1919), Gough & Hanson (1923), Jenkin (1923), Masing (1926) and Soderberg (1939).

In 1926, a book entitled the Fatigue of Metals was published by Gough [9] in the United Kingdom. A year later, a book bearing the same title was published by Moore [9] and Kommers [9] in the United States. By the 1920s and 1930s, fatigue had evolved as a major field for scientific research. Investigations in this time period also focused on corrosion fatigue of metals (Haigh, 1917; McAdam, 1926; Gough, 1933), damage accumulation models for fatigue failure (Palmgren, 1924; Miner, 1945), notch effects on monotonic and cyclic deformation (e.g., Neuber, 1946), variable amplitude fatigue (Langer, 1937), and statistical theories of the strength of materials (Weibull, 1939). A prolific researcher of this period was Thum (e.g., Thum, 1939) who, along with many German colleagues, reported experimental results on such topics as fatigue limits, stress concentration effects, surface hardening, corrosion fatigue and residual stresses in numerous publications [9].

The notion that plastic strains are responsible for cyclic damage was established by Coffin (1954) and Manson (1954) [9]. Working independently on problems associated with fatigue due to thermal and high stress amplitude loading, Coffin and Manson proposed an empirical relationship between the number of load reversals to fatigue failure and the plastic strain amplitude. This so-called Coffin-Manson relationship has remained the most widely used approach for the strain- based characterization of fatigue.

With the application of fracture mechanics concepts to fatigue failure, increasingly more attention was paid to the mechanisms of subcritical crack growth. Conceptual and quantitative models were developed to rationalize the experimentally observed fatigue crack growth resistance of engineering materials (e.g., Laird & Smith, 1962; McClintock, 1963; Weertman, 1966; Laird, 1967; Rice, 1967; Neumann, 1969; Pelloux, 1969).

Concomitant with this research, there was expanding interest in understanding the processes by which the stress intensity factor range could be altered by the very history of crack advance. An important contribution in this direction came from the experimental results of Elber (1970, 1971) who showed that fatigue cracks could remain closed even when subjected to cyclic tensile loads [9].

B. Fatigue Failures on Railcar wheelset

To see accidents due to fatigue failure on wheelset, accident in Sheffield, United Kingdom in 1884 that led to derailment was the broken axle of a train moving at 80 km/h. Twenty-four people lost their lives. Hoddinott examined the accidents related to axle failures taking root from mechanical loads, electrical arcing and corrosion in his article. For instance, an accident at Rickerscote in 1996 was reported as a complete fracture of an axle and consequent derailment of a two-axle freight wagon containing liquid carbon dioxide. The derailed wagons blocked the adjacent line and were run into by a traveling post office train going in the opposite direction. One person was killed and there were 10 injuries.

From the beginning of 1997, axle failures have occurred on rail vehicles of the Istanbul Transportation Co. that have been in service for Istanbul city rail transportation. Finally, in 2007 after the vehicle entered the station in Istanbul Esenler, the axle of the vehicle broke and the wheel fell between the rail and the switch as a result of fatigue fracture [10].

Meral Bayraktar[10], investigated the reason behind the train axle failure in February, 2009. The experts reported that the fracture occurred at the transition section having radius between the wheel and gear box. From the result of examination of fracture surface is 10% less than the total surface. Also, it is clear that two different regions have been detected on surface. While 90 % of the section surface has shown the growth of fracture by the time, 10% of the section surface has been pointed out as instantaneously broken. The forces affecting the axle are tension and low stress. The edges of the fracture move along rapidly because of the poor but effective environmental notch impact. After many investigations they concluded that the reason behind the axle failure is that the fractures result from fatigue.

On Thursday 9 February 2006, passenger train travelling from Melbourne to Sydney derailed near Harden in New South Wales. An inspection by the driver found one wheel on the trailing bogie of the leading power car had derailed. During recovery operations the axle of the derailed wheel was found to have completely sheared with a crack in the radius relief area between the gear and wheel seats. The ATSB's investigation concluded that impacts from track ballast from unknown location(s) had led to the formation of the cracks in the axles. The investigation also concluded that routine testing of the axles carried out by the operator's maintenance contractor, using magnetic particle inspection (MPI), was ineffective and resulted in the fatigue cracks going undetected for a considerable period of time. A number of safety actions have been undertaken by Rail Corp and the Independent Transport Safety and Reliability Regulator of New South Wales which include measures

aimed at the early detection and prevention of axle fatigue cracks in XPT and other diesel fleet rail vehicles to limit the risk of further axle failures. Additionally, the Australian Transport Safety Bureau has issued a safety advisory notice to all rail vehicle operators in Australia that they should consider the risks associated with axle failures as a result of fatigue cracks initiated by ballast strikes and review their maintenance practices accordingly [11].

Fig 2.2 Fractured surface of an axle [11]

In 2010, In Germany Bundesanstalt für Arbeit state there were train accident because of train axle failure. And the customers accused the manufacturers that produced that product. But the court ordered to investigate the problem first by using different scientific techniques.

C.Klinger, D.Bettge, R.Hacker, T.Heckel, D.Gohlke and D.KlingBeil [12] started to solve the problem. The broken railway axle model was ICE3. The axle failures caused derailment of the train and property damage.

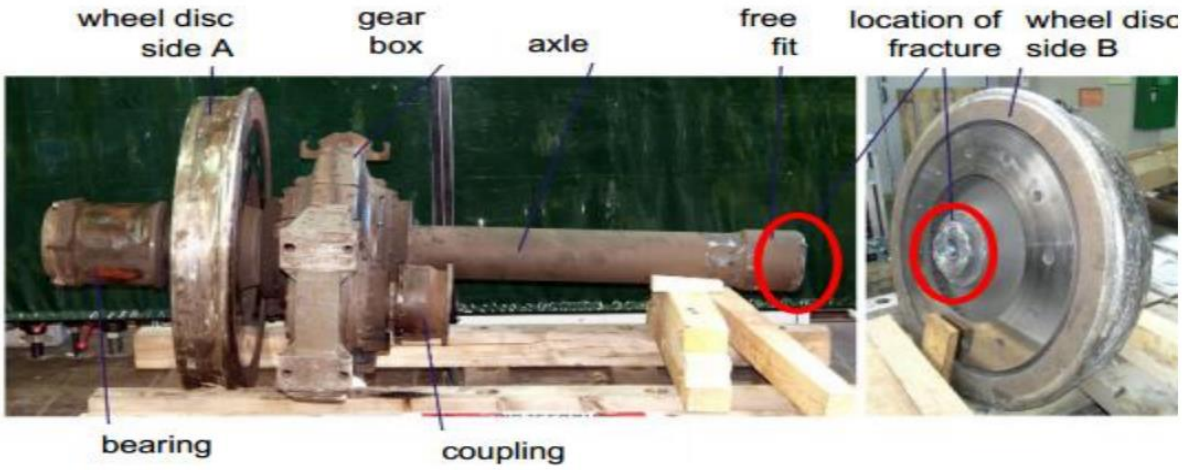

Fig 2.3 Broken wheels set and gear box [12]

They first separated the broken Wheelset and they tested mechanical test like tensile and impact tests. They did the chemical analysis and follows fractography. Then they do the metallographic and identification of purity. The result of fractography test was - Fatigue crack caused by rotation bending - Residual fracture about 1/5th of fracture surface - Successful allocation of the fracture surface to each other Metallographic investigation - Micro structure – OK - Hardness – OK - Microstructure – OK - Grain Size – OK - Surface Roughness – OK. Then they finally hypothesized the root cause for the fracture. The axle was nonmetallic inclusion of unacceptable size from the production. It was operating with a very high cycles in service. And the initiation of fatigue crack in the recess (three center curve) shows it was highly utilized axle. They investigated also there were fast crack propagation due to high stresses [12].

Cosmin Locovei, Aurel Rădulă, Mircea Nicoară and Laurenłiu Roland Cucuruz [13] did a research and wrote an article about Analysis of Fatigue Fracture of Tank Wagon Railway Axles in 2011 in Romania. The article was focused on the fracture mechanism of railway axles due to the fatigue of material. The purpose of the article was to numerically predict the number of cycles (or kilometers) to fracture of tank wagon railway axles in various theoretical conditions. The stresses in the axles were calculated by finite element methods. The number of cycles to fracture was calculated using closed form solution of NASGRO equation for fatigue crack development starting from an initial crack detectable by means of non-destructive testing. In order to demonstrate the deep negative impact of forbidden thermal treatments and operations applied to railway axles, residual stresses of these treatments were calculated and new numerical predictions of number of cycles to fracture have been made [13].

G. Fischer, V. Grubisic and M. Grosse-Hovest [14] wrote a research article about ‘Methodology for Reliable Durability Validation of Wheelset-Axles’. In their study they concluded that an “infinite life” design of wheelset axles is not possible based on practical experience and scientific investigations. And much greater vertical and lateral forces acting on axles were often found by the service measurements, compared with the values on which different standards for strength assessment of axles were based. In particular as a result of modified characteristics of rail vehicles, such as higher speed and adaptive matching to the track section (tilt technique), the stresses and number of cycles reached are much greater than those covered by the standards. An estimate of the maximum allowable nominal stresses according to the standard with the help of Woehler curves up to 10 and the properties determined with small specimens as proposed in some norms do not

constitute a reliable basis for assessing fretting fatigue of higher strength new materials. Suitable validation tests are necessary for this purpose. The experience with regard to load values and permissible stresses on which the standards are based should be validated using corresponding safety factors. The large number of fractures in operation resulting from fatigue –particularly due to fretting fatigue –and re-call actions and inspections this entails, call for revision of the design concepts used so far and adaptation to the state of technology. Optimum and reliable design of wheel set axles requires determination of the operational loads and of the fatigue strength of axles. A corresponding procedure must ensure that these decisive influencing factors are appropriately considered for the design of wheel set axles as proposed in this paper [14].

At present time the procedures for design and calculation of the axles and wheels are defined by different International standards. Therefore, axle and wheel resistance to failure is a key issue in designing and correctly maintaining railway vehicles, to ensure high safety standards and, at the same time, to optimize life-cycle costs from a system point of view.

C. Fatigue and overloading in case of AALRT

When we come to our case, now in Ethiopia, The AALRT is giving service to its customers. But the service is not safe due to improper train loading and traction conditions. Different parts of the train are facing failure (like the wheel and rail) before their service life span.

Solomon Kibebew [5] is a former 2015 batch ERC (AAU) institute student worked on the "Analysis of effect of train overload on disc brake of AALRT" by different loading conditions by taking overloading condition of maximum 420 passengers per train.

Etaferahu Birhanu [6] is another former batch of Addis Ababa university who study Overloading effect on the life cycle of car body structures in case of AALRT using different case of loading (maximum 408 passengers/ train) and traveling speed of 20 km/hr.

When we come to fatigue on wheelset**, Kidanemariam G/tsadik** is a former 2014 batch ERC (AAU) institute student. He worked on the fretting damage (fatigue on the press fitted area of wheel and axle) on train wheel set when the train is on the condition of empty. He tried to analyze the fretting fatigue life of the wheel set and found 29469 cycles before failure [15].

Worku Leta [16] another colleague, 2017 batch of AAIT mechanical engineering department did" Analysis of Rolling Contact Fatigue Failures of Railway Wheels Due to cyclic Load" and tried to find the available life of railway wheel and get fatigue life of 168080 cycles for the maximum loading condition.

This research mainly tries to analyze mechanical fatigue on the wheel set in case of AALRT railcar. It is done according to AALRT operating and loading condition. Here different approaches and new analysis ideas are used to analyze the stress and force and fatigue life of the AALRT axle. ERC (Ethiopian Railway Corporation) employees are interviewed and explained that the trains are operating relatively slow and beyond their operating load limit. This will have effect on the fatigue life of the train axle and wheel.

2.2 Theoretical Foundation of Wheelset Fatigue Analysis

Railway Axles and wheels were one of the first components which were subjected to large numbers of repeated cycles. Because of the loading geometry the axle is in approximately 4-point bending and torsion, and each time the axle rotates, an element of material on the surface of an axle goes from a compressive state to a tension state of equal magnitude.

Bending stress and strains of the Wheel set is calculated from loading forces – vertical (weight of the wagon and load), horizontal (Lateral) forces from the rail, also from curves and crossings and braking forces. From bending moments are than calculate bending stresses in all cross sections of the axle.

Also the torsional stress from the gearbox of the train, horizontal (Lateral) forces on the wheel from the rail. After that based on the yield criterion (common yielding criteria known as the von Mises yield criterion) we calculate the von mises stress and Calculated stresses must be smaller than permissible stress that is determined as fatigue limit of the axle and wheel divided by safety factor.

2.2.1 Fatigue design approaches

The three main approaches in fatigue design philosophy are Safe-Life, Fail-Safe and Damage-Tolerant [17].

A). Safe-Life (finite lifetime concept): - In the Safe-Life philosophy products are designed to survive a specific design life with a chosen reserve.

B). Fail-Safe (infinite lifetime concept): - Design to keep stress below threshold of fatigue limit, so as to reduce some of this waste of useful fatigue life, and maintain or improve the

operating safety of a component in the later stages of its life. This is the main philosophy we use on this research.

C). Damage-Tolerant: - users need to inspect the part periodically for cracks and to replace the part once a crack exceeds a critical length. This approach usually uses the technologies of nondestructive testing and requires an accurate prediction of the rate. of crack-growth between inspections. This is often referred to as damage tolerant design or "retirement-for cause" [18].

2.2.2 Fatigue analysis methods

The three major fatigue life methods used in design and analysis are the stress-life method, the strain-life method, and the linear-elastic fracture mechanics method. These methods attempt to predict the life in number of cycles to failure, N, for a specific level of loading. Life of $1 \leq N \leq 103$ cycles is generally classified as low-cycle fatigue, whereas high-cycle fatigue is considered to be $N > 103$ cycles [19].

A. Stress-life (S-N) method

The stress-life method, based on stress levels only, is the least accurate approach, especially for low-cycle applications & Stress Life is concerned with total life and does not distinguish between initiation and propagation. However, it is the most traditional method, first formulated in the 1850s to 1870s and based on S-N curves (Stress – Cycle curves). Fig 2.4 is a typical S-N curve that shows the stress amplitude with number of cycles. Since it is the easiest to implement for a wide range of design applications, has ample supporting data, and represents high-cycle applications adequately [19].

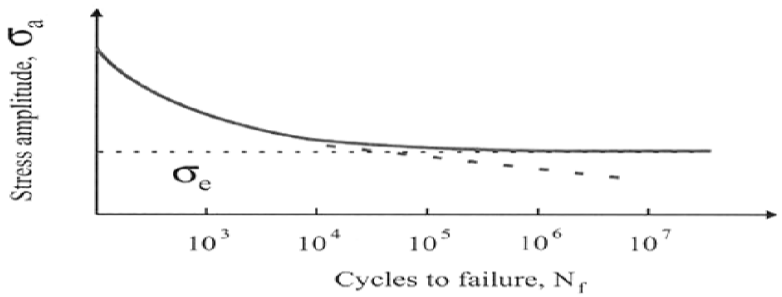

Fig 2.4 S-N Curve for stress life approach [19]

In terms of cycles, Stress Life typically deals with a relatively High number of cycles which are more than 10^3 (10,000) cycles, it shouldn't use to estimate fatigue lives below 10,000 cycles [20].

B. Strain-life (ε-N) method

This method is also called Critical Location (CLA) approach, Local Stress-Strain, E-N or Crack Initiation. It was first formulated in the 1960s. This approach is best suited for low cycle fatigue problems refers to fewer than 10^3 (10,000) cycles [20].

The strain-life method involves more detailed analysis of the plastic deformation at localized regions where the stresses and strains are considered for life estimates. Fig 2.5 shows us how the strain of a typical material changes with number of cycle.

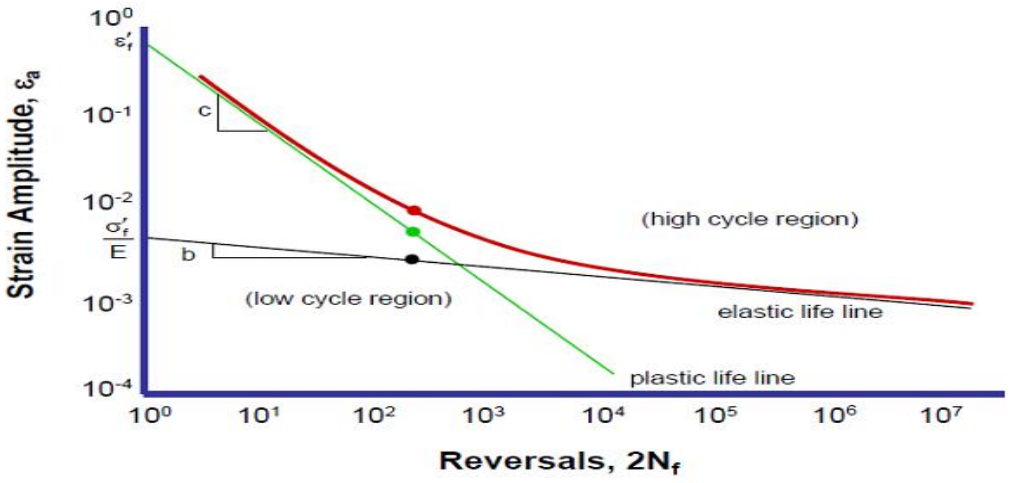

Fig 2.5 Strain Approach for constant amplitude loading [21]

This method is especially good for low-cycle fatigue applications. In applying this method, several idealizations must be compounded, and so some uncertainties will exist in the results. For this reason, it will be discussed only because of its value in adding to the understanding of the nature of fatigue [19].

C. Fracture mechanics method

The fracture mechanics method assumes a crack is already present and detected. It is then employed to predict crack growth with respect to stress intensity. It is most practical when applied to large structures in conjunction with computer codes and a periodic inspection program [19].

2.2.3 Basic Fatigue Terminologies, [1, 20,22, 23]

Before we go to the detail FEM fatigue analysis for the Wheelset the reader should have a clear understanding and knowhow to the following terms.

Consider the case of constant amplitude, proportional loading, with min and max stress values σ_{min} and σ_{max}[8]

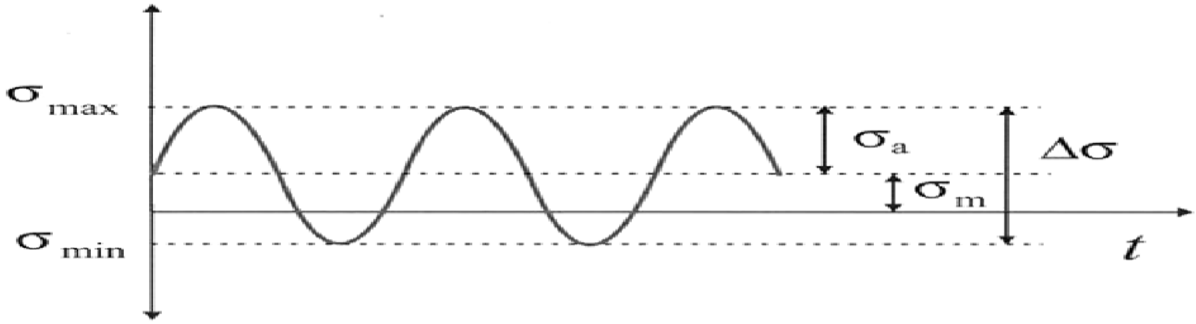

Fig 2.6 Terminologies for Constant amplitude loading [20]

- **Stress range, $\Delta\sigma$** is defined as $(\sigma_{max} - \sigma_{min})$
- **Mean stressσ_m** is defined as $(\sigma_{max} + \sigma_{min})/2$
- **Stress amplitude** or alternating stress is $\sigma_a = \Delta\sigma/2$
- **Stress ratio R** is $(\sigma_{min}/\sigma_{max})$
- **Fully-reversed loading** occurs when an equal and opposite load is applied. This is a case of $\sigma_m = 0$ and R = -1.
- **Zero-based loading** occurs when a load is applied and removed. This is a case of $\sigma_m = \sigma_{max}/2$= and **R** = 0.

A. Endurance Limit

Endurance or Fatigue Limit is a value on S-N diagram which a laboratory test specimen gives infinite life. Record is kept of the number of cycles required to produce failure at a given stress, and the results are plotted in stress-cycle curve as shown in Fig 2.8. A little consideration will show that if the stress is kept below a certain value as shown by dotted line in Fig. 2.8, the material will not fail whatever may be the number of cycles. This stress, as represented by dotted line, is known as endurance or fatigue limit (σ_e) [1].

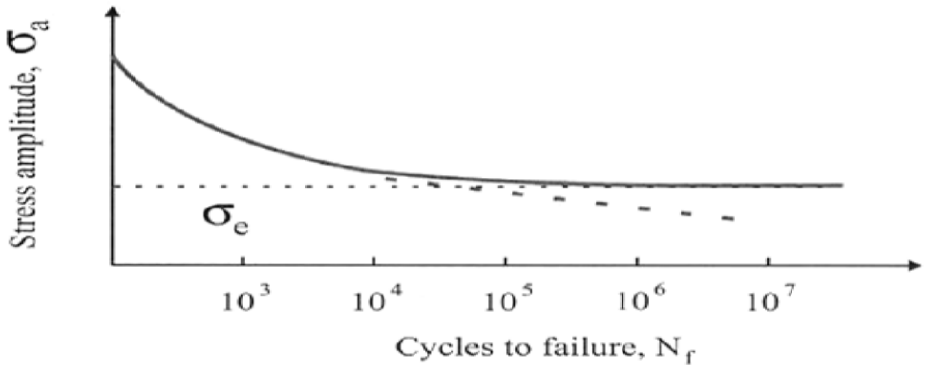

Figure 2.7 S-N Curve for stress life approach [20]

Finding the Endurance Limit using the rotating beam experiment is time consuming where it requires testing many samples and the time for each test is relatively long. Therefore,

scientists try to relate the endurance limit to other mechanical properties which are easier to find (such as the ultimate tensile strength) [1].

For Steel

$$S_e = 0.5\, S_{ut}\,, S_{ut} \leq 200\ ksi\ (1400\ MPa)$$
$$S_e = 100\ Ksi\ \ , S_{ut} > 200\ ksi\ (1400\ MPa)$$
$$S_e = 700\ Mpa\,, S_{ut} \geq 1400\ Mpa$$

For cast Iron

$$S_e = 0.4\, S_{ut}\,, S_{ut} \leq 60\ ksi\ (400\ MPa)$$
$$S_e = 24\ Ksi\ \ , S_{ut} > 60\ ksi\ (1400\ MPa)$$
$$S_e = 160\ Mpa\,, S_{ut} \geq 1400\ Mpa$$

S_e is the endurance limit value obtained for the test specimen. It is unrealistic to expect the endurance limit of a mechanical or structural member to match the values obtained in the laboratory. The endurance limit of an actual element subjected to any kind of loading will be estimated based on Marin's modification factors,

B. Endurance Limit Modification Factors

Marin identified factors that quantified the effects of surface condition, size, loading, temperature, and miscellaneous items. To account for these conditions a variety of modifying factors, each of which is intended to account for a single effect, is applied to the endurance limit value of test specimen obtained under laboratory conditions. Consequently, we may write; [19]

$$S_e = S_e{}' * K_a K_b K_c K_d K_e \qquad \text{(Eq. 2.1)}$$

Where ;

$S_e = endurance\ limit\ of\ actual\ element$

$S_e{}' = endurance\ limit\ of\ test\ specimen$

$K_a =$ surface factor

$K_b =$ size factor

$K_c =$ load factor

$K_d =$ temperature factor

$K_e =$ miscellaneous effects factor

Surface Factor K_a

The surface of a rotating-beam specimen is highly polished, with a final polishing in the axial direction to smooth out any circumferential scratches. The surface modification

factor depends on the quality of the finish of the actual part surface and on the tensile strength of the part material.

$$K_a = aS_{ut}{}^{b} \qquad \text{(Eq. 2.2)}$$

Where $S_{ut}$is the ultimate strength of the material and *a* and *b* are to be found in Table 2.1. [19]

Table 2.1 Value of Surfaced Factor constants [19]

Surface finish	Factor a ($S_{ut} in\ MPa$)	Exponent b
Ground	1.58	-0.085
Machined or Cold – drawn	4.51	-0.265
Hot rolled	57.7	-0.718
As – forged	272	-0.995

Size factor Kb: The rotating beam specimens have a specific (small) diameter. Parts of larger size are more likely to contain flaws and to have more non-homogeneity.

The size factor K_b for bending and torsion is given by

$k_b = 0.91 * d^{-0.157}$ For diameter from 2 inch to 10 inch

For axial the size factor $K_b = 1$

Loading Factor (K_c)

[1] The load factor K_c is given by

For Bending,$\boldsymbol{K_c = 1}$

For Torsion,$\boldsymbol{K_c = 0.59}$

For Torsion,$\boldsymbol{K_c = 0.85}$

The loading factor is 1 for combined load and Von mises stress is used

Temperature Factor (K_d)

When the operating temperature is below room temperature the material becomes more brittle. When the temperature is high the yield strength decreases and the material becomes more ductile and creep may occur.

$$K_d = 1 \text{ for temprature } \leq 450\ ℃$$

Reliability Factor (K_e)

The endurance limit obtained from testing is usually reported at mean value [1].

Reliability	K_e
90%	0.897
95%	0.868
99%	0.814
99.9 %	0.753

C. High and low cycle fatigue

In fatigue analysis Life of $1 \leq N \leq 103$ cycles is generally classified as low-cycle fatigue, whereas high-cycle fatigue is considered to be $N > 103$ cycles. In general, to for high number of cycles we use stress based fatigue analysis known as stress life analysis while for low cycle fatigues we can use strain based fatigue analysis [7].

D. Finite and Infinite Life

We also distinguish a finite-life and an infinite-life region. Finite life region covers life in terms of number of stress reversals up to the knee point [19]

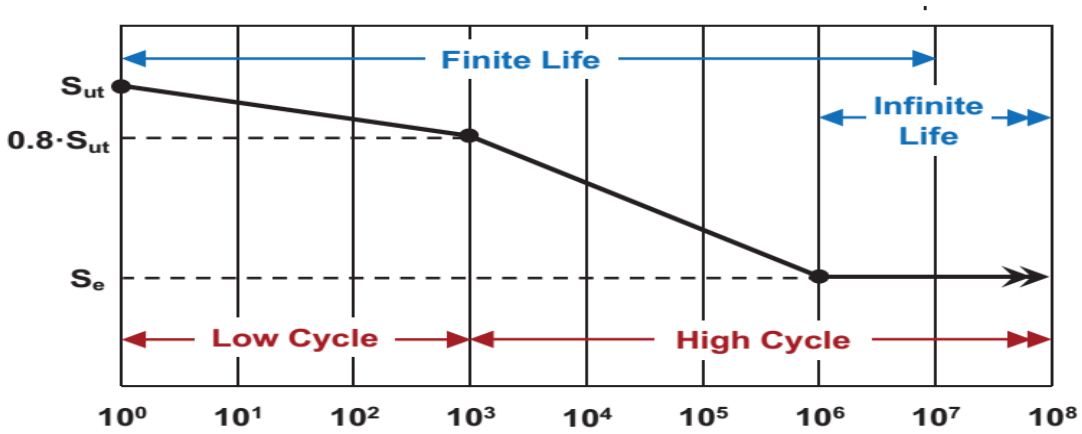

Fig 2.8 Typical S-N diagram for steel in Log – Log scale [19]

E. Fatigue stress concentration factor, K_f

In the development of basic stress equations for tension, compression torsion and bending, it was assumed that no longer geometric irregularities occur in the member under consideration. But it is difficult to design a machine component without permitting some changes in the cross section of the member.

Therefore, equations in basic stress equation no longer describe the state of stress in the part of these locations. The existence of irregularities or discontinuities, such as holes,

grooves, or notches, in a part increase the magnitude of stresses significantly in the immediate vicinity of the discontinuity. Fatigue stress concentration factor,

$$K_f = \text{Maximum stress in notched specimen} / \text{Maximum stress in notch free specimen}$$

F. Failure criteria

A Haigh diagram plots the mean stress, usually tensile strength, along the x-axis and the oscillatory stress amplitude along the y-axis. Lines of constant life are drawn through the data points. The infinite life region is the region under the curve and the finite life region is the region above the curve [19].

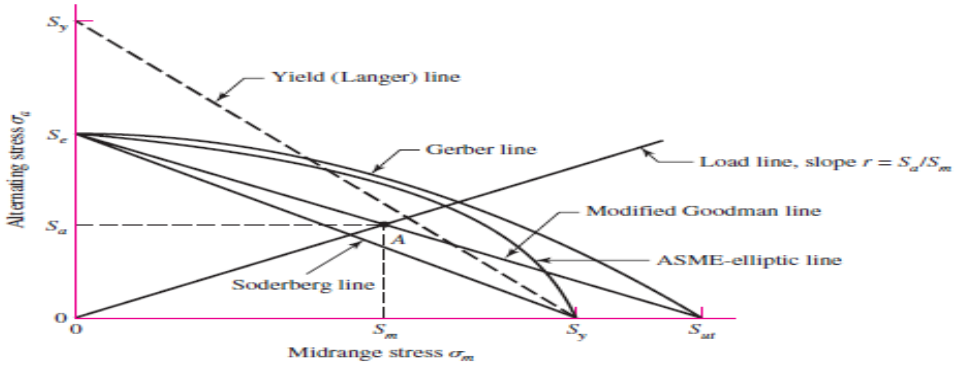

Fig 2.9 Fatigue criteria [19]

The two most widely accepted methods are those of Goodman and Gerber. Experience has shown that test data tends to fall between the Goodman and Gerber curves. Goodman is often used due to mathematical simplicity and slightly conservative values. For design applications the stresses σ_a and σ_m can replace S_a and S_m in the above equations and each strength is divided by a factor of safety F.S [19].

The resulting equations are:

Goodman's Criteria

$$\frac{1}{F.S} = \frac{\sigma'_m}{S_{ut}} + \frac{\sigma'_a}{S_e} \qquad (Eq.2.4)$$

Soderberg's Criteria

$$\frac{1}{F.S} = \frac{\sigma'_m}{S_{yt}} + \frac{\sigma'_a}{S_e} \qquad (Eq.2.5)$$

Gerber's Parabolic Criteria

$$\left(\frac{F.S * \sigma'_m}{S_{ut}}\right)^2 + \frac{(F.S * \sigma'_a)}{S_e} = 1 \qquad (Eq.2.6)$$

Therefore For this research we use Goodman's criteria since it is recommended for ductile materials.

G. Bending stress on high speed and low speed trains

On high speed trains the bending load and stress increases with the increase in speed due to dynamic acceleration rate i.e. the load increasing rate of the static load relative to the accelerated gravity force. But this situation is worked only for very high speed trains.

According Hirakawa [24], who recognize the design philosophy difference between the Japanese Shinkansen (based on the old standard V max = 210 Km/hr.) and European TGV and ICE (new revised standard vmax 350 km/hr.) and he says that increase in speed causes an increase in axle bending stresses. The maximum value of dynamic stress and static stress increases with the increase in velocity; but he also implies that this effect is only significant at very high speeds which the traveling speed up to 350 Km/hr. but the effect is nonexistent for speeds less than 60 km/hr.

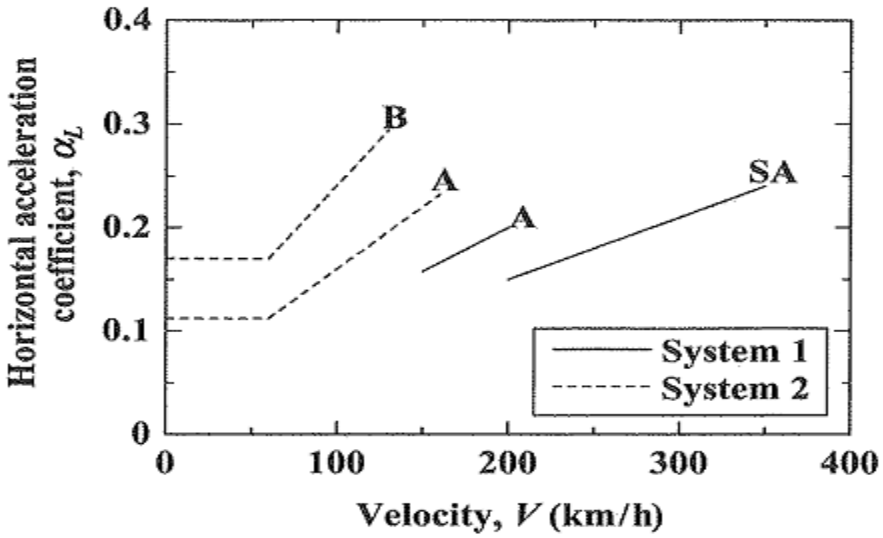

Fig 2.10 Increase in horizontal acceleration force with speed

As we can see from fig 2.10 since the dynamic acceleration coefficient is not dependent on the velocity for low and medium speed trains below 60 km/hr., the effect of increasing axle bending stresses with speed is nonexistent.

CHAPTER 3

RESEARCH METHODS

3.1 Research methods

To achieve the scope of the thesis the following methodological approaches are performed.

3.1.1 Data collection

Necessary data like passenger number, train carrying, railcar specifications, material property etc… are gathered from AA LRT project office. And also different research works, articles, journals, and other related documents are used to perform the thesis work.

3.1.2 Analysis

For the analyses of fatigue life, stress, strain factor of safety etc…of the wheel set of the AALRT railcar under different loading and traction conditions the researcher employs different analytical and Numerical approaches.

To determine bending, torsional and lateral forces and stress we use different mechanic theories (static and dynamic), and Hertzman theory of contact mechanics to determine elliptical contact patch between wheel and rail and to calculate contact stresses for the analytical calculation.

For FEA analysis the researcher uses different Software. To modeling of wheel set and the rail based on the specifications Solidwork 2013 is used. For analysis of the effects of different loading and traction conditions on the wheelset Finite element software ANSYS 15.0 is used.

For data analysis of results and discussions the researcher uses data analysis softwares like Origin and EXCEL

3.2 Data Collection

Below data are collected from ERC Kality Depot. Based on this fatigue analysis of the axle and wheel is done.

3.2.1 Specifications

A. Rolling stock

The trains shall be 70% low-floor articulated 6-axle modern trams, consisting of three modules, bidirectional driving. Two tramcars shall be able to operate with double heading [8].

- Train formation: Mc+Tp+Mc
- Mc module: motor car with driver's cab
- Tp module: trailer without driver's cab and with pantograph

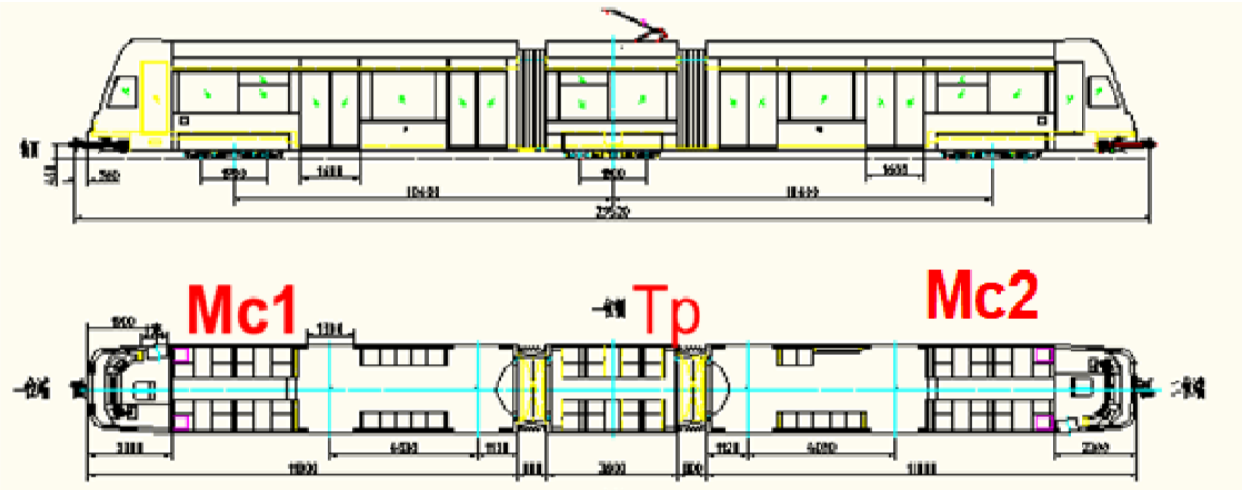

Fig 3.1: AALRT Rolling stock

Table 3.1 Basic parameter of the AALRT Line [8]

Basic Technical Parameter	Value
Track gauge	1435 mm
Minimum radius of vertical Curve	1000 m (auxiliary line)
Minimum radius of Horizontal Curve	25 m
Maximum Gradient	5 ‰
Rated voltage	DC 750 V
Train length (exclusive of train couplers)	28.8 m

Table 3.2: Basic Technical Parameter of the Train [8]

Basic Technical Parameter	Parameter Value
Max. Operating speed	70 Km/hr.
Distance between backs of wheel flanges	1,377.7 (-1,+2) mm
Wheel base	18000 mm
Axle Load	11.5 t
Wheel diameter (new/worn)	660/580 mm
Bogie weight	≤ 4 t
Maximum width	2650 mm
Height	3610 mm
Center to center distance between both bogies	10400 mm
Axle distance of motor unit	1900 mm
Axle distance of trailer unit	1800 mm

Table 3.3 Main electric parameters of traction motor [8]

Parameters	Value
Rated power	130KW
Number of poles	6
Number of phases	3
Rated voltage	500 V
Power factor	0.74
Net voltage	750V, Max. 900V, Min .525V
Gear ratio	6.05
Rated current	215A
Connection	Y
Rated rotate speed	1,800r/min
The highest rotate speed	4,377r/min

B. Axle Specifications

Table 3.4 Axle type [4,8]

Axle type	Material	Axle Load	Wheel diameter	Bogie weight
Hallow	Steel (A1N)	11.5 Ton	660 mm	4 Ton

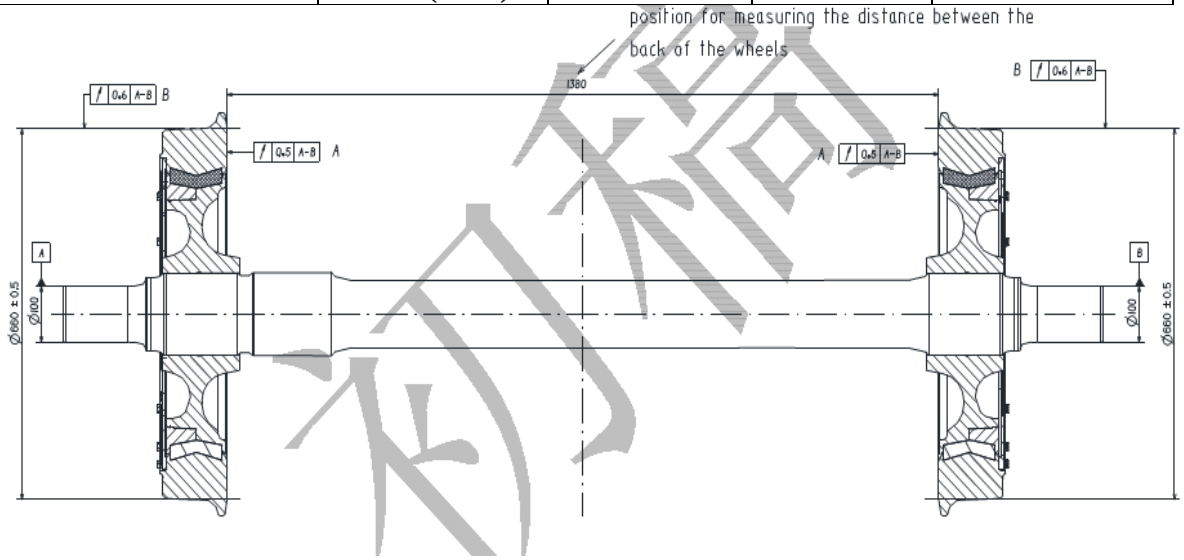

Fig 3.2 Front view of AALRT Wheelset [8]

Table 3.5 : Chemical composition of the Axle Material [15]

Steel Grade	C	Si	Mn	P	S	Cr	Cu	V	Ni
AIN	0.37	0.46	1.12	0.04	0.04	0.03	0.3	0.05	0.3

Table 3.6 Mechanical property of the Axle Material [22]

Mechanical Property of AIN Steel	Value
Young's Modulus	200 GPa
Elastic Modulus	210 GPA
Poisson's Ratio	0.26
Shear Modulus	7.69×10^{10}
Density	7300 Kg/m3
Ultimate Tensile strength	650 Mpa
Compression Strength	650 MPa
Yield strength	320 Mpa

C. Wheel Specification

Table 3.7 Chemical composition of wheel [16]

Material	C	Si	Mn	Mo	Cr	N	S	P	V
Wheel	0.58	0.34	0.75	0.02	0.15	0.01	<0.001	0.010	<0.005

Table 3.8 Mechanical Property of wheel material [16]

Wheel Material	**Yield stress (Mpa)**	**Ultimate Tensile strength (MPa)**	**Young's Modulus (GPa)**	**Poison's ratio**	**Density (kg/m3)**
	640	880	207	0.3	7800

Table 3.9 Mechanical Property and chemical composition of rail material [25]

Rail Material	**Tensile strength(Mpa)**	**Hardness (HV)**	**% C**	**% Si**	**% Mn**	**% Cr**
	950	267	0.7	0.3	1	0.3

Table 3.10 Main dimension of Wheel/Rail [16]

	Radii of curvature (mm)	**Gauge (mm)**	**Poisons Ratio**	**Young's Modulus**
Wheel	$R_1^W = 330$	1435	0.3	207
	$R\,_2^{\,w} = \infty$			
Rail	$R_2^r = 330$	1435	0.3	207
	$R\,_1^{\,r} = \infty$			

3.2.2 Data Collections of Different Loading Conditions

A. Number of Passenger

From ERC data, for rated passenger loading condition - 6 persons/m2, for over-crowed loading condition - 8 persons/m2, unaccepted overloading condition - 10 persons/m2 [4,5].

Passenger loading capacity and unacceptable load of a locomotive is summarized in the following table.

- To find the total passenger number in the train;

  Total number of passenger = standing passenger + sitting passenger

Table 3.10: seating and standing passenger loading value of a train [4]

Number of passengers	Seated	Standing	Total
Case 1 Loading capacity (AW_1) (standing:0 persons/m^2)	65	0	65
Case II Loading capacity (AW_3)(standing: 8 persons/m^2)	65	252	317
Case III Loading Capacity (AW_4) (standing: 10 persons/m^2)	101	319	420

B. Data Analysis of Passenger weight and traction conditions

Table 3.8 (a) Passenger weight of different cases

Loads	Car body weight	Passenger mass	Luggage (Kg)	Total mass	Total Weight (N)	Load per wheel (N)
Case 1 Loading (standing:0 persons/m^2)	44000	3900	0	47900	469899	39158.25
Case II Loading (standing: 8 persons/m^2)	44000	19020	0	63020	618856.4	51571.36
Case III Loading Capacity (standing: 10 persons/m^2)	44000	25200	820	70020	686896.2	57307.88

Note: -Take 60 kg as average weight of each passenger.

Table 3.8 (b) Different traction conditions

Traction Conditions	V(km/hr)	W (rad/sec)	T(Nm)	Traction Conditions	V(km/hr)	W (rad/sec)	T(Nm)
1	10.0	8.4	15444.0	8	40.0	33.7	3861.0
2	15.0	12.6	10296.0	9	45.0	37.9	3432.0
3	20.0	16.8	7722.0	10	50.0	42.1	3088.8
4	25.0	21.0	6177.6	11	55.0	46.3	2808.0
5	30.0	25.3	5148.0	12	60.0	50.5	2574.0
6	35.0	29.5	4412.6	13	65.0	54.7	2376.0
7	37.0	31.2	4172.7	14	70.0	58.9	2206.3

I.e. the above torque and angular velocity values are calculated by taking Motor power of 130 Kw for the case of AALRT [8].

CHAPTER 4

ANALYTICAL AND NUMERIC ANALYSIS

4.1 Analytical Calculations

4.1.1 Load on axle and wheel

A. Vertical Downward Load

Assumption

The total weight of the vehicle supported by the vehicle wheel set is equally distributed to all axles of the vehicle and the two wheels of an axle

Vertical Load on axle

Total weight = Total mass (passenger + vehicle) * Gravitational constant

Since on train has 3 bogies and 6 axles, weight applied on a single axle will be

Load supported by a single axle

$$Axle\ load\ = \frac{Total\ weight(\ load)}{No\ of\ axles}$$

Load supported by a single wheel

$$Wheel\ load\ = \frac{Axle\ load}{2}$$

Table 4.1 Summary of Loading Cases

Loads	Total mass	Total Weight (N)	Load per axle (N)	Load per Wheel (N)
Case 1 Loading (AW_1) (standing:0 persons/m^2) in kg	47900	469899	78316.5	39158.25
Case II Loading (AW_2)(standing: 8 persons/m^2) in kg	63020	618856.4	103142.73	51571.36
Case III Loading Capacity (AW_3) (standing: 10 persons/m^2) in kg	70020	686896.2	114615.76	57307.10

B. Rotational Moment

The other thing that the railway axle subjected to the torque or the twisting moment that enables the axle to rotate and give traction force for the vehicle**.** The stress set up by this torsion is known as torsional shear stress and it is zero at the centroid axis and maximum at the outer surface. [7, 19]

The maximum torsional shear stress on the railway axle is at the outer surface of and may be obtained from the following equation:

$\tau_{max} = \frac{16\,T}{\pi d^3}$ For solid Shaft

$T = \frac{\pi}{16} * \tau * \frac{D^4 - d^4}{D}$ For Hallow shaft

In order to calculate the torque on the wheelset first we should determine the torque transferred from the motor through gear box to the wheel set. Therefore, we should find the gear ratio of the axle box using power, torque and angular velocity of the wheel and the motor output shaft.

Power and Torque relationship

$$P = \frac{2 * \pi * N * T}{60} = T * \omega \qquad (Eq. 4.2)$$

Where

- P = Power
- N = rotational speed (RPM)
- T = Torque (Nm2)
- ω = Angular speed

From AALRT specification [table 3.3] of the LRT low floor train motor specification we know that the rated output power of the motor P, [8]

P = 130 KW at 1800 RPM

R= Gear ratio = 6.05

Since the power output from the motor is depend on input current and voltage from the line, the researcher assumes to take as constant of 130 kW, based on the specification to calculate torque for different traction conditions.

Rearranging equation (4.2) output torque of the electric motor will be

$$T = \frac{60\,P}{2 * \pi * N} = \frac{P}{\omega} \qquad (Eq. 4.3)$$

$$T_M = \frac{60 * 130000\ watt}{2 * \pi * 1800\ rpm} = 689.7\ Nm$$

Therefore, the axle torque will be

$$T_A = T_M * R \qquad \text{(Eq. 4.4)}$$

Where $T_A = Axle\ Torque$

$T_M = Motor\ output\ torque$

$R = Gear\ Ratio = 6.05$

From the gear ratio the torque (twisting moment) on the axle will be

$$T_A = 6.05 * 689.7\ Nm = 4172.68\ Nm$$

Also Axle and wheel rotational speed will be 297.5 Rpm and velocity wills 37.5 Km/hr.

For other traction conditions (10 km\hr. to 70 Km/hr.) the calculated torque are summarized in a tabulated form [table 3.8 b]

C. Lateral Force

Lateral forces $F_1\ and\ F_2$ that acts on the wheelset from the rail are calculated using Equation ,

$$F_l = \gamma * V$$

Where $\gamma = inclination(cant)of\ the\ wheelset\ running\ on\ the\ rail$ *(1/40 in case of AALRTS)*

$V = inclination(cant)of\ the\ wheelset\ running\ on\ the\ rail$ *(1/40 in case of AALRTS)*

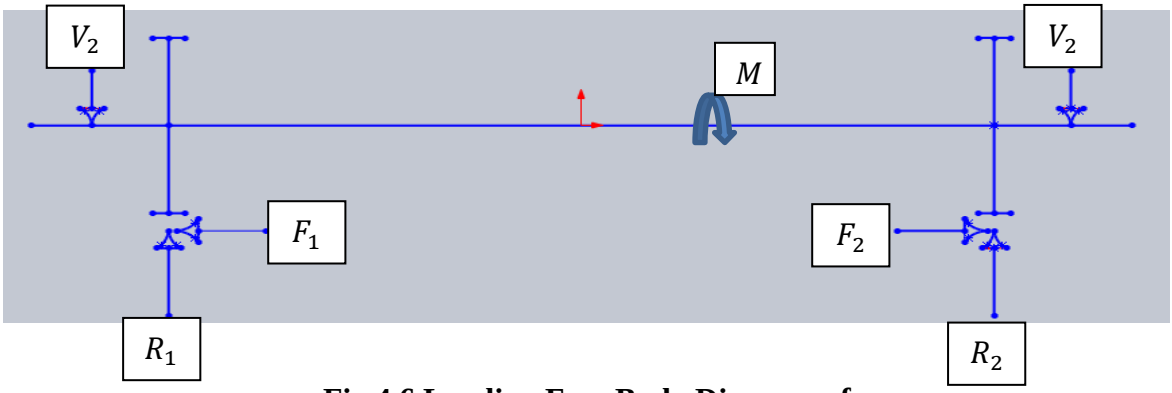

Fig 4.6 Loading Free Body Diagram of

4.1.2 Stress on the wheel

Hertz Contact Theory for the Wheel and Rail [16]

Since Heinrich Hertz published his contact theory in 1882, it has been extensively applied in many engineering fields which deal with contact problems. When a wheel and a rail are brought into contact under the action of the static wheel load, the contact area and the pressure distribution are usually determined using the Hertz theory Motion in the rolling direction.

Here we use two and three dimensional in the sense that the contacting bodies are two and three dimensional. Hertz solution can be used to predict the shape and size of the contact area and the normal pressure carried by its. In Hertz contact theory, no plastic deformation in the contact patch is assumed, and the radii of the curvature of wheel and rail profiles in the contact patch are assumed to be constant. According to Hertz theory, the normal pressure is distributed as an ellipsoid over the elliptic contact area.

The general conditions considered during the wheel/rail contact simulation are the assumption of the Hertz contact theory. As explained in the previous the common Hertz assumptions are:

- The strains are small and within elastic limit
- The surfaces are continuous and non-conforming
- The area of contact is much smaller than characteristic dimensions of the contacting bodies.
- Each body can be considered as elastic half space

Analysis of Load Distribution and Contact Area

Based on the above assumptions, Hertz proposed the solution for the determination of contact area and pressure distribution between two bodies in contact. Setting out from two bodies which come in contact with each other, the origin is set as the point where the first contact occurs. If both bodies are approximated by quadratic functions close to the origin and brought into contact, then the contact area is elliptical. In the case of a railway, the four main curvatures can be considered to be in perpendicular planes. Their directions correspond to the main axes of the frame: *O-xy.*

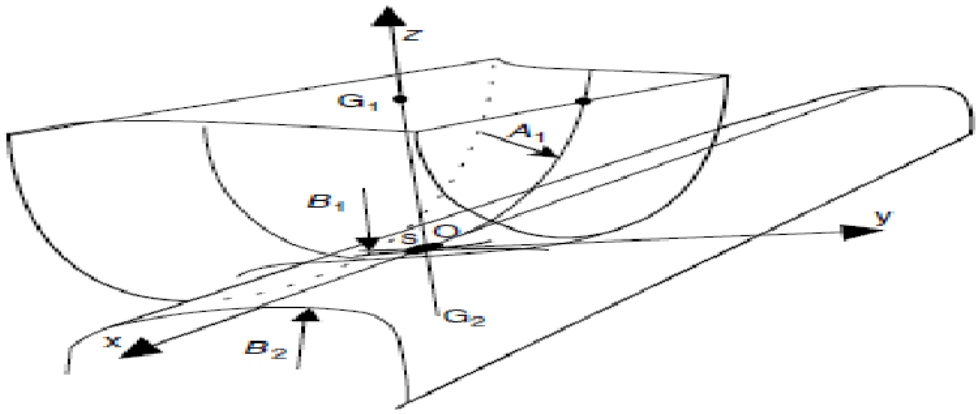

Fig 4.1 Hertz contact between wheel and rail

In the 3D railway case, the above-mentioned curvatures and radii will be:

Wheel: $\frac{d^2Z_1}{dx^2} = 2A_1 = \frac{1}{R_{1w}}$ (Eq. 4.6)

Wheel: $\frac{d^2Z_1}{dy^2} = 2B_1 = \frac{1}{R_{2w}}$ (Eq. 4.7)

Rail: $\frac{d^2Z_2}{dx^2} = 2B_2 = \frac{1}{R_{2w}}$ (Eq. 4.8)

Where $R_{1w}$the longitudinal radius of the wheel at the contact point is,$R_{2w}$is the transversal radius of the wheel profile and R_{2r} is the transversal radius of the rail profile. In the railway case, the curvature A_2 is generally neglected as the rail principal rolling radius $R_{1r}$is ∞. Before being loaded, the vertical relative distance d (x, y) between the two bodies can be written as:

$Z_1 + Z_2 = d\ (x, y) = Ax^2 + By^2$ (Eq. 4.9)

$A = \frac{1}{2r_n}\&B = \frac{1}{2}\left(\frac{1}{R_{wx}} + \frac{1}{R_{rx}}\right)$ (Eq. 4.10)

A and B are principal curvature of the two bodies and strictly positive.

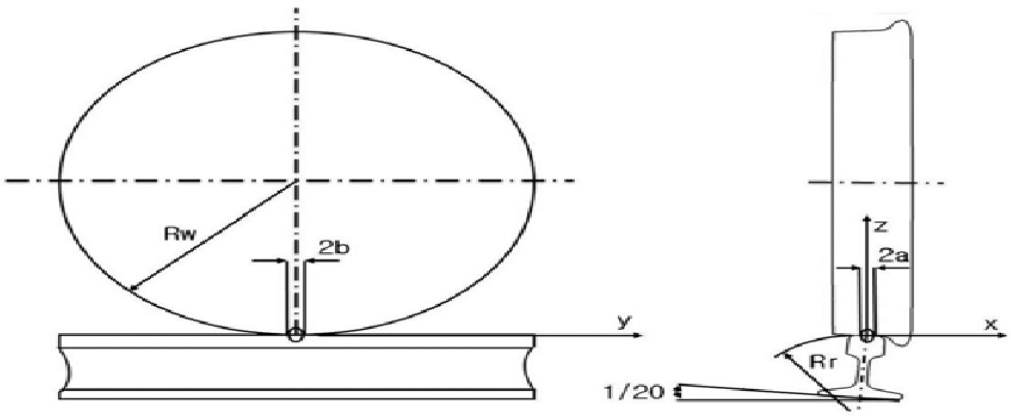

Fig 4.2 Wheel rail contact area

If two elastic nonconforming bodies contact together then according to the Hertz contact theory, the contact area is elliptical in shape with a major semi-axis **a,** and a minor semi-axis **b** [45]. The ellipsoidal normal contact pressure distribution p(x,y) is expressed by:

$$P(x,y) = \frac{3w}{2\pi ab}\sqrt{1-\left(\frac{x}{a}\right)^2-\left(\frac{y}{b}\right)^2} \qquad \text{(Eq. 4.11)}$$

Where: *a* and *b* are the half width of the contact area in the longitudinal *x* and lateral *y* directions, respectively, W is the applied normal load at the contact as shown in Fig.4.1 The contact ellipse semi-axes a and b are determined as follows:

$$a = m\sqrt[3]{\frac{3\pi w(k_w+k_r)}{4(A+B)}} \qquad \text{(Eq. 4.12)}$$

$$b = n\sqrt[3]{\frac{3\pi w(k_w+k_r)}{4(A+B)}} \qquad \text{(Eq. 4.13)}$$

Where modulus and k_r are given by;

$$K_w = \frac{1-{v_w}^2}{\pi E_w} = \frac{1-0.3^2}{\pi * 207 * 10^9} = 1.4 * 10^{-12}\,\frac{m^2}{N}$$

$$K_r = \frac{1-{v_r}^2}{\pi E_r} = \frac{1-0.3^2}{\pi * 207 * 10^9} = 1.4 * 10^{-12}\,\frac{m^2}{N}$$

m and n are Hertz coefficients and they are given as a function of the angle θ $(0^\circ - 180^\circ)$

$$\theta = \cos^{-1}\left(\frac{A-B}{A+B}\right)$$

Then the modulus $(A + B)$ and $(A - B)$ are given by

$$A + B = \frac{1}{2}\left(\frac{1}{R_{1w}} + \frac{1}{R_{2w}} + \frac{1}{R_{1r}} + \frac{1}{R_{2r}}\right) \qquad \text{(Eq. 4.13)}$$

$$A - B = \frac{1}{2}\left(\sqrt{\left(\frac{1}{R_1^w} - \frac{1}{R_2^w}\right)^2 + \left(\frac{1}{R_1^r} - \frac{1}{R_2^r}\right)^2 + 2\left(\frac{1}{R_1^w} - \frac{1}{R_2^w}\right)\left(\frac{1}{R_1^r} - \frac{1}{R_2^r}\right)cos2\varphi}\right) \qquad \text{(Eq. 4.14)}$$

Where:

- R_{w1} And R_{r1} are the wheel nominal rolling radius and the rail lateral section curve radius, respectively.
- E_w and E_r are the Young's moduli of the wheel and rail materials
- v_w and v_r are the Poisson's ratios of the wheel and rail materials, respectively.
- The angle of φ is between the radius of the wheel and rail and θ is the angle between the principal axes.(For the wheel and rail $\varphi = \frac{\pi}{2}$)

After substituting value from table 3.8 on eq. 4.13 & eq. 4.14, the modulus $(A + B)$ and $(A - B)$ will be

$$A + B = \frac{1}{2}\left(\frac{1}{330\,mm} + \frac{1}{\infty} + \frac{1}{\infty} + \frac{1}{300\,mm}\right) = \frac{0.00318}{mm} = 3.18/m$$

$$A - B = \frac{1}{2}\left(\sqrt{\left(\frac{1}{330} - \frac{1}{\infty}\right)^2 + \left(\frac{1}{\infty} - \frac{1}{300}\right)^2 + 2\left(\frac{1}{330} - \frac{1}{\infty}\right)\left(\frac{1}{\infty} - \frac{1}{300}\right)cos2(90^\circ)}\right) = 0.000314/mm$$

Therefore, angle between the principal axes θwill be

$$\theta = \cos^{-1}\left(\frac{0.000314}{0.00318}\right) = 80.41^\circ$$

By using the following table (the Hertz coefficient) and linear interpolation method the value of m and n for the chosen wheel can be easily obtained.

Table 4.1 Hertz coefficients

θ(deg)	M	N	θ(deg)	m	n	θ(deg)	m	N
0.5	61.4	0.1018	10	6.604	0.3112	60	1.486	0.717
1	36.86	0.1314	20	3.813	0.4125	65	1.378	0.759
1.5	27.48	0.1522	30	2.731	0.493	70	1.284	0.802
2	22.26	0.1691	35	2.397	0.530	75	1.202	0.846
3	16.5	0.1964	40	2.136	0.567	80	1.128	0.893
4	13.31	0.2188	45	1.926	0.604	85	1.061	0.944
6	9.79	0.2552	50	1.754	0.641	90	1.0	1.0
8	7.86	0.285	55	1.611	0.678			

By interpolation method, we can calculate m and n

$$\theta_1 = 85^\circ, m_1 = 1.061, n_1 = 0.944, \theta_2 = 90^\circ, m_2 = 1.0, n_2 = 1.0$$

$$m = m_1 + \frac{m_2 - m_1}{\theta_2 - \theta_1}(\theta - \theta_1)$$

$$m = 1.061 + \frac{1.0 - 1.061}{90^\circ - 85^\circ}(80.41^\circ - 85^\circ) = 1.1169$$

$$n = n_1 + \frac{n_2 - n_1}{\theta_2 - \theta_1}(\theta - \theta_1)$$

$$n = 0.944 + \frac{1.0 - 0.944}{90^\circ - 85^\circ}(80.41^\circ - 85^\circ) = 0.8926$$

After that the contact ellipse semi-axes a and b are determined as follows for different loading cases:

a. Case I

$$a = m\sqrt[3]{\frac{3\pi w(k_w + k_r)}{4(A+B)}}$$

$$a = 1.1169 * \sqrt[3]{\frac{3 * \pi * 39280.87\ N * (1.4 * 10^{-12} + 1.4 * 10^{-12})\ {}^{m^2}/_{N}}{4 * (3.18/m)}} = 0.0048\ m$$

$$b = 0.8926 * \sqrt[3]{\frac{3\pi w(k_w + k_r)}{4(A+B)}}$$

$$b = 0.8926 * \sqrt[3]{\frac{3 * \pi * 39280.87\ * (1.4 * 10^{-12} + 1.4 * 10^{-12})}{4 * \left(\frac{3.18}{m}\right)}} = 0.0038\ m$$

According to Hertz theory contact pressure, P_0 (Hertz stress) occur will be

$$P = P_0 = \frac{3w}{2\pi ab}$$

$$P = P_0 = \frac{3 * 39280.87}{2\pi * 0.0048 * 0.0038} = 1028.24\ MPa$$

Shear force and Stress on Wheel

$$\tau \cong \frac{1}{3} P_{Max} = 342.74\ Mpa$$

b. Case II

$$a = m\sqrt[3]{\frac{3\pi w(k_w + k_r)}{4(A+B)}} = 0.0053\ m$$

$$b = 0.8926 * \sqrt[3]{\frac{3\pi w(k_w + k_r)}{4(A+B)}} = 0.0042\ m$$

According to Hertz theory maximum contact pressure, P_0 (Hertz stress) will be

$$P = P_0 = \frac{3w}{2\pi ab} = \frac{3 * 51571.36}{2\pi * 0.0053 * 0.0042} = 1106.17\ MPa$$

Maximum Shear force and Stress on Wheel

$$\tau = \frac{1}{3} P_{Max} = 368.72 Mpa$$

c. Case III

$$a = m\sqrt[3]{\frac{3\pi w(k_w + k_r)}{4(A+B)}} = 0.00549\ m$$

$$b = 0.8926 * \sqrt[3]{\frac{3\pi w(k_w + k_r)}{4(A+B)}} = 0.0043\ m$$

According to Hertz theory maximum contact pressure, P_0 (Hertz stress) will be

$$P = P_0 = \frac{3w}{2\pi ab} = \frac{3 * 57307.88}{2\pi * 0.0054 * 0.0043} = 1178.4\ MPa$$

Maximum Shear force and Stress on Wheel

$$\tau = \frac{1}{3}P_{Max} = 392.8\ Mpa$$

4.2 Finite Element Analysis

The finite element analysis (FEA) is a computing technique that is used to obtain approximate solutions to boundary value problems. It uses a numerical method called finite element method (FEM). FEA involves the computer model of a design that is loaded and analyzed for specific results, such as stress, deformation, deflection, fatigue tool, mode shapes, temperature distributions, and so on. The wheel set of AALRT train was modeled using solid work and was imported for further FEM analysis to ANSYS work bench 15.0. The simulation is carried out using 3D model in static structural analysis and for fatigue analysis the researcher uses stress based analysis with Goodman's failure criteria.

4.2.1 Modeling

Based on the specifications and collected data from AALRT 2D drawing of the wheel and the axle is done using solid work 2013 software. After that the 2D drawing of the wheel set translated to 3D modeling and assembled using assembly module on the solid work Software.

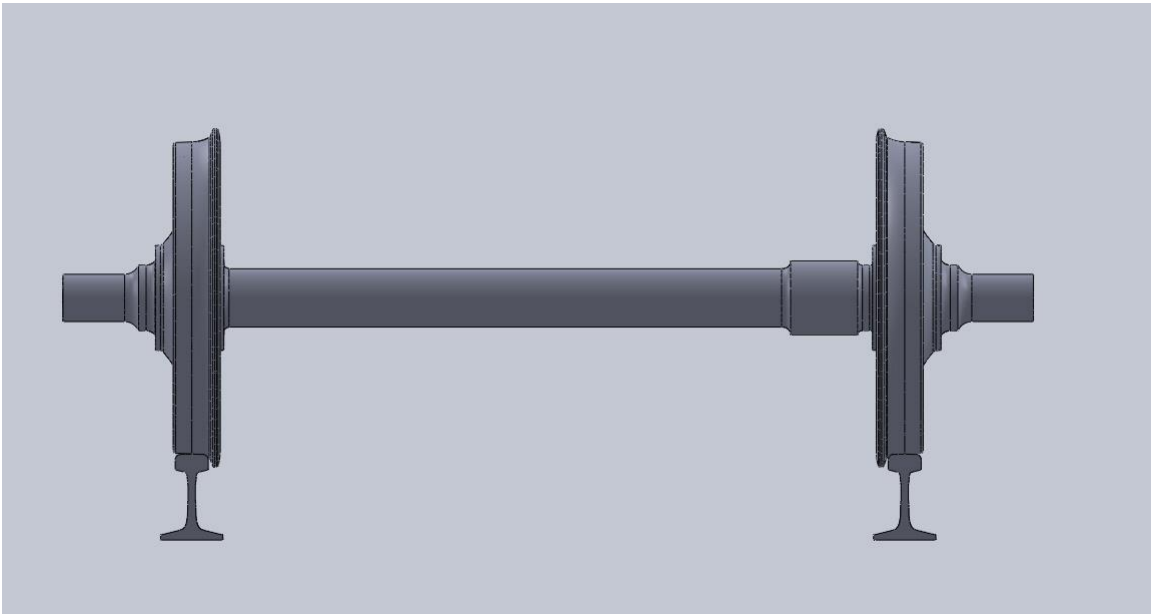

Fig 4.3 wheel set assembly

4.2.2 Material selection

Material data are defined, modified, and used in Workbench Simulation for structural analyses using Engineering Data Module. Material properties include Young's modulus, ultimate strength, yielding strength, Poisson's ratio and density of the axle and the wheel are filled based on the specifications.

4.2.3 Geometry

Geometry module opens the Design Modeler application, which can be used to import CAD models from other software like Solidwork or to sketch a new 2D or 3D geometry. For this research the wheel set of AALRT rail car was modeled using solid work and was imported for further FEM analysis to ANSYS work bench 15.0.

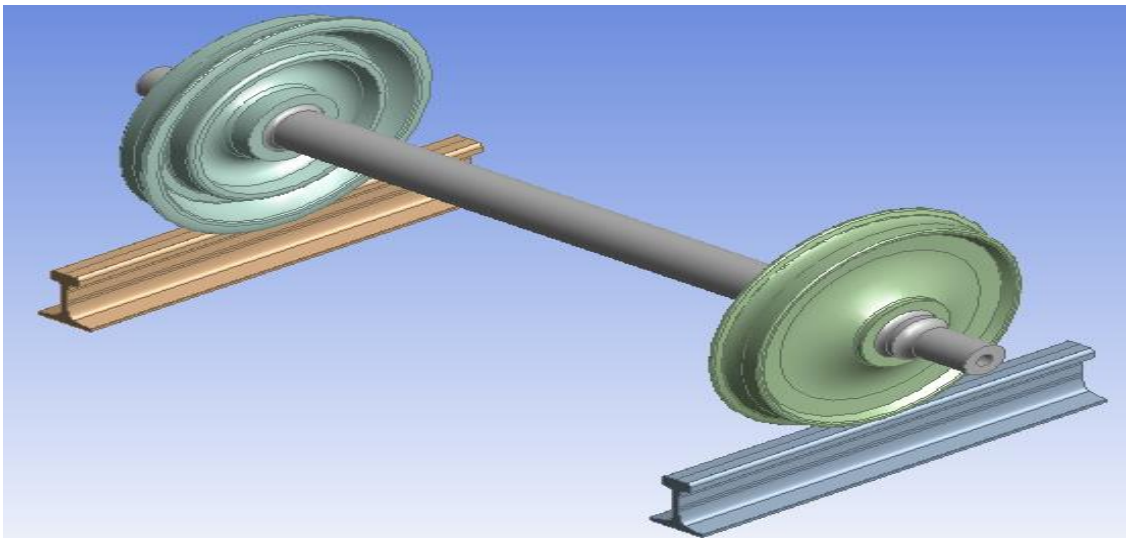

Fig 4.4 Imported Geometry

4.2.4 Meshing

In the finite element analysis, the basic concept is to analyze the structure, which is an assemblage of discrete pieces called element, which are connected together at a finite number of point called nodes. A network of these elements is known as a mesh. Mesh is discretizing the solid object to finest parts to perform the analysis to get the precise value at each and every element of the meshed object.

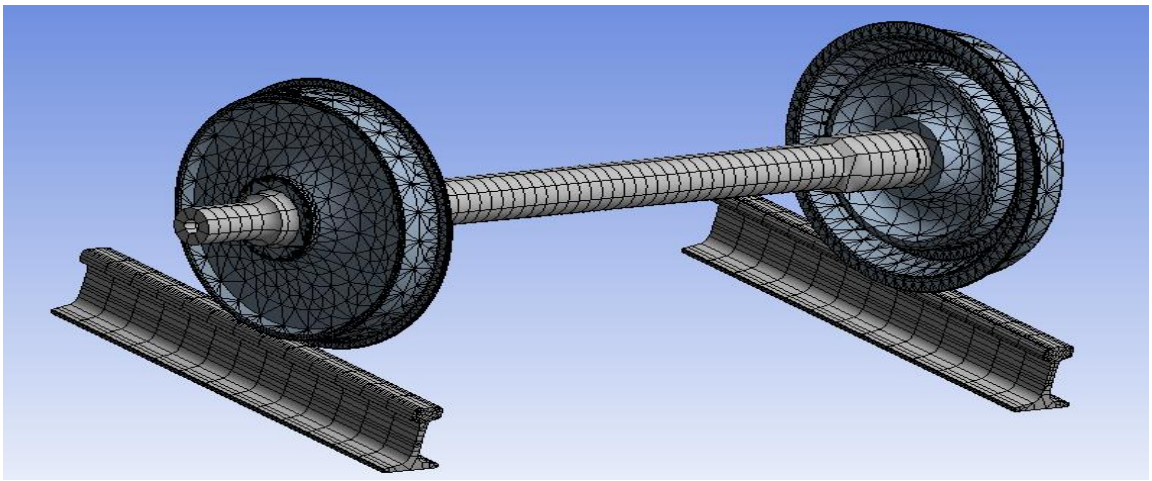

Fig 4.5 Meshing

The wheelset model including the rail considered in this thesis consists of 41314 numbers of elements and 87269 numbers of nodes. The size of the meshing type in this research can be categorized as a coarse size mesh.

For this fatigue life analysis in order to reduce the computation time and computer memory requirement we are going to use the wheel set model excluding the rail part and the researcher doesn't use mesh optimization on different parts.

Below here the researcher tries to see the effect of different meshing types (Fine, medium and Coarse) for a typical loading and traction condition of the wheelset (excluding the rail) on von mises stress result.

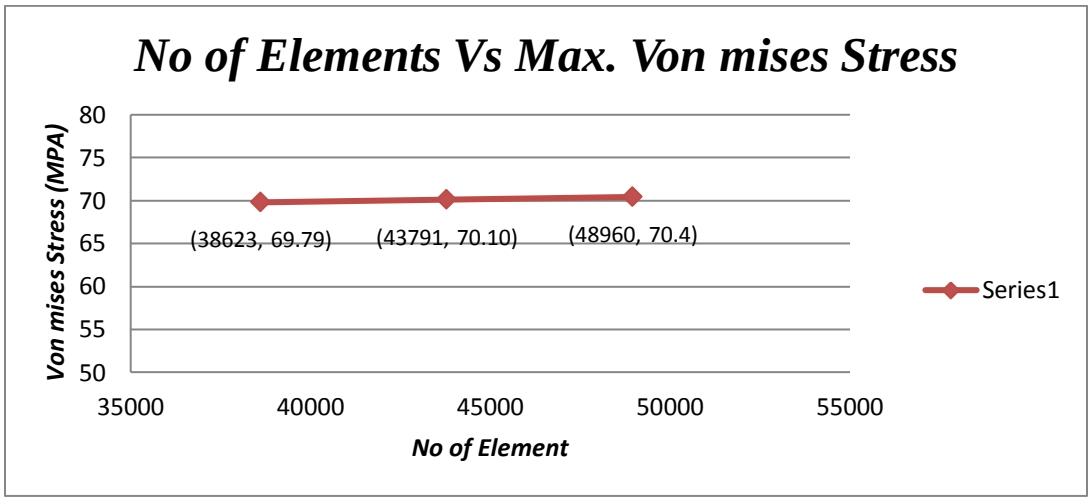

Fig 4.6 Number of element Vs. Von mises Stress

4.2.5 Loadings

On Ansys work bench after material selection, geometry and meshing loadings and boundary conditions must be defined based on the actual environment of the system. On static structural module there are four types of loadings but for this research we use only inertial loads like acceleration, rotational velocity, gravity and structural load acts on a part or a system

These loadings are applied based on physical characters and real conditions of the AALRT.

Rotational velocity for this research we take the maximum speed of the train as 70 km/h or 58.9 rad/sec based on the specification of AALRT Railcar and to check the effect of this travelling velocity on the fatigue life the researcher uses 14 different traction rotational

velocities with corresponding torque. This rotational velocity is defined as a component which the whole body rotates about y axis.

Acceleration another inertial load the researcher applies on the wheelset assembly is acceleration. the researcher applies the acceleration as a step process based on the collected data, during starting (1.1 m/s2), free run (0 m/s2) and retardation during coasting 1 m/s2) in x – Direction as a component load that acts on the entire model.

Standard earth gravity is also applied in negative Z direction.

Displacement also all model components are only allowed to displace in a longitudinal direction i.e. in x-axis

Structural Loads The vertical and lateral forces acted on the wheel and axle are applied based on the 3 loading conditions. To ensure to achieve the satisfactory results, some constraints should be applied at the nodes and some constrains to the all components. For the fatigue analysis since the type loadings are different (fully reversed due to bending and fluctuating due to torsion and lateral force from the rail on the wheel, we are going to use different environments for the modeling and we combine the solutions from each environment using solution combination module. The researcher takes the ambient temperature of Addis Ababa city as$25\ ℃$.

Summary of types of loads applied on the Model for FEA analysis:

- Vertical down ward bending load (V_1 & V_2) in " - Z direction"
- Upward Reaction forces from the rail on wheel rail contact (R_1 & R_2) in +Z
- Lateral force from the rail at wheel rail contact (F_1 & F_2) in "+Y & -Y Direction"
- Standard earth gravity (-Z Direction)
- Rotational velocity (all body) and Displacement (X direction)

Position and magnitude of applied loadings on the wheel set

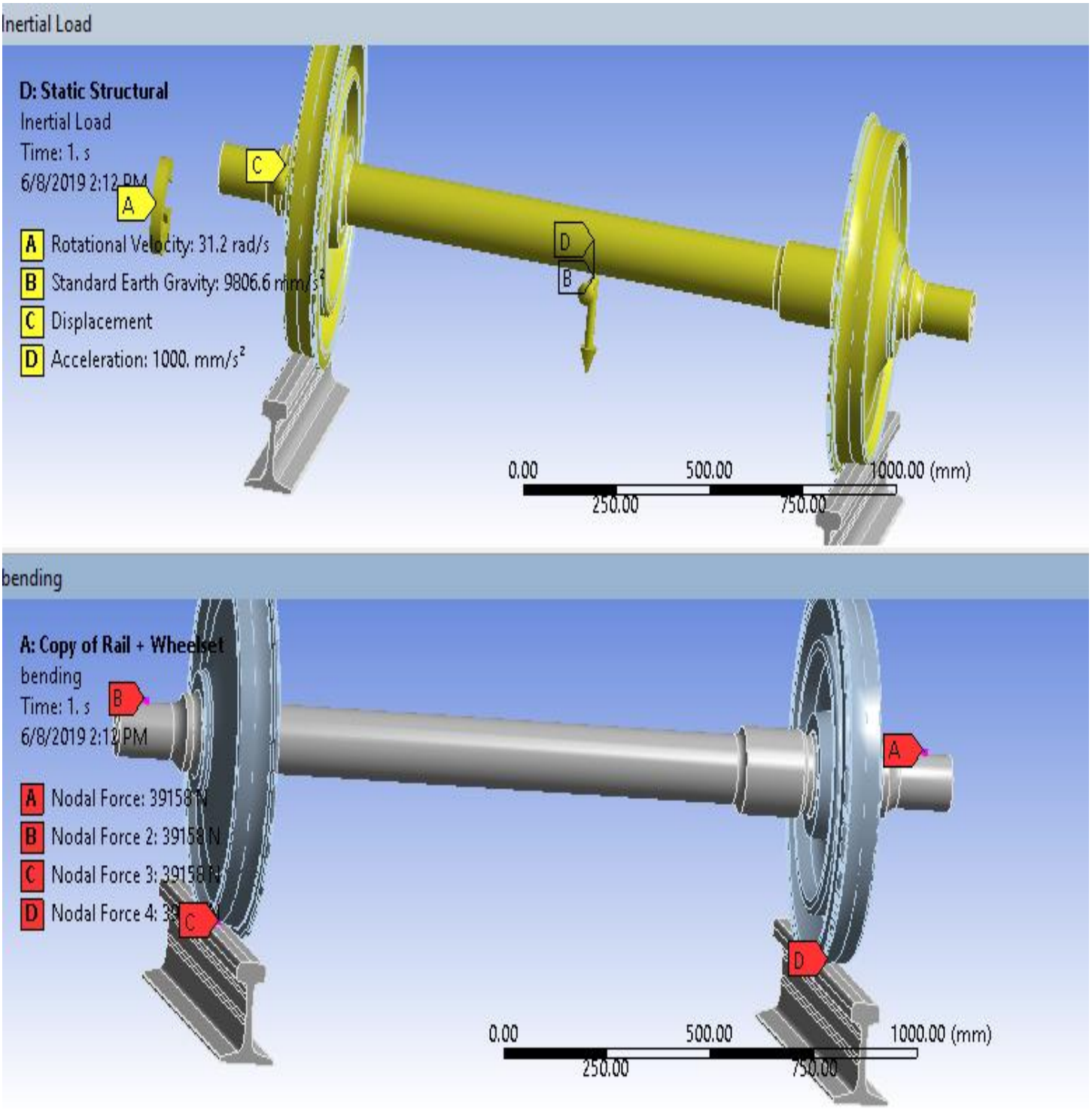

(a)

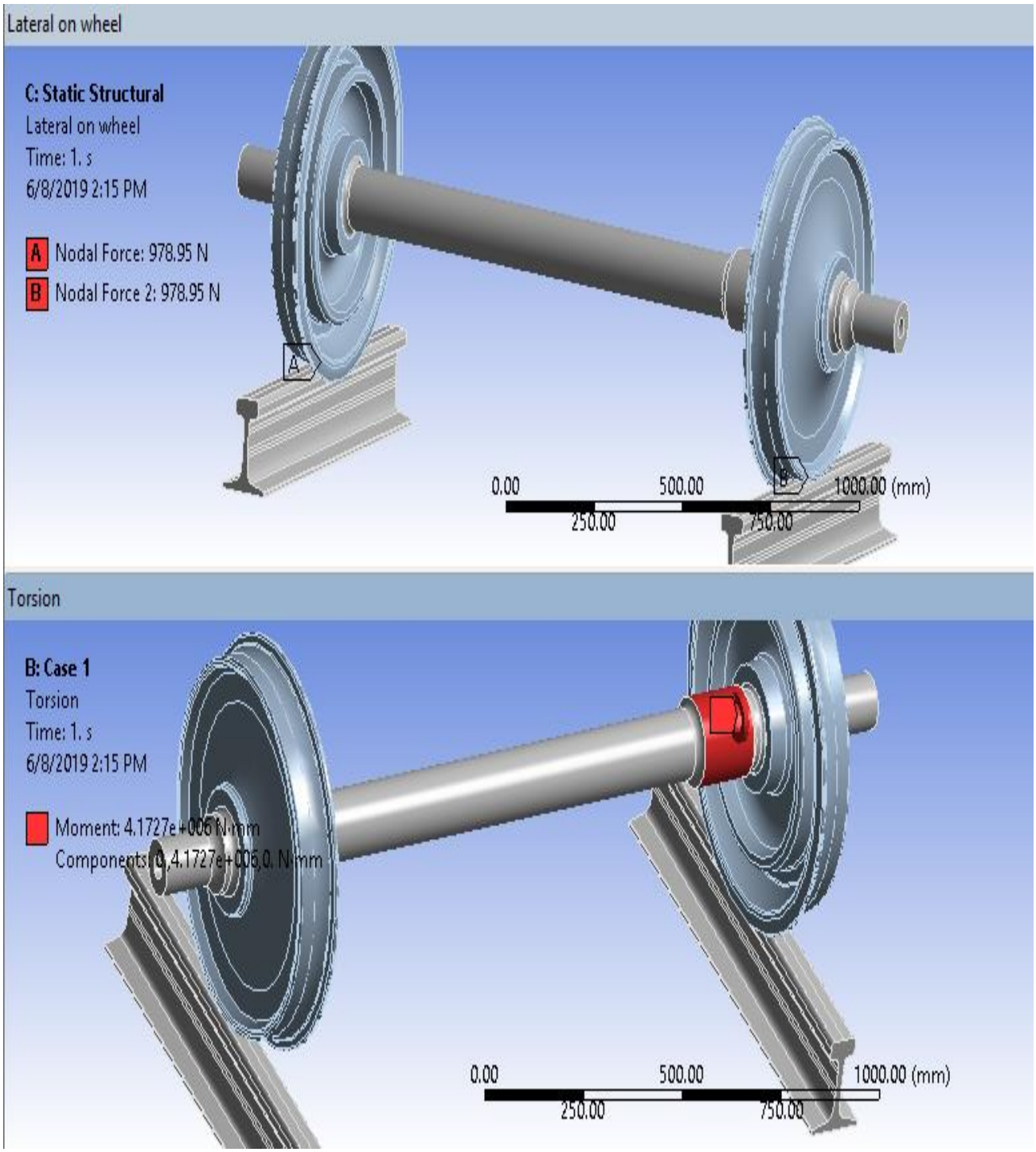

(b)

Fig 4.7 (a) and (b) boundary conditions and loading for case I

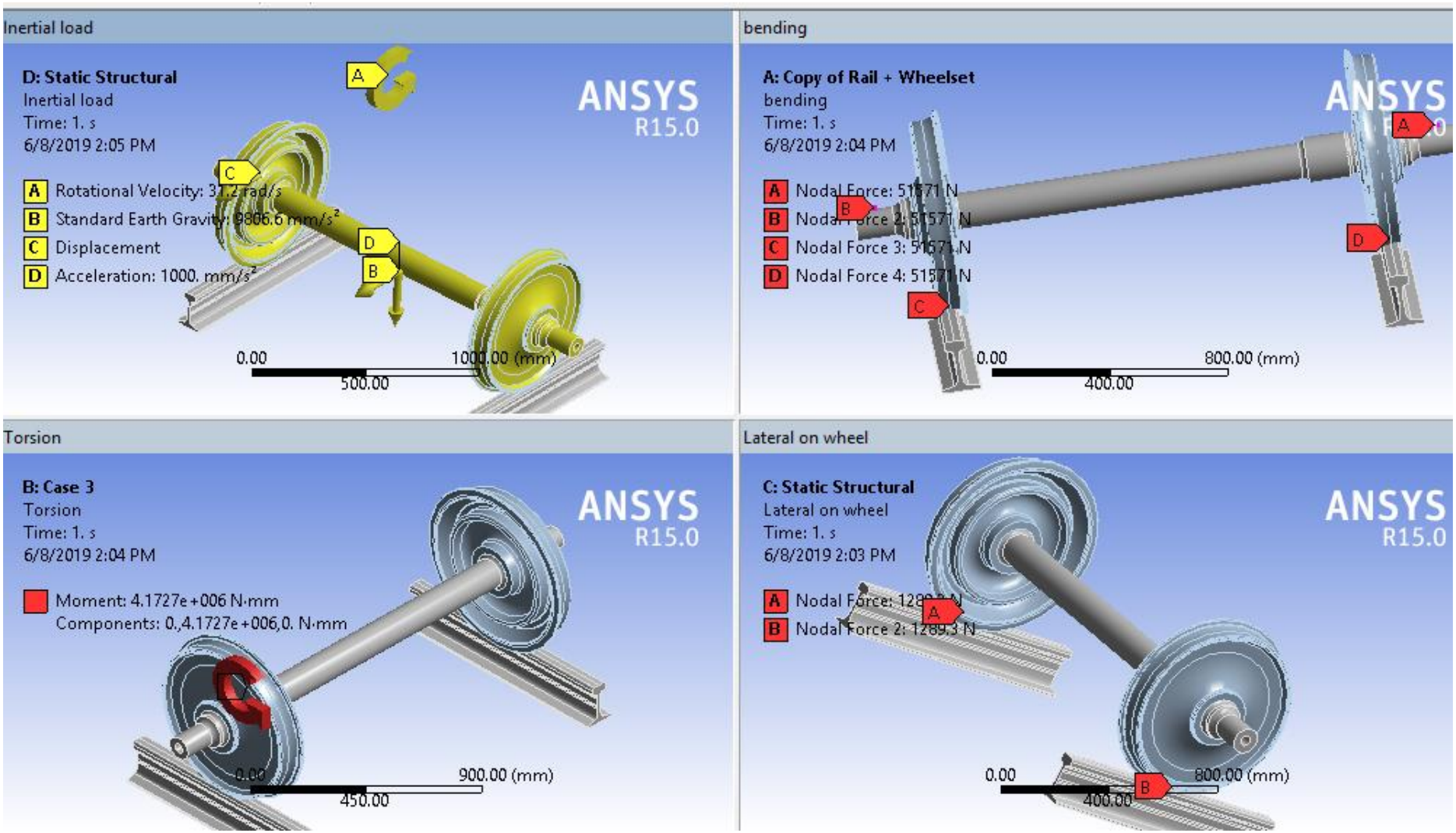

Fig 4.8 boundary conditions and loading for case II .

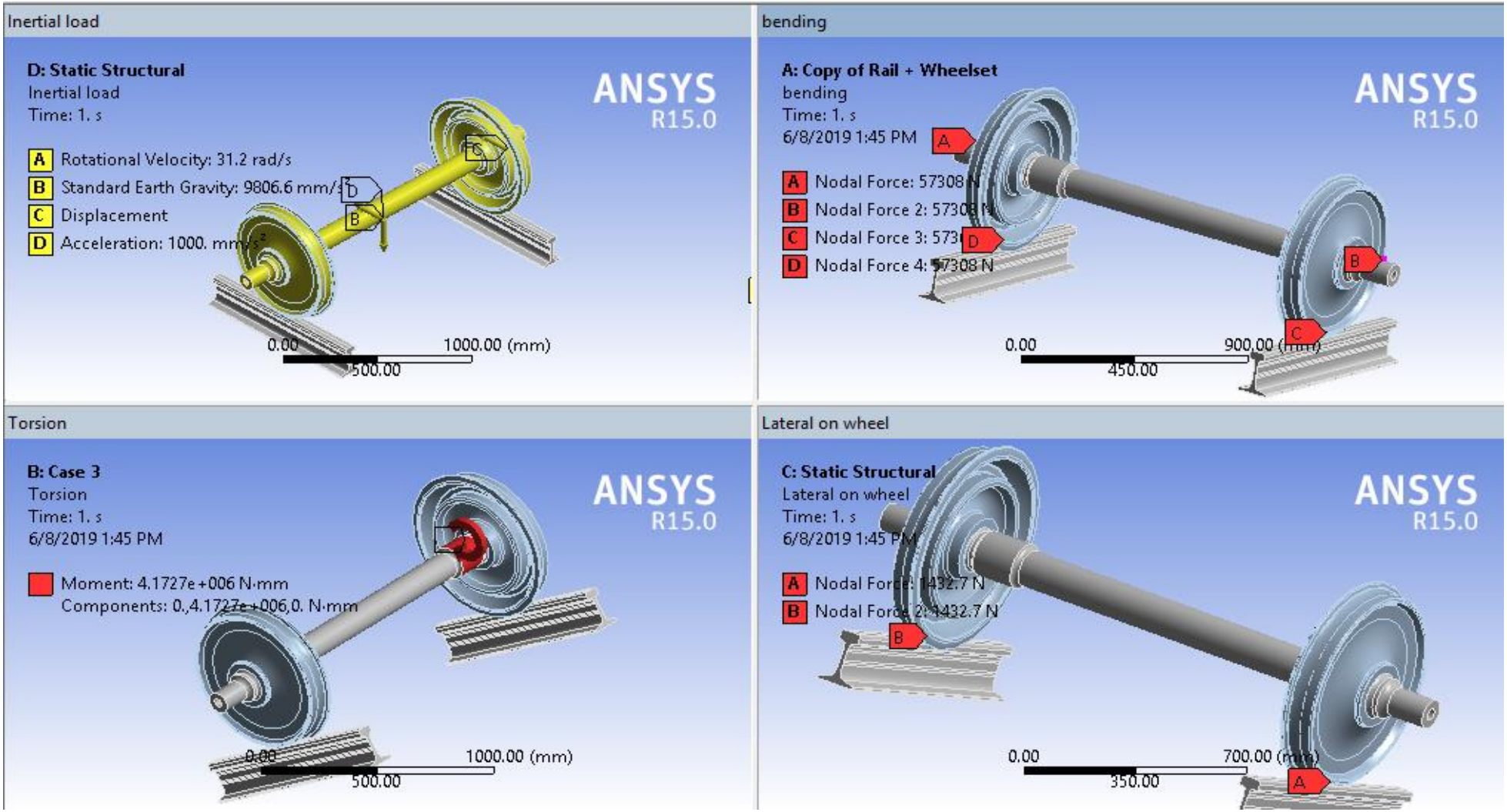

Fig 4.9 boundary conditions and loading for case III

CHAPTER 5

RESULTS AND DISCUSSIONS

Introduction

The analysis is performed by using finite element model which consist fatigue analysis. A static structural analysis is used to determine the stresses, deflection, strains, safety factor, and fatigue results of structures caused by loads and different boundary conditions.

The results obtained based on primary and the secondary data with the application of Finite Element Method analysis software under different loading and traction condition are illustrated by figures and graphs. The loading and traction conditions are taken from calculated load summary [table 4.1].

5.1 Results

5.1.1 Results of Different Loading Conditions

A. Von Mises stress

Von Mises stress is one of the results we can get from Ansys work bench. A common way to express three dimensional stresses (multi-directional stresses) build up in many directions is to summarize them into an "Equivalent" stress, also known as the "Von Mises" stress. Concept of Von mises stress arises from distortion energy failure theory. According to this theory yielding would occur when total distortion energy absorbed per unit volume due to applied loads exceeds the distortion energy absorbed per unit volume at the tensile yield point. In figure 5.1 (a) and (b) we can find results of Von mises stress for different loading conditions.

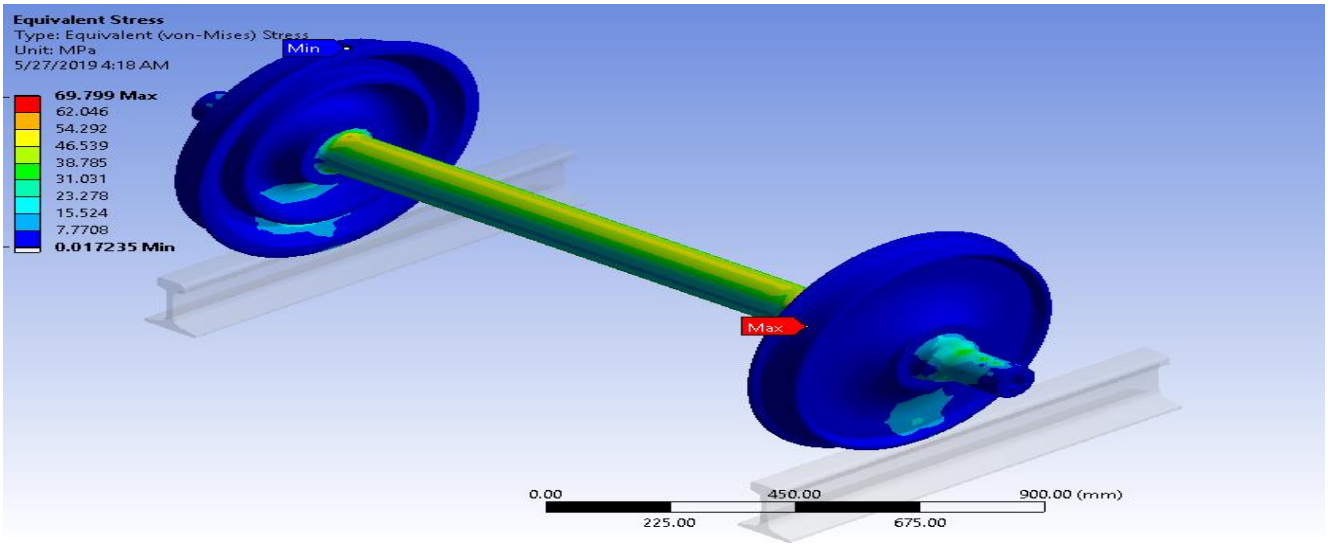

(a)

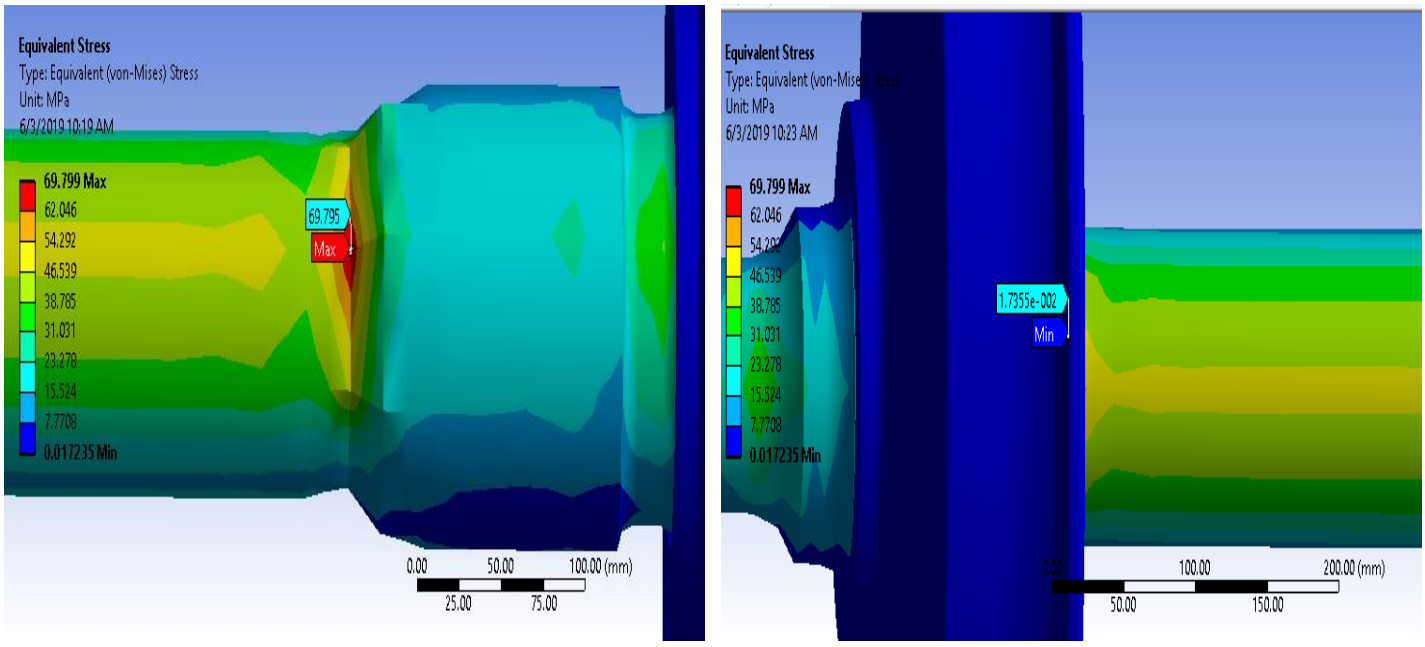

(b)

Fig 5.1 (a) and (b) maximum and minimum Von Mises stress for Loading case I

- For Case I, the first Loading condition with rated torque as shown in above figure, the maximum von miss stress is 69.79 MPa and the minimum von miss stress is 0.0172 Mpa. as we can see from the fig above the maximum Von mises stress is on the axle middle section where the wheel set is coupled with the gear box assembly, the red color shows that maximum stress develops on that area and minimum at the thread of the wheel since it doesn't subject to any type of loading.

- Also similarly for the second loading condition (51571.36 N) the maximum Von miss stress will be 90.82 MPa which increases directly with proportional to the loading of passengers by considering the rated torque and traction

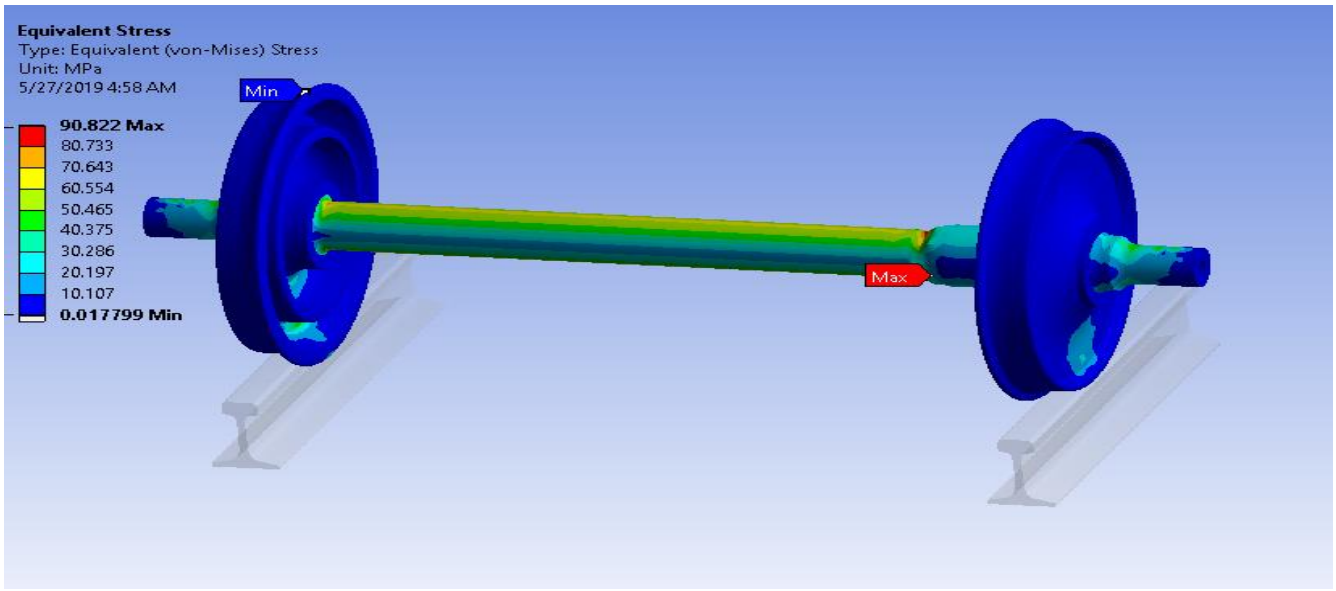

(a)

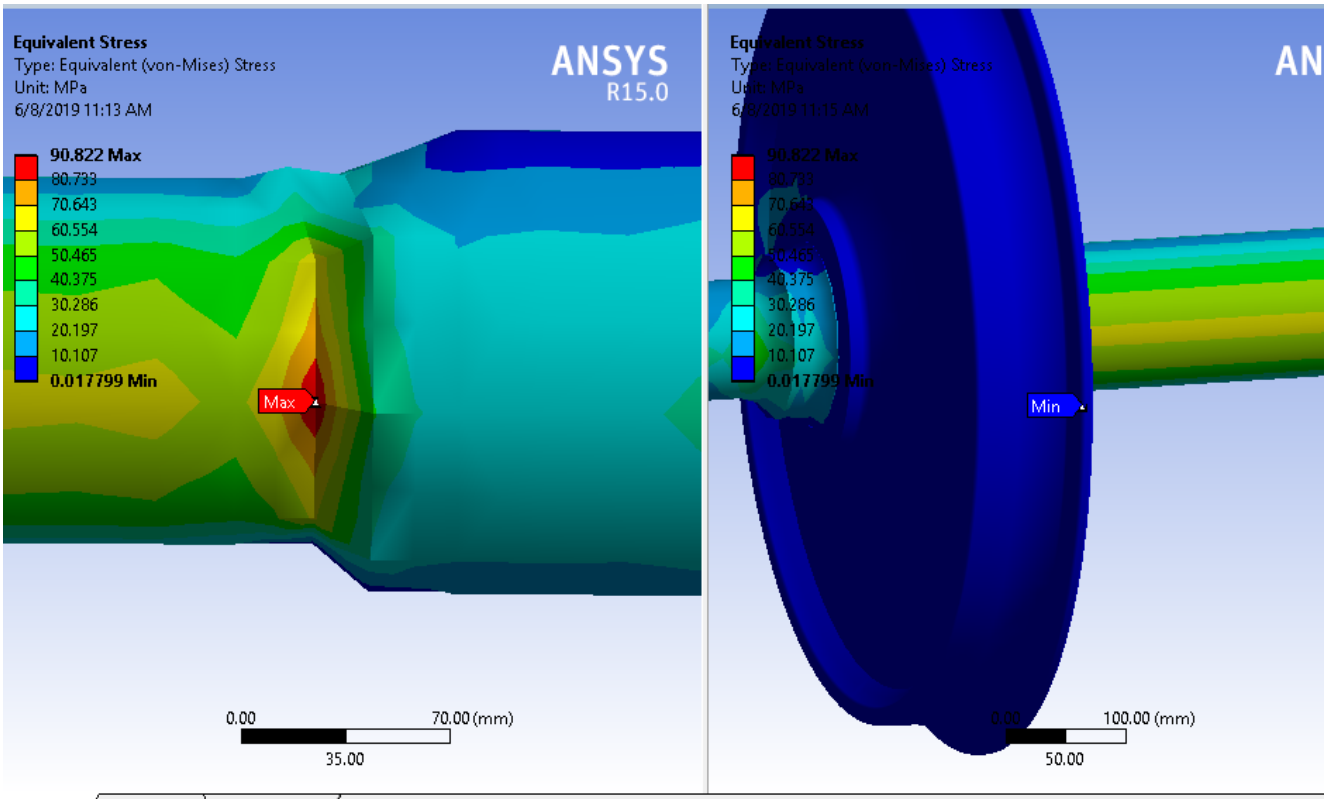

(b)

Fig 5.2 (a) and (b) Contour plot of von Mises stress for Loading case II

- Similarly, the fig 5.3 shows us the maximum and the minimum Von mises stresses Induced on the wheelset for the loading case III (57307.88 N) using the rated torque

and traction condition. The maximum Von mises stress is 100.59 MPa and the minimum will be 0.018 MPa on the axle and wheel respectively.

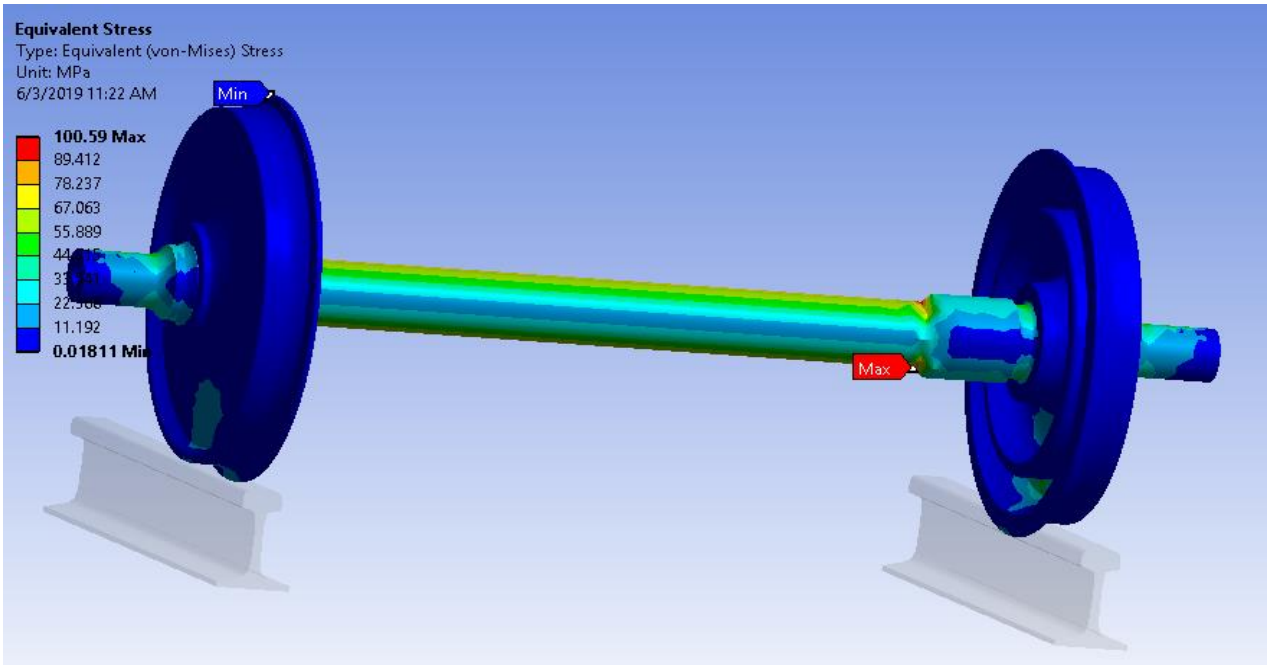

Fig 5.3 Contour plot of von Mises stress for Loading case III.

B. Maximum Principal Stress

Another theory of failure is based on maximum principal stress which states that failure in any material occurs when the principal stress in that material due to any loading exceeds the principal stress at which failure occurs in one dimensional loading test. In figure 5.4 we can find maximum principal stress of the wheel set under different loading conditions.

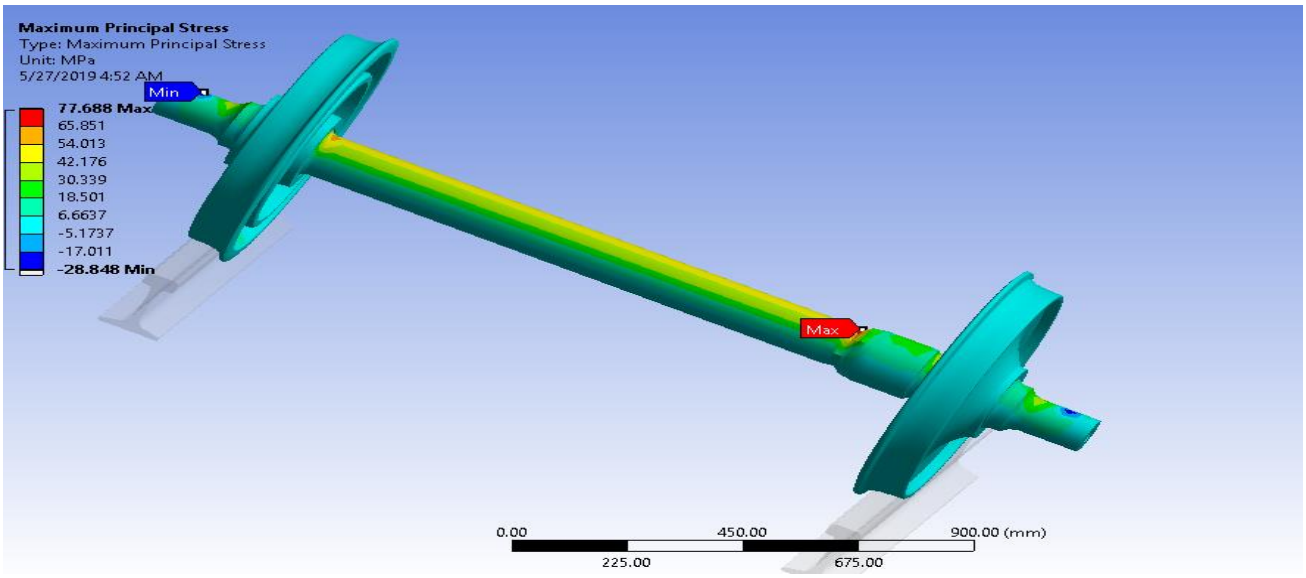

(a)

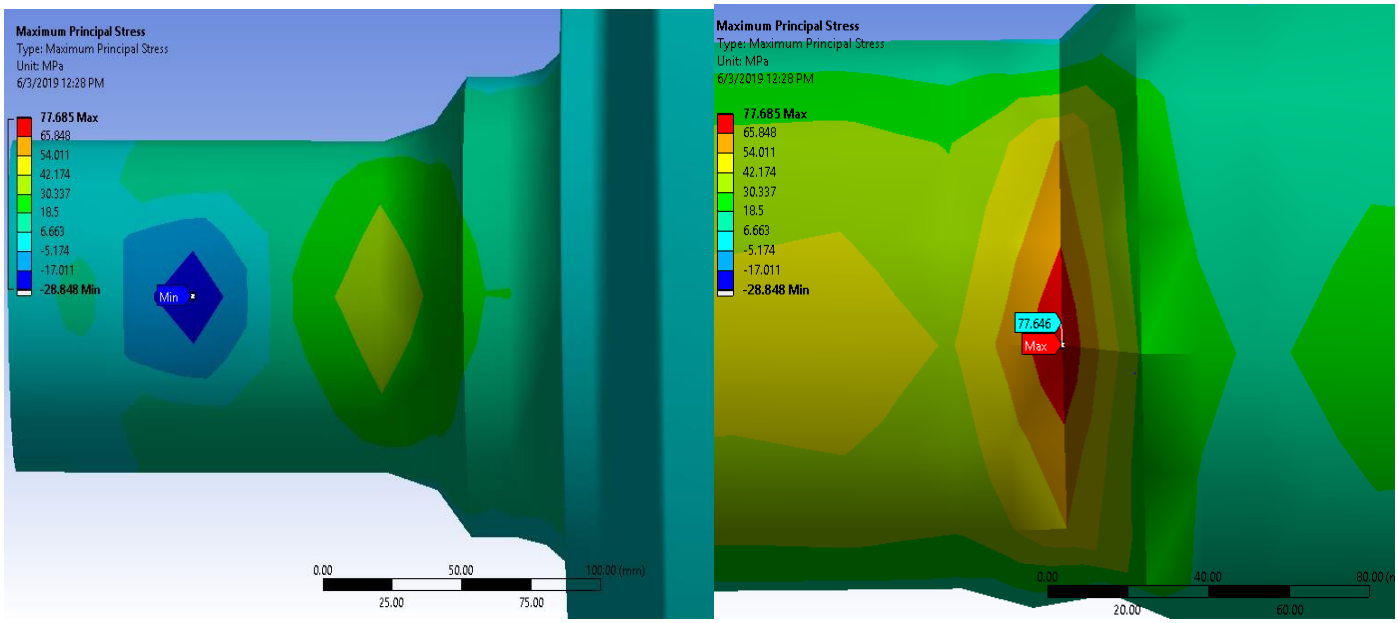

(b)

Fig 5.4 (a) and (b) Contour plot of Maximum Principal Stress for loading case I.

- From fig 5.4 we can see that the maximum principal stress for loading case I is 77.68 Mpa at the middle section of the axle where the gearbox is coupled with the wheelset

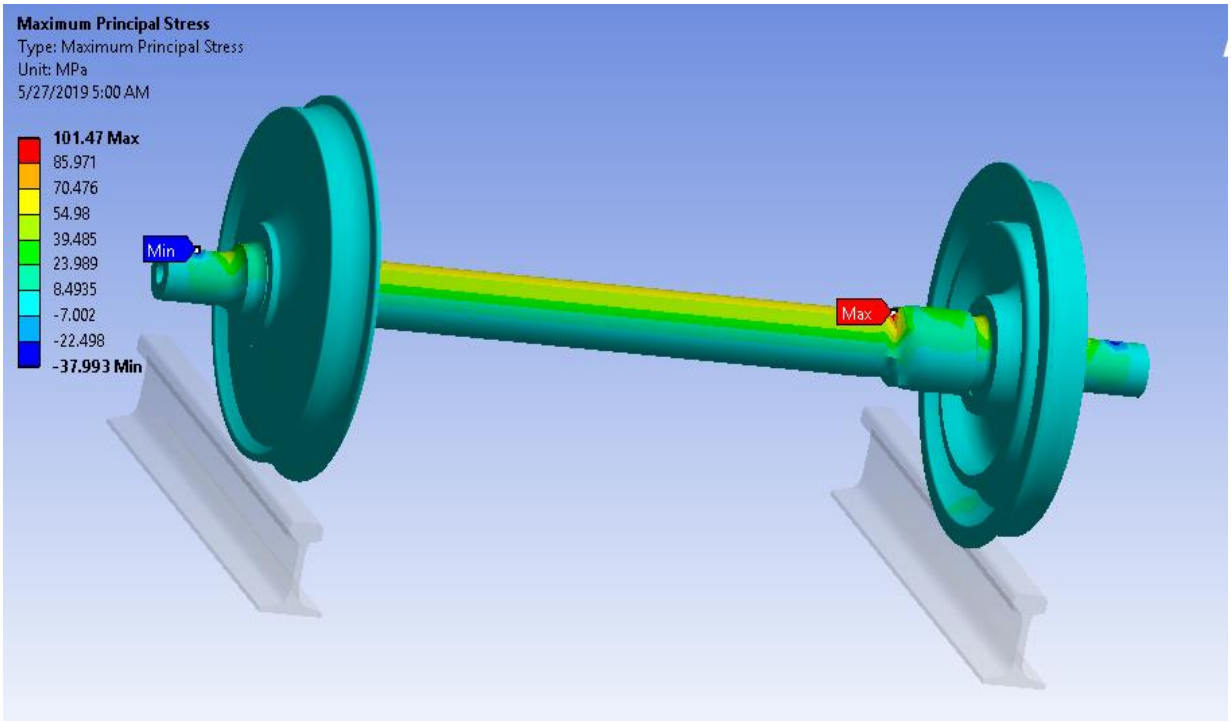

(a)

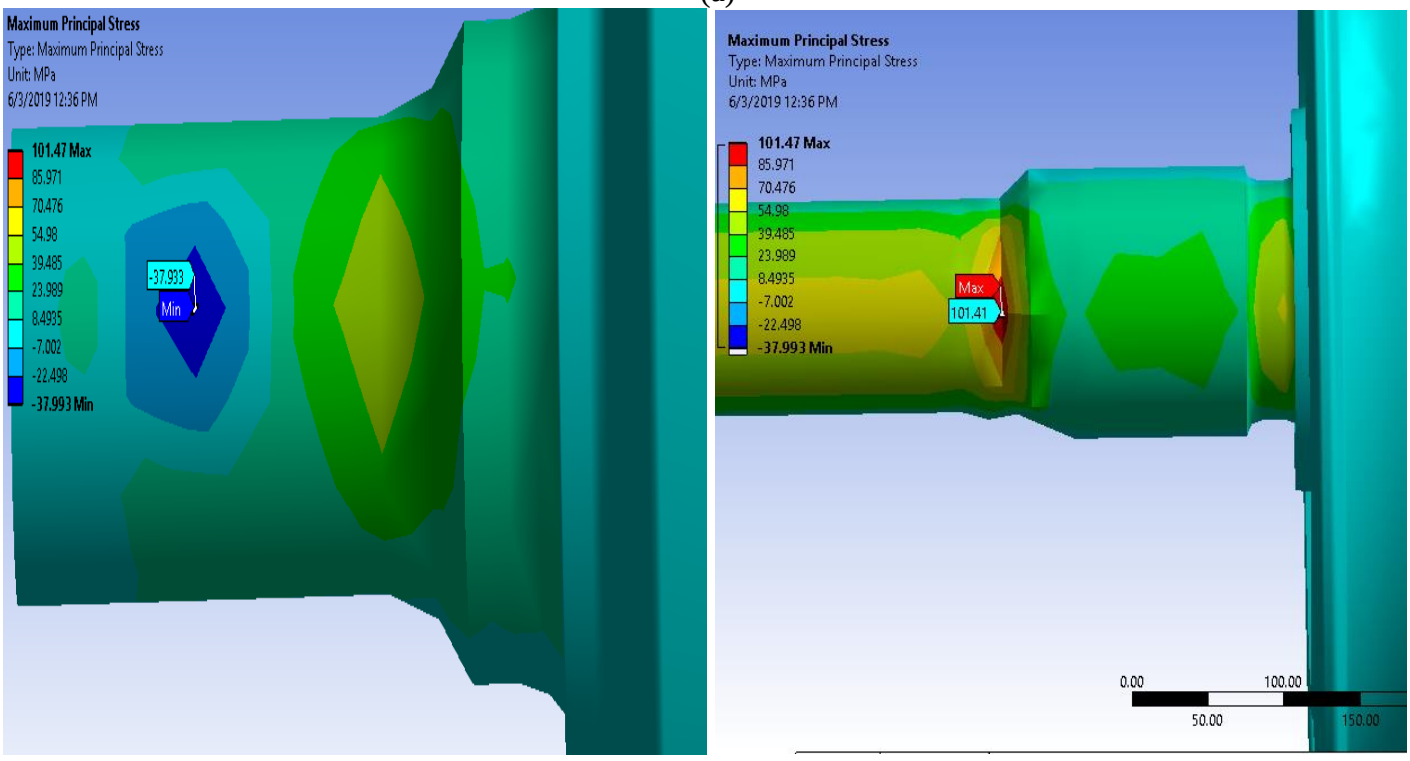

(b)

Fig 5.5 Contour plot of Maximum Principal Stress for loading case 2

- Also the maximum principal stress for loading case II will be 101.47 Mpa which increases proportionally with the passenger loading.

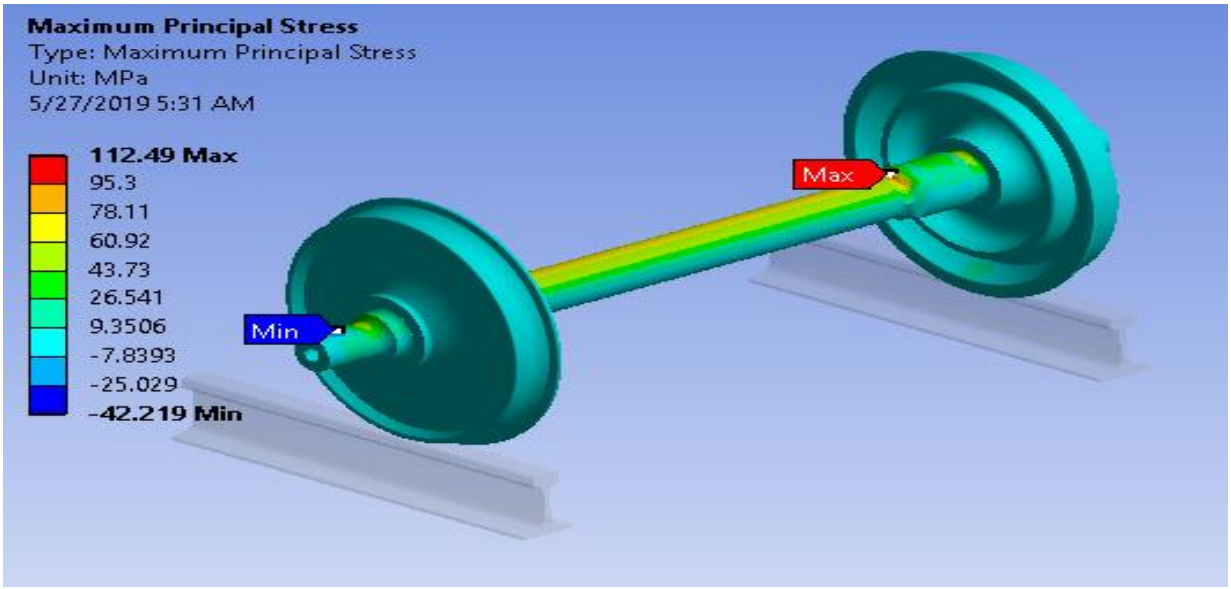

(a)

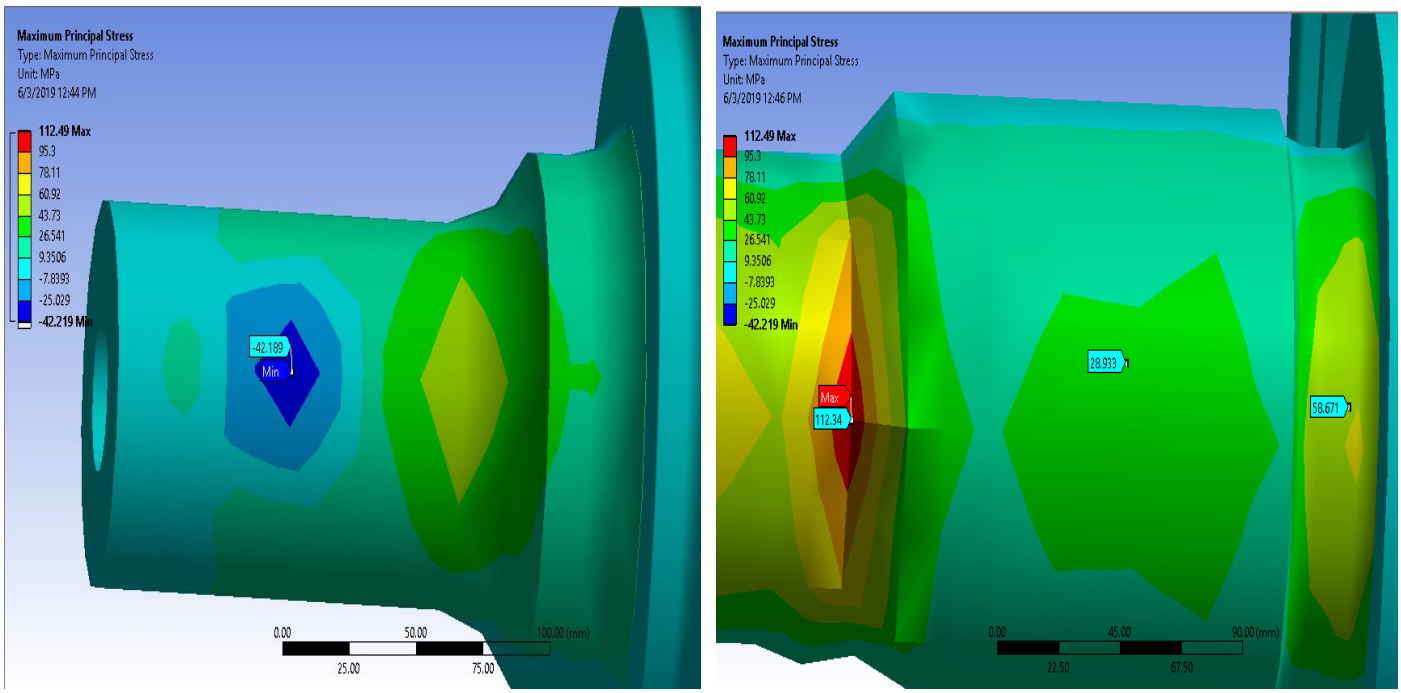

(b)

Fig 5.6 (a) and (b) Contour plot of Maximum Principal stress for loading case III

- Also for loading case III the maximum principal stress will be 112. 49 Mpa

C. Fatigue Life

This result contour plot shows the available life for the given fatigue analysis. Here are some results of fatigue life from Ansys work bench under different loading conditions

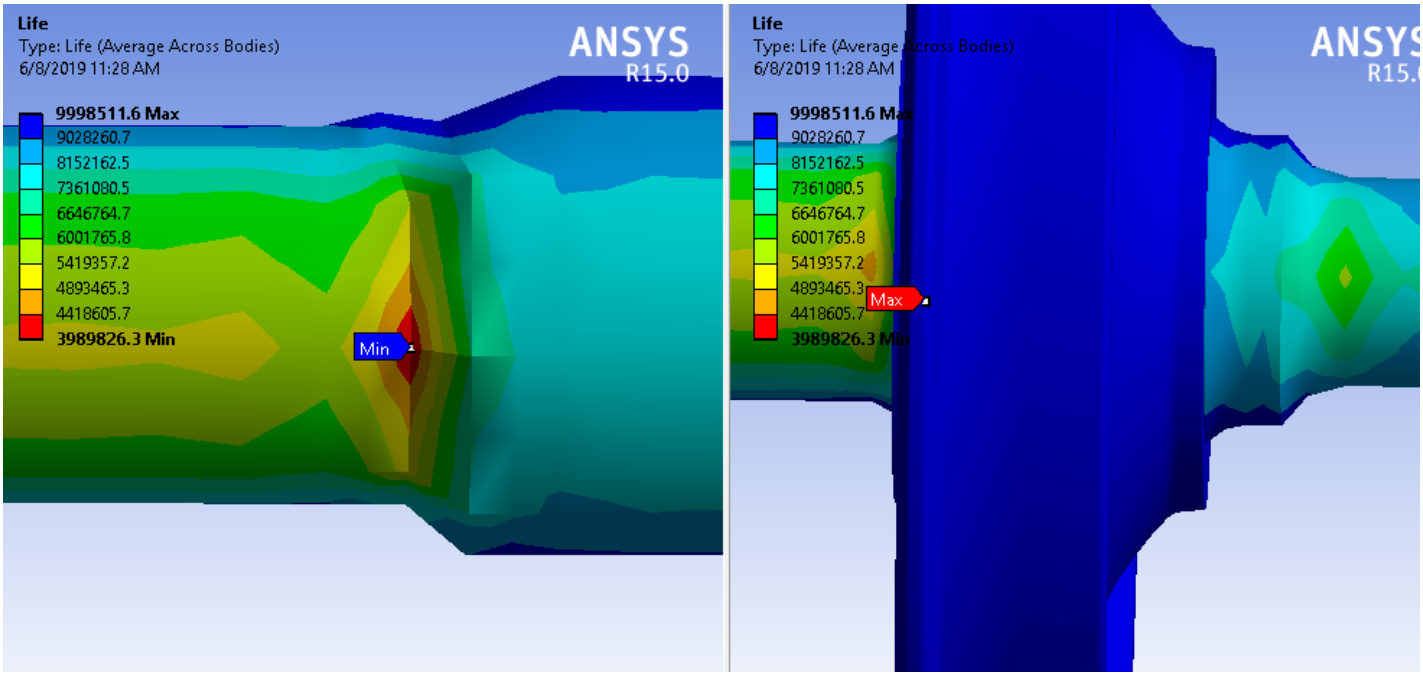

(a)

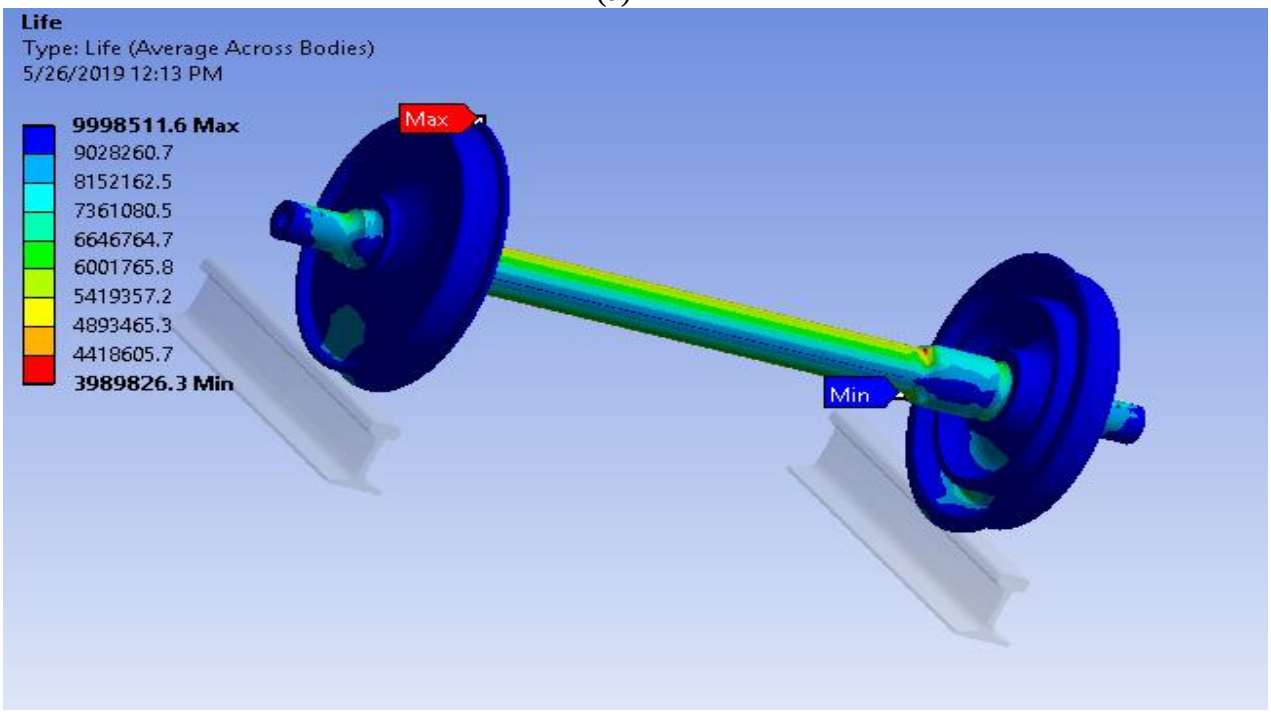

(b)

Fig 5.7 Contour plot of Fatigue Life for loading case 1.

- For case 1 loading condition fatigue life is shown in Figure 5.7. The maximum fatigue life is on the wheel and its value is 9998511.6 cycles and the minimum value is 3989826.3 on the axle cycles. This result shows us the available life for the given fatigue analysis. Since

there were some difficulties finding documents and standards of AALRT railcars expected life we compare this results to the steel family fatigue life.

- Figures 5.8 and 5.9 show us the fatigue life of the wheelset for the second and third loading condition respectively. From the result we can see that minimum fatigue life on the wheelset will be decreased inversely proportional to the loading. For case 2 it will be 2945128.5 cycles before failure which actually decreases in million from the first loading case and for the third loading condition it becomes 2548694.6 cycles also decreased in millions.

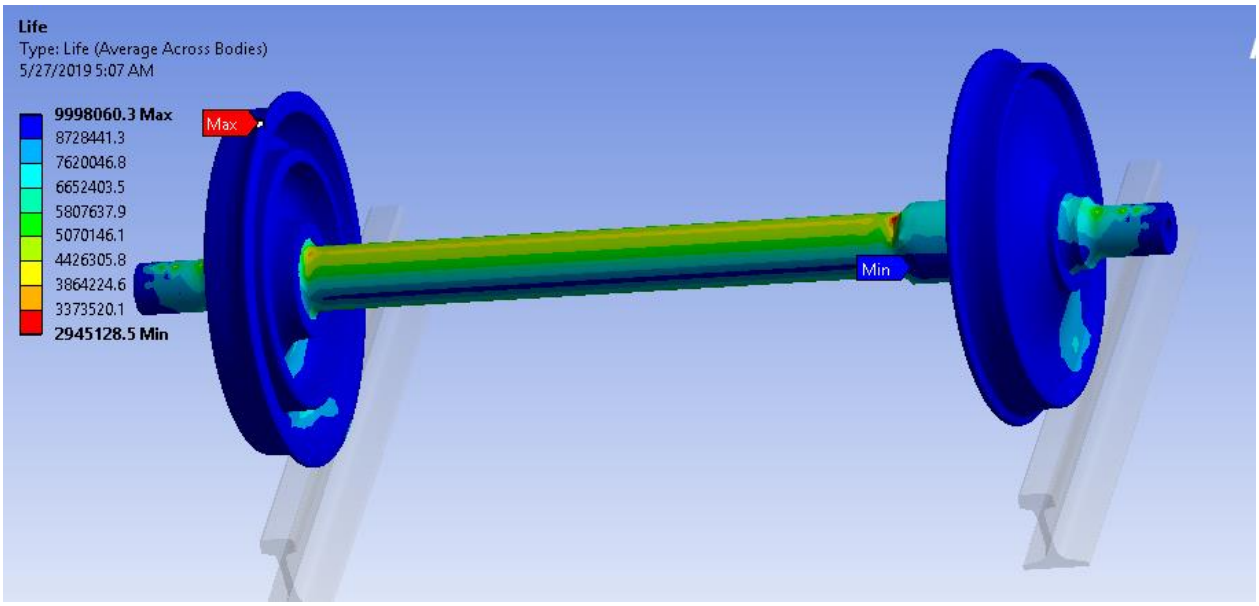

(a)

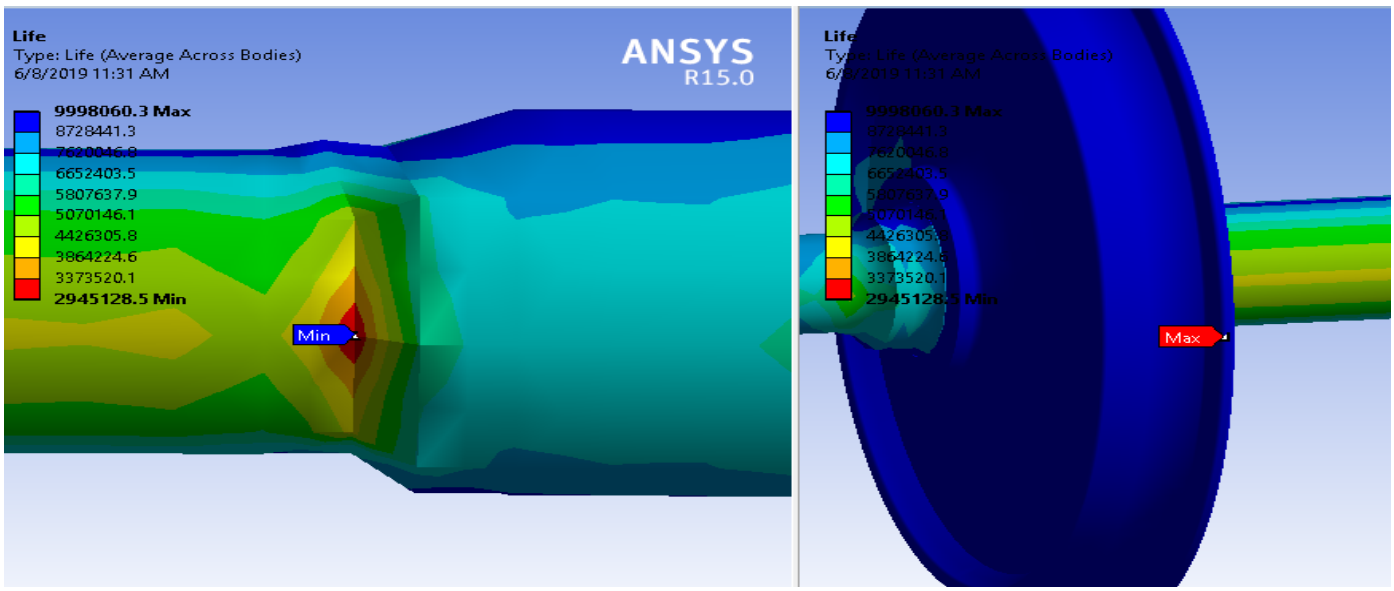

(b)

Fig 5.8 (a) and (b) Contour plot of Fatigue Life for loading case II.

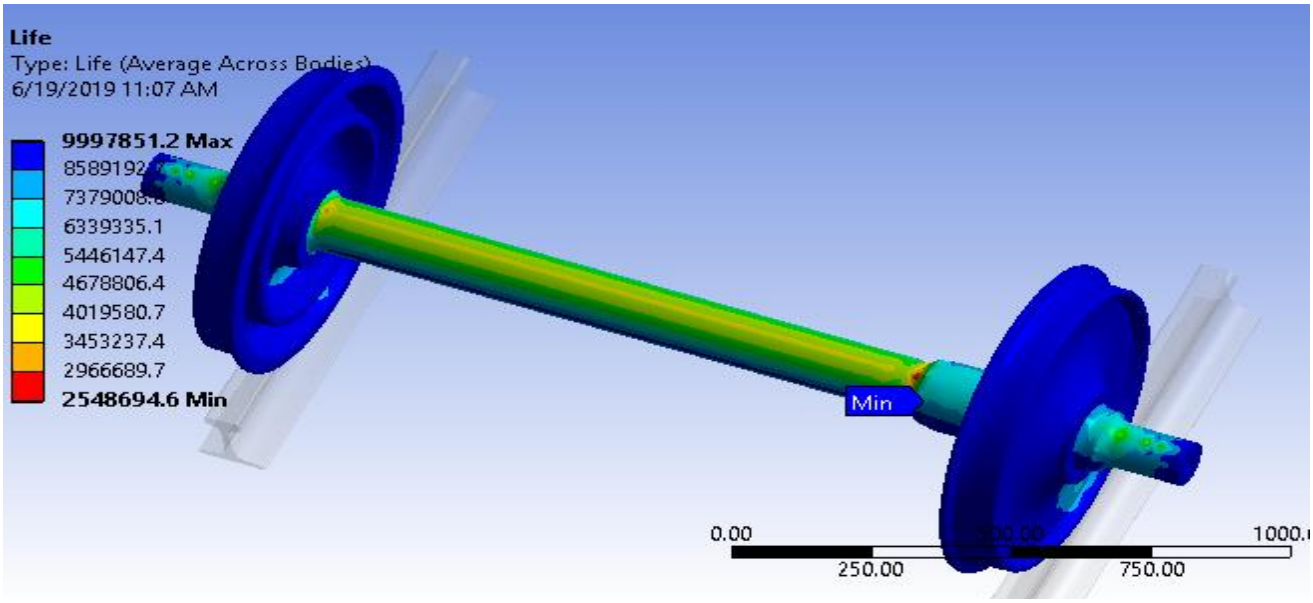

Fig 5.9 Contour plot of Fatigue Life for loading case III.

D. Equivalent alternative stress

In a Stress Life fatigue analysis, one always needs to query an SN curve to relate the fatigue life to the stress state. Thus the "equivalent alternating stress" is the stress used to query the fatigue SN curve after accounting for fatigue loading type, mean stress effects, multi-axial effects, and any other factors in the fatigue analysis. The maximum equivalent alternating stress shown in figure 5.10 is 34.39 MPa for case I.

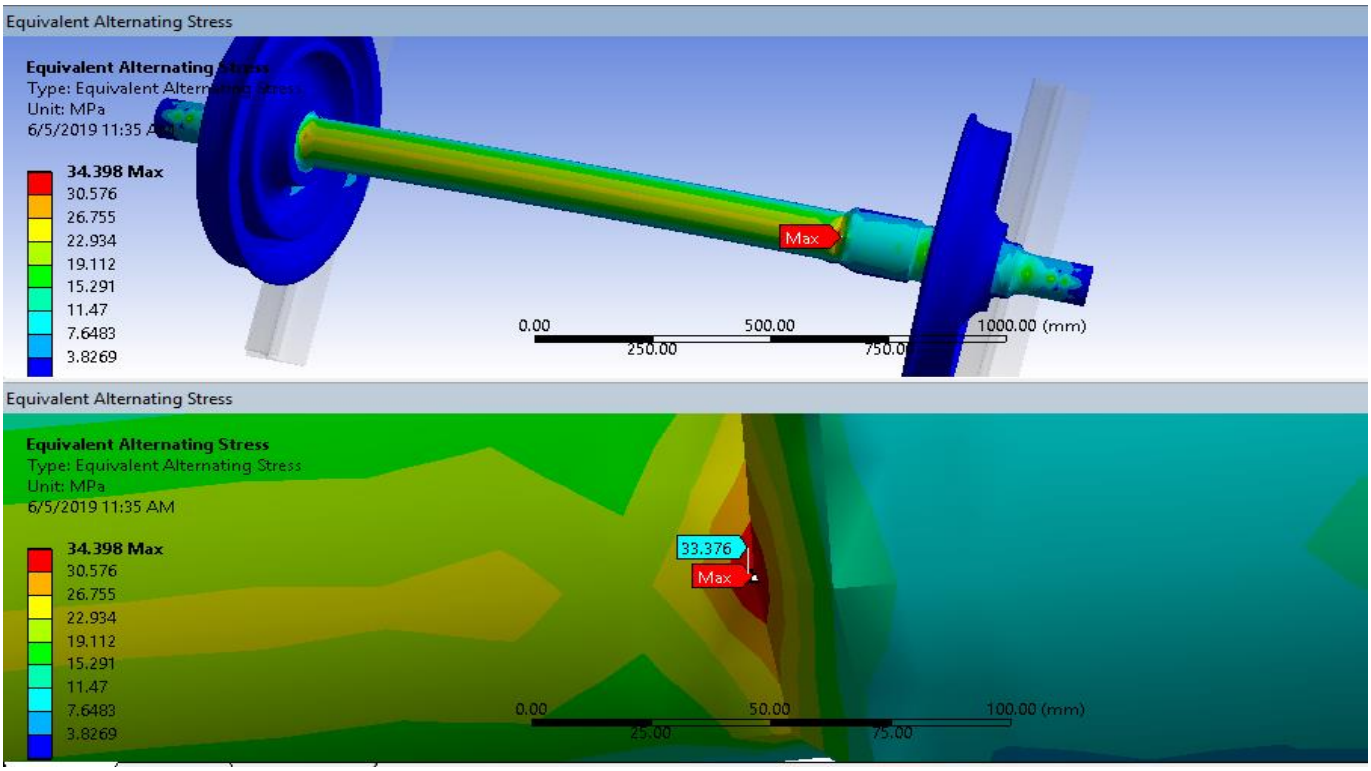

Fig 5.10 Contour plot of Equivalent alternating stress for loading case I

- Also as we see from fig 5.11 the equivalent alternating stress for loading case II will be 45.76 and it shows increment relative to loading case I the minimum will be 5.08 MPa on the wheel thread.

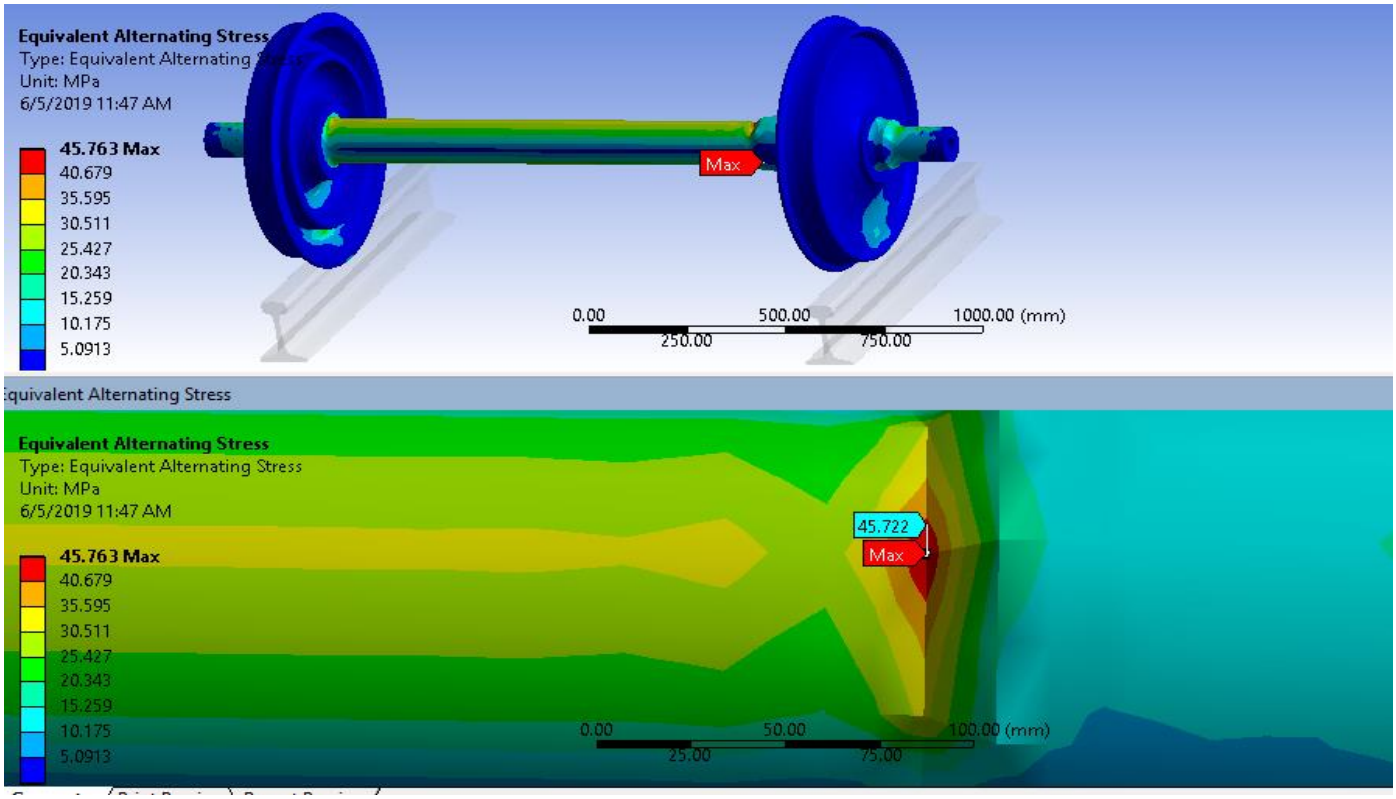

Fig 5.11 contour plot of Equivalent alternating for loading case II

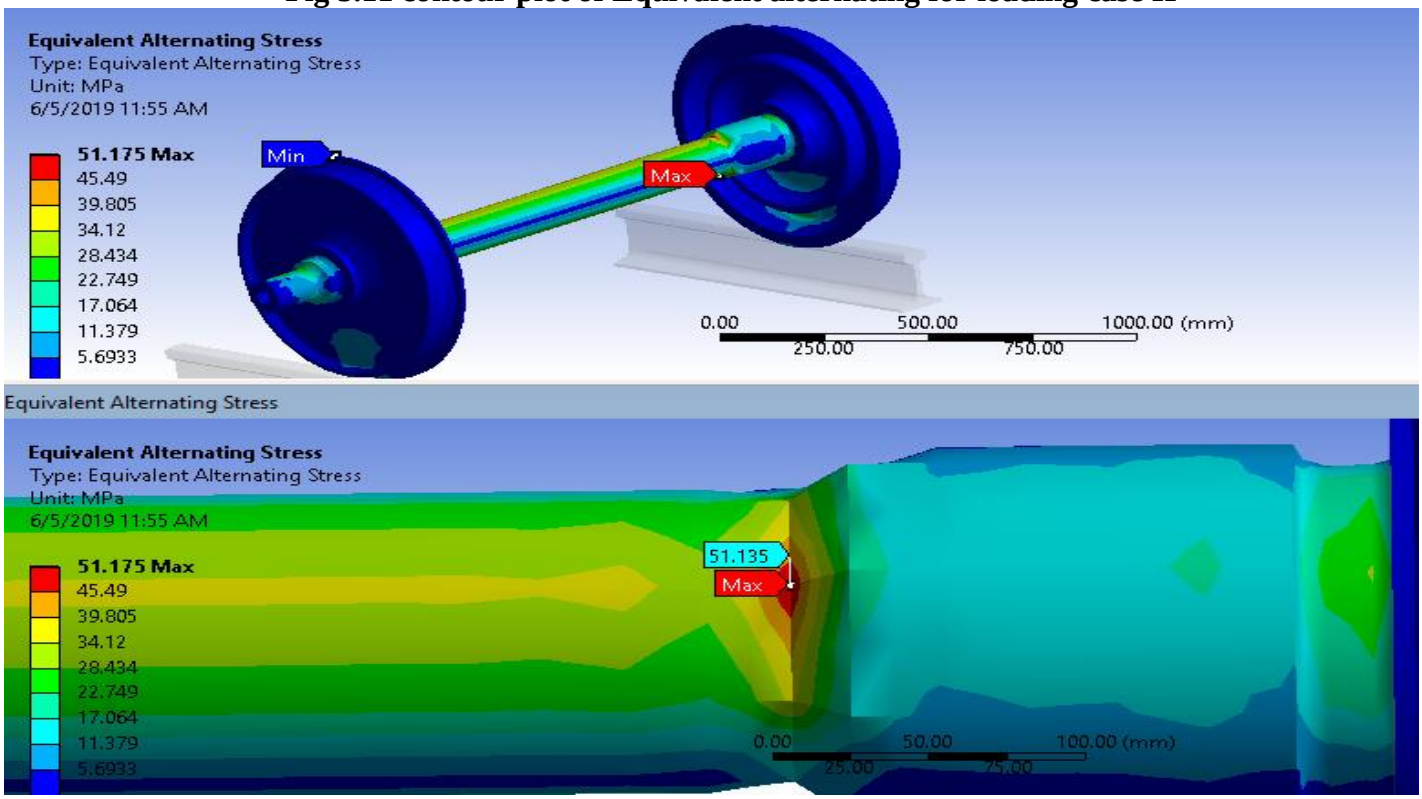

Fig 5.12 contour plot of Equivalent alternating for loading case III.

- From fig 5.11 and 5.12 we can see that the equivalent alternating stress increases to 45.76 Mpa for loading case II and 51.17 Mpa for loading case III. The Equivalent alternating stress also increases with the increase of passenger loading.

E. Factor of safety

Factor of safety is ability of a system's structural capacity to be viable beyond its expected or actual loads at a given design life. The maximum Factor of Safety displayed in Ansys is 15. To compare results of factor of safety from Ansys to the standard factor of safety of AALRTs wheelset material there was some challenges of accessing documents of AALRTs railcar. There for the researcher use common factor of safety standard for known material and uncertain loading condition which shows the factor of safety value should lay between 3 – 4 values [26].

Figure 5.13 below indicates that at the axle middle section where the torque from the gearbox transmitted to the wheelset assembly is where the minimum value of factor of safety will be 4.58.

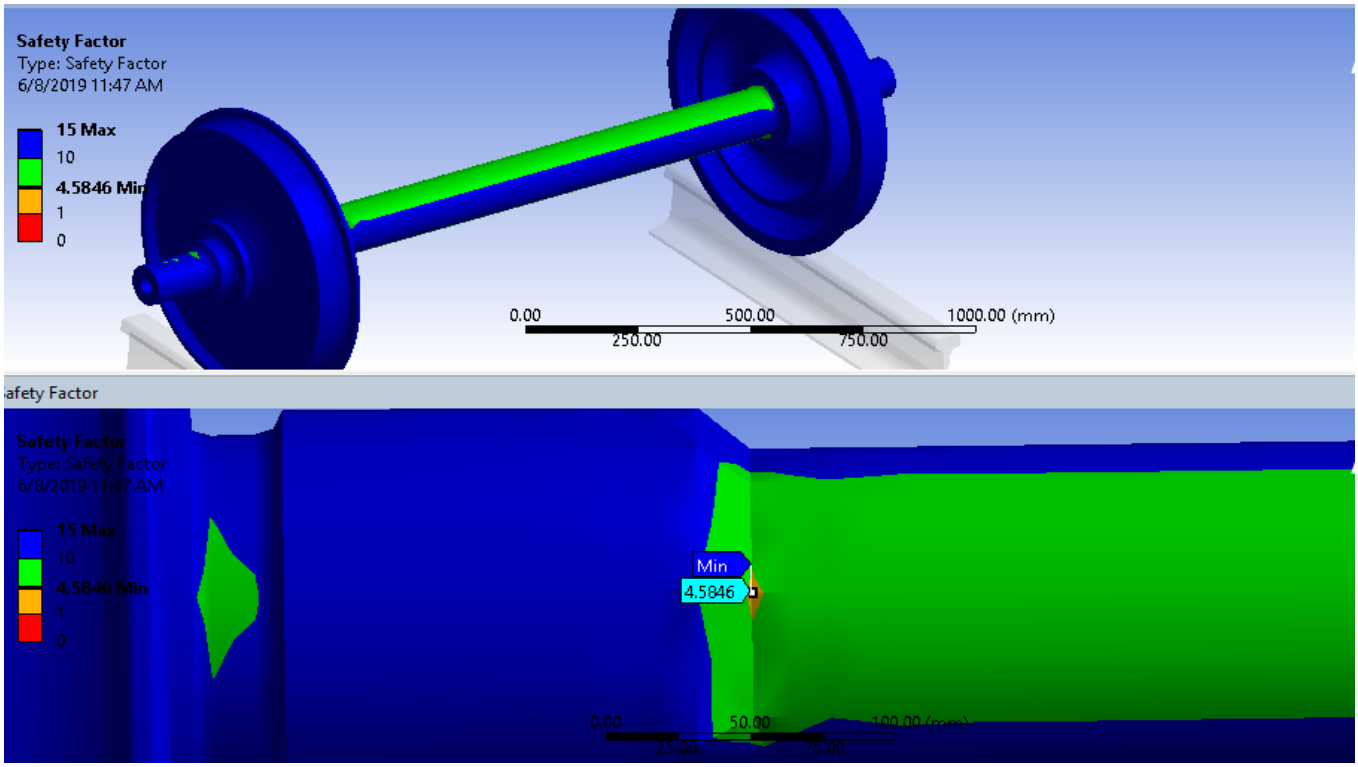

Fig 5.13 Contour plot of Factor of safety for loading case I

- Also the fig 5.14 and fig 5.15 show us the values of factor of safety for loading case II and loading case III. It decreases to 3.52 for case II and to 3.18 on loading case III which

shows us loading more passengers on the train more than its capacity decreases the safety of the wheelset also the safety of the rail car and passengers.

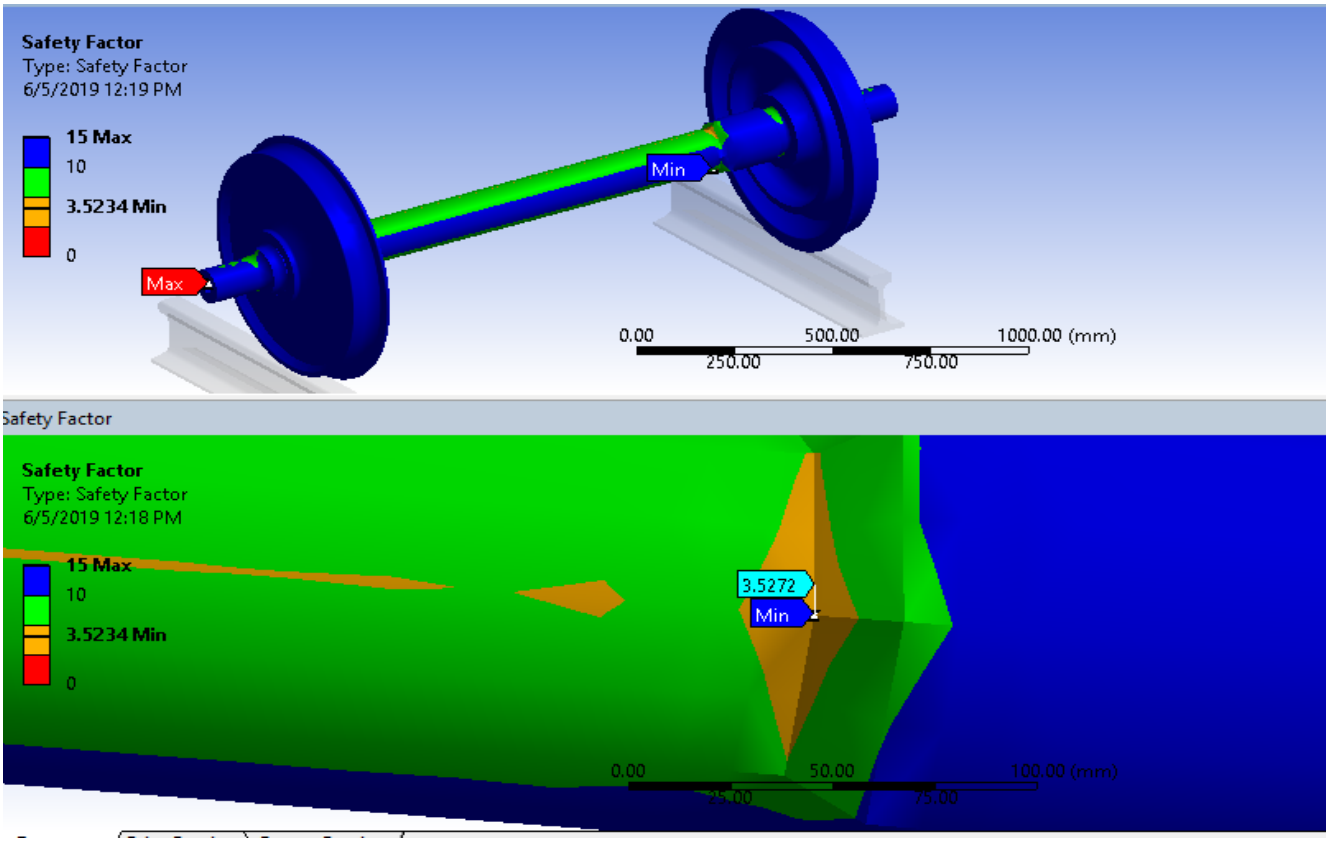

Fig 5.14 Contour plot of Factor of safety for loading case II

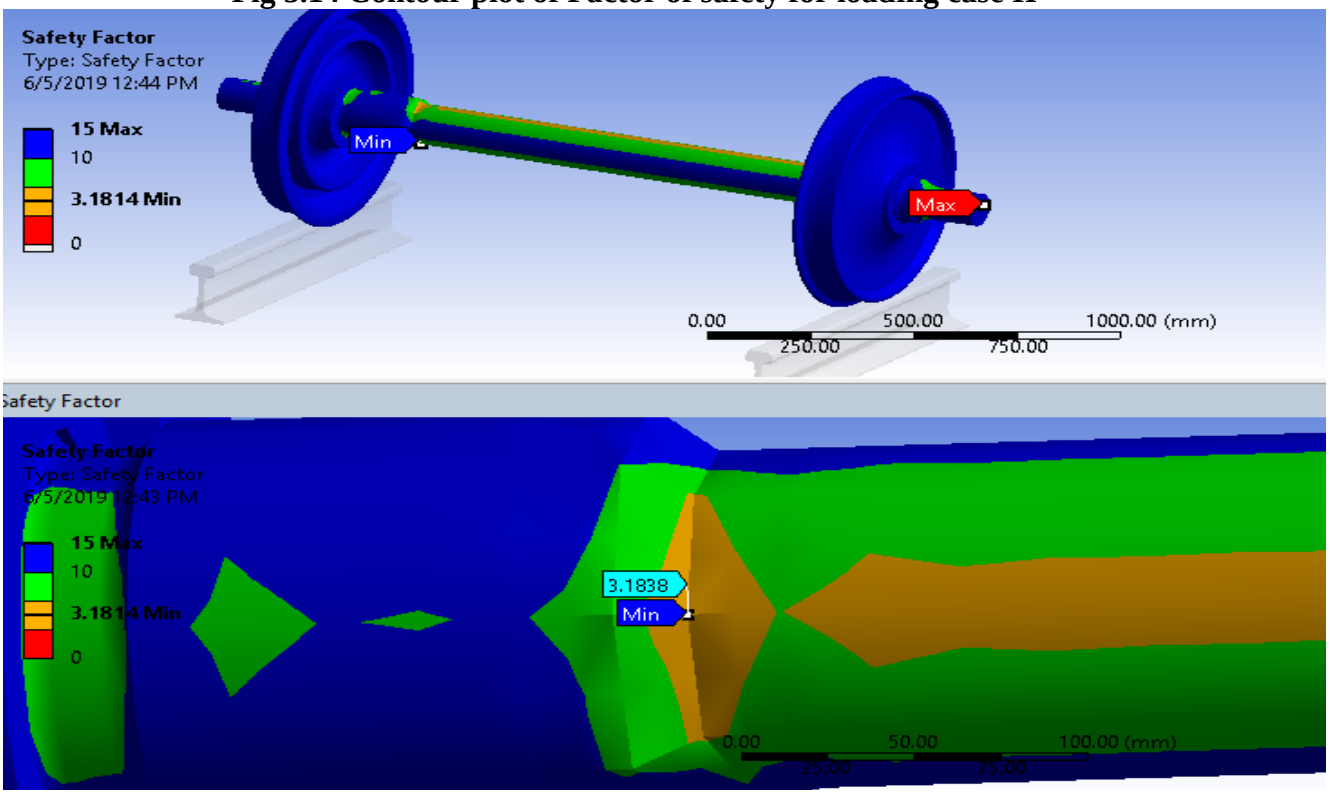

Fig 5.15 Contour plot of Factor of safety for loading case III.

F. Normal and shear stress

A stress induced on a body by Forces that are perpendicular to area resisting the force is known as normal stress while if the force acts in a parallel to the resisting area the resulting stress is called shearing stress. Below here we can see results of normal stresses and shear stresses induced on the wheelset under different loading conditions.as shown in the fig 5.16 the maximum normal stress induced on the axle end section which support the vertical load from the vehicle and the maximum shear induced on the middle section which the gear box is coupled with the axle using rubber couplings.

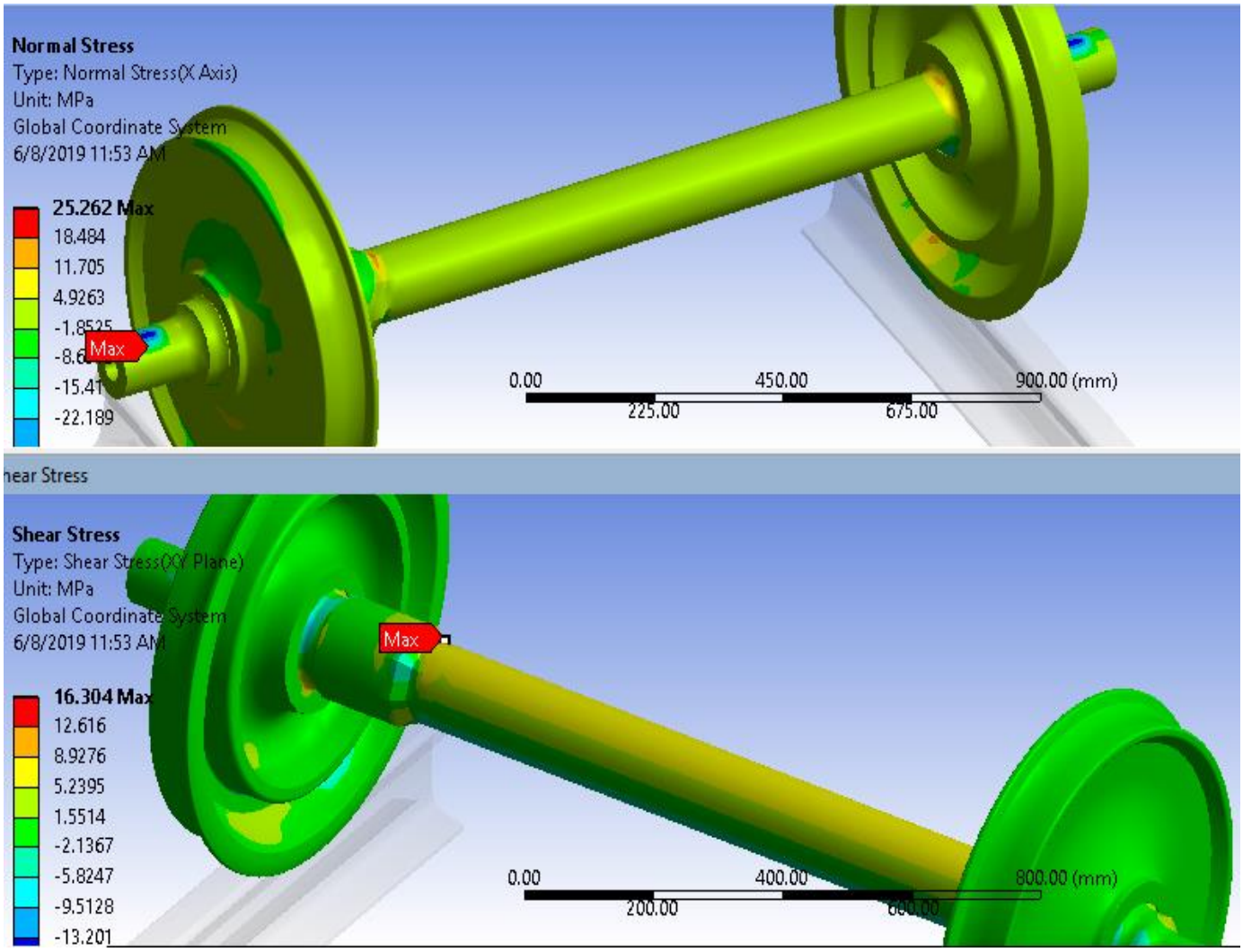

Fig 5.16 Contour plot of Maximum Normal and shear stresses for loading case I.

- For loading case I the maximum normal stress is 25.26 Mpa and maximum shear stress is 16.30 Mpa

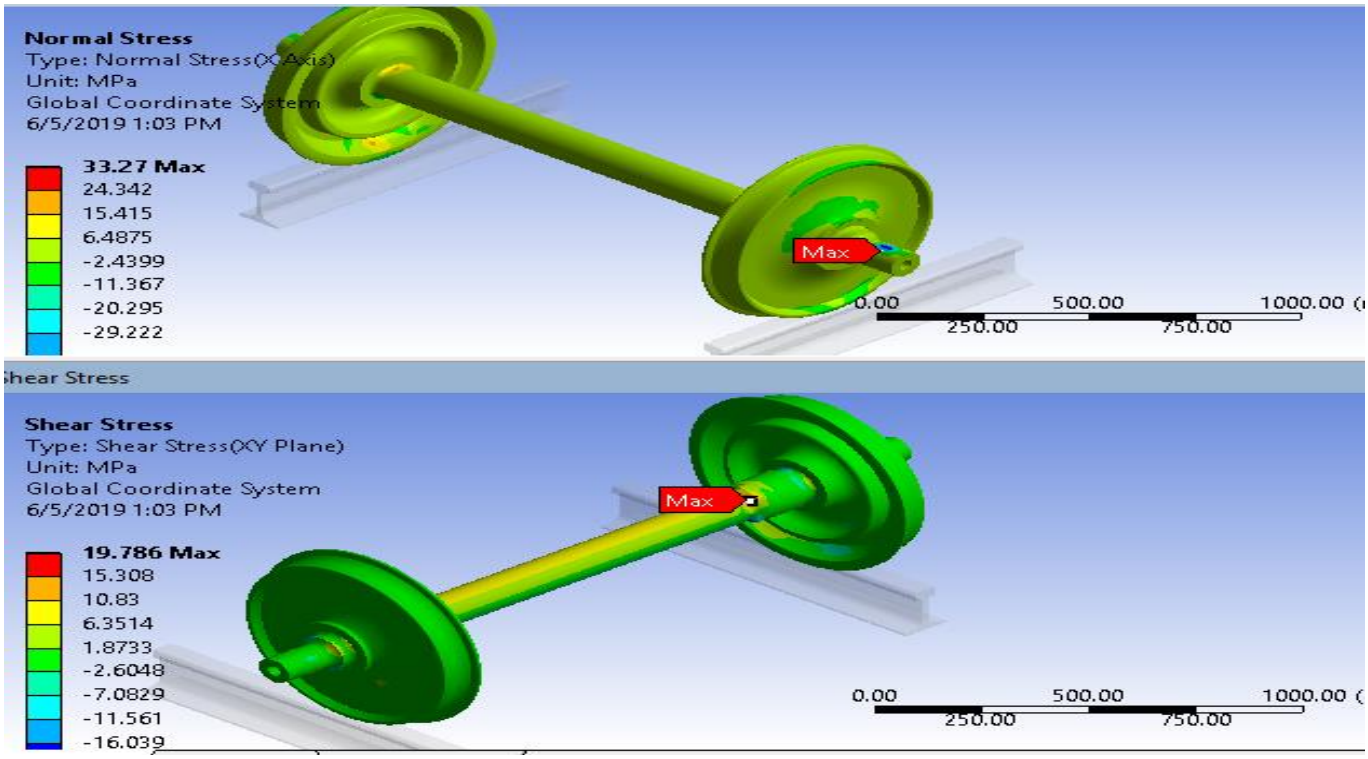

Fig 5.17 Contour plot of Maximum Normal and shear stresses for loading case II

- For loading case II the maximum normal stress is 33.27 Mpa and maximum shear stress is 19.78 Mpa and it increases with Number of loading of passengers.

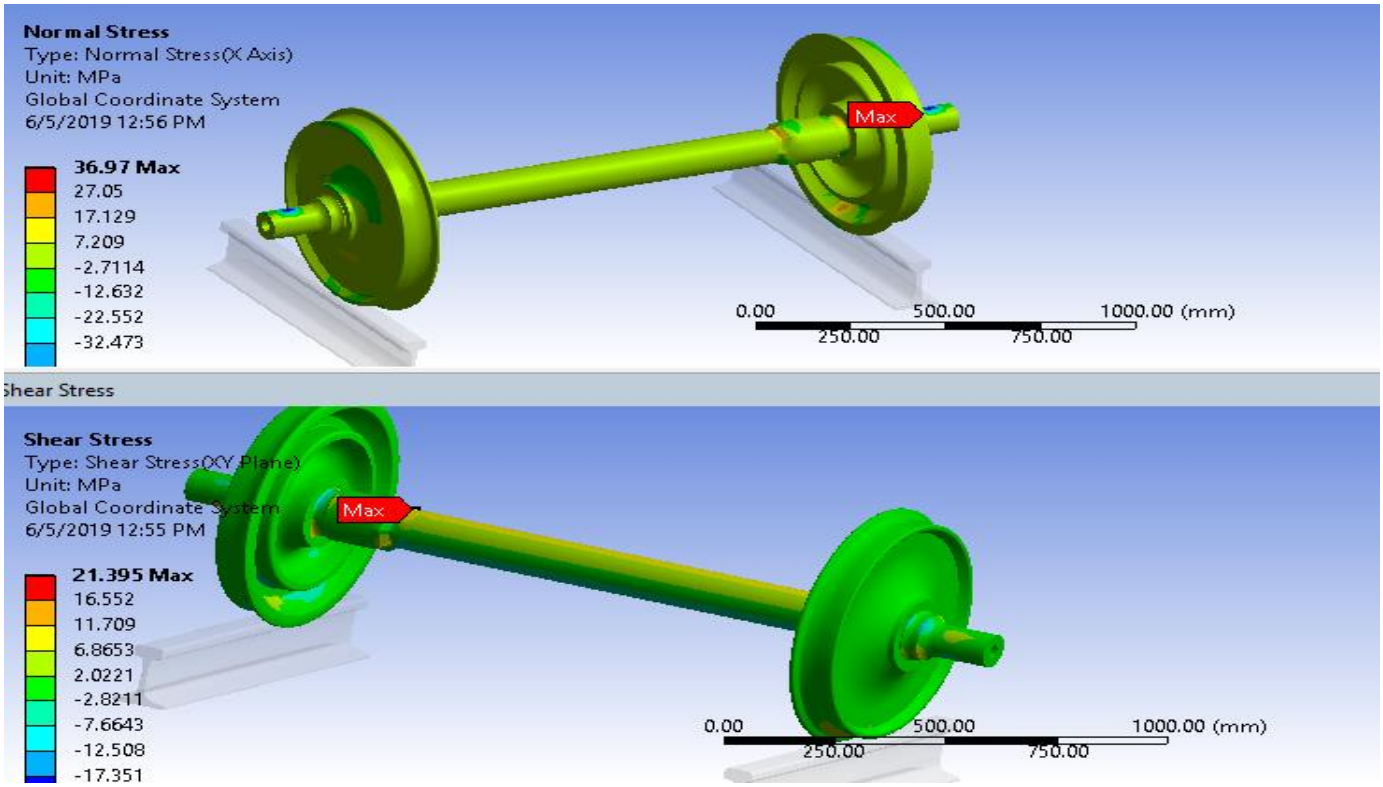

Fig 5.18 Contour plot of Maximum Normal and shear stresses for loading case III.

- Also for loading case III the maximum normal stress will be 36.9 Mpa and maximum shear stress is 21.3 Mpa

G. Directional Deformation

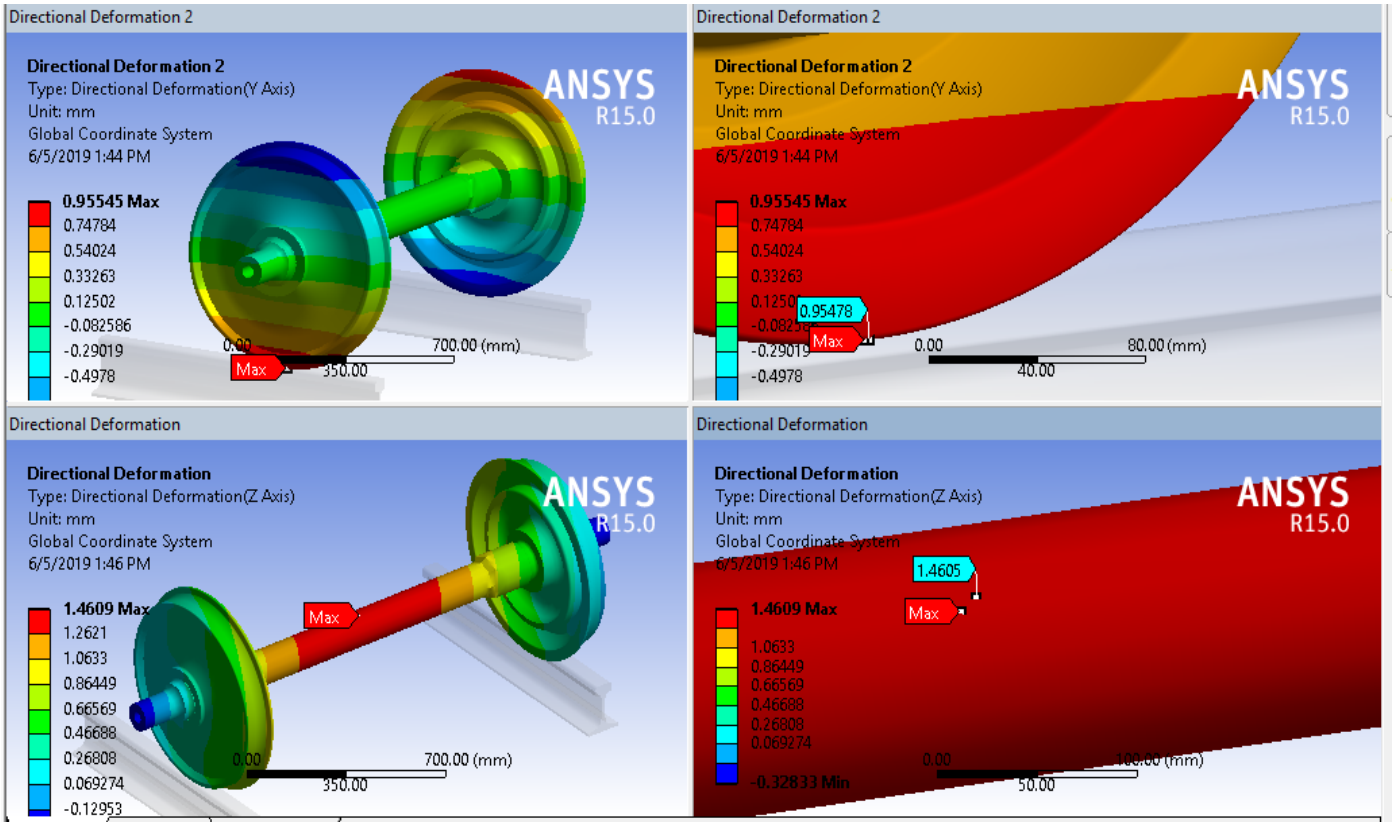

Fig 5.19 Contour plot of Directional deformation for loading case 1.

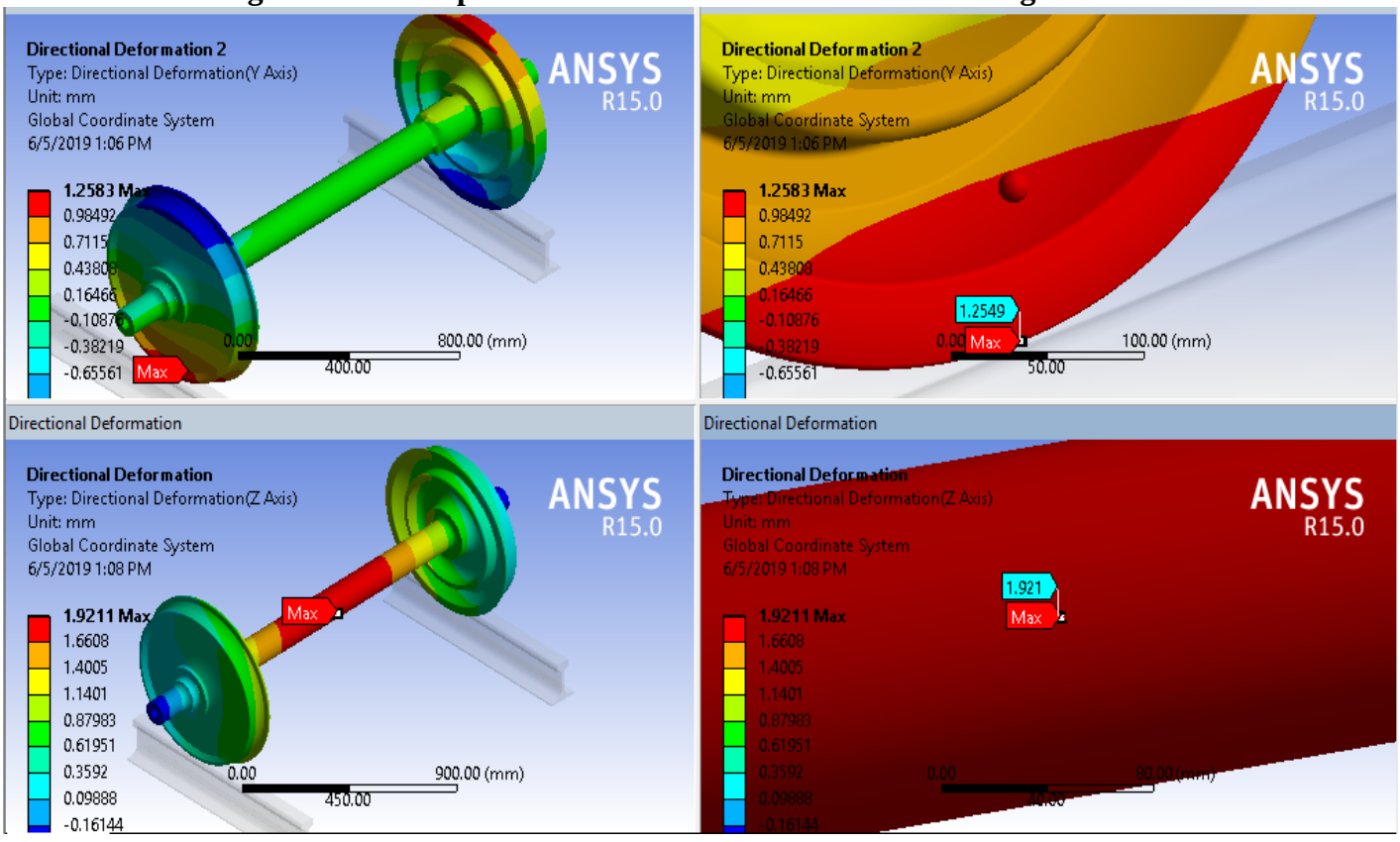

Fig 5.20 Directional deformation for loading case II.

- As we can see from Fig 5.19 the directional deformation in Y and Z direction for loading case I is 0.95mm respectively, and it increases to mm 1.25 and 1.92 mm for loading case II.

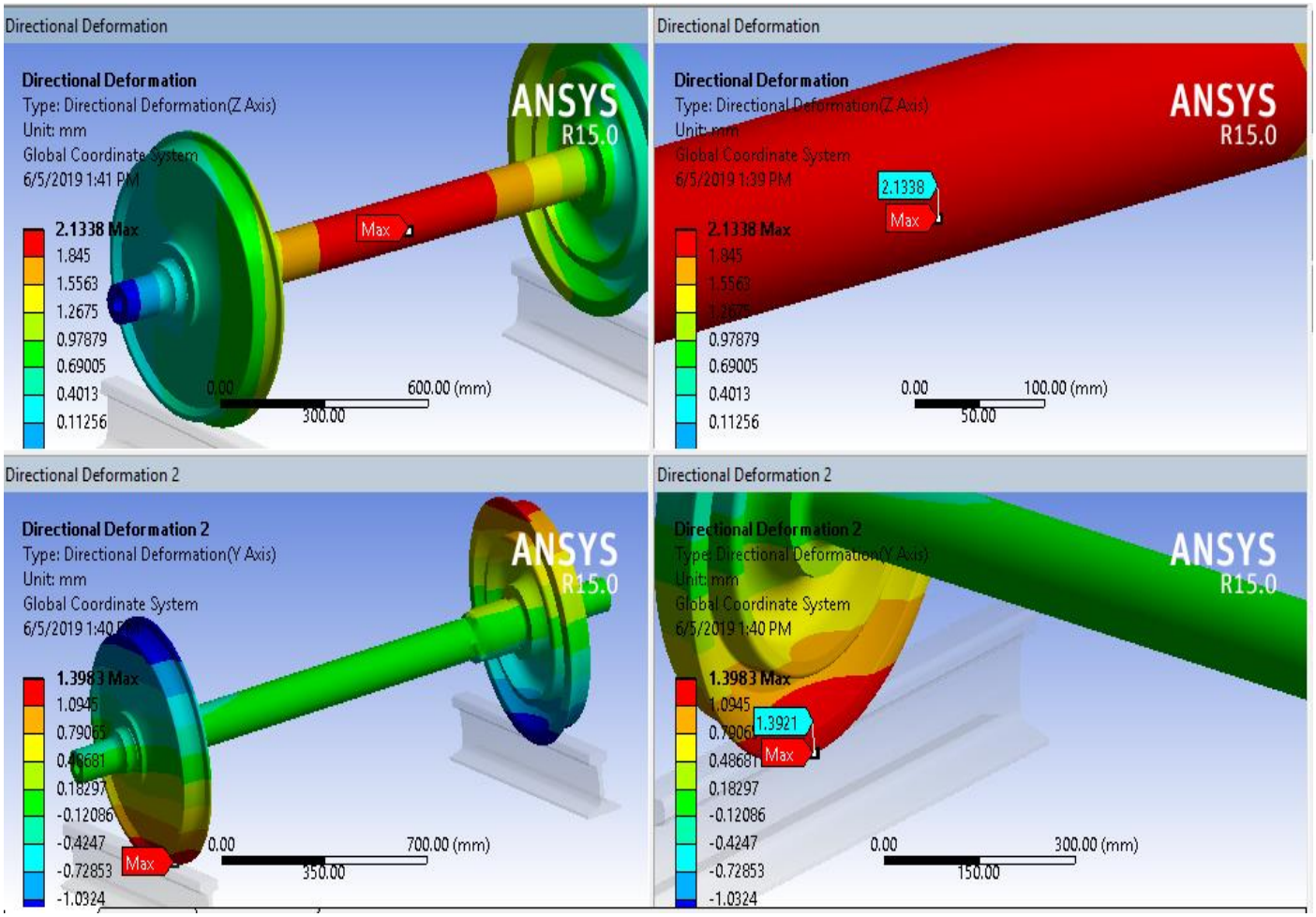

Fig 5.21 Contour plot of Directional deformation for loading case III.

For loading case III as we can see from fig 5.21 the directional deformation in y and z direction increases to 1.39 mm and 2.13 mm respectively.

5.1.2 Results of Different Traction Condition

In order to have the research focused the researcher only displays the results of three selected traction conditions ,20 km/hr. (actual traveling speed of AALRT train), 40 km/hr. and 70 km/hr. (maximum traveling speed AALRT train) with the overloading case of 57307.88 N/wheel. Other results of traction condition in all three loading conditions are summarized in a table form on appendix C table

A. Von Mises Stress

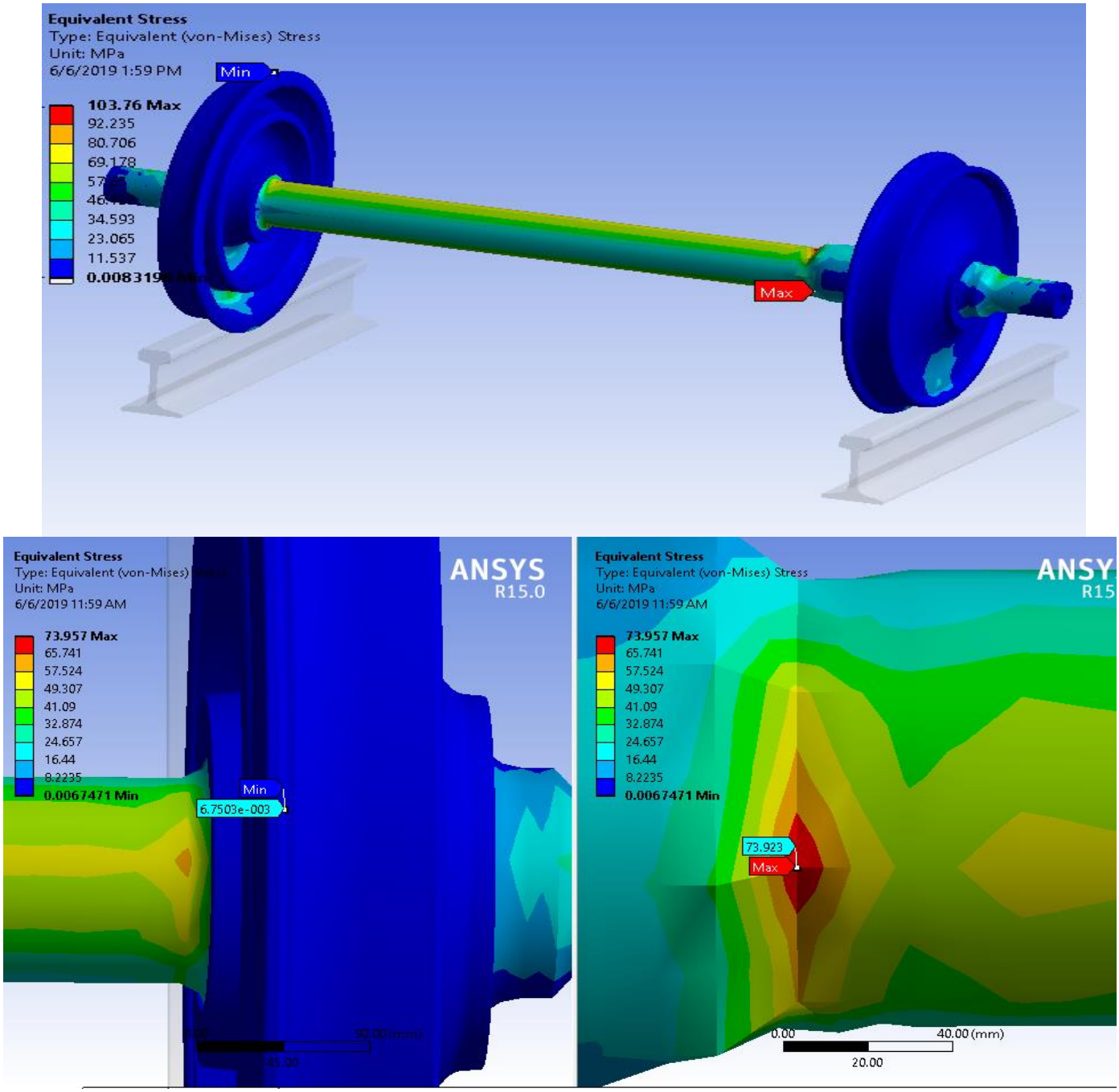

Fig 5.22 Contour plot of von Mises stress for traction condition I (20 km/hr.) .

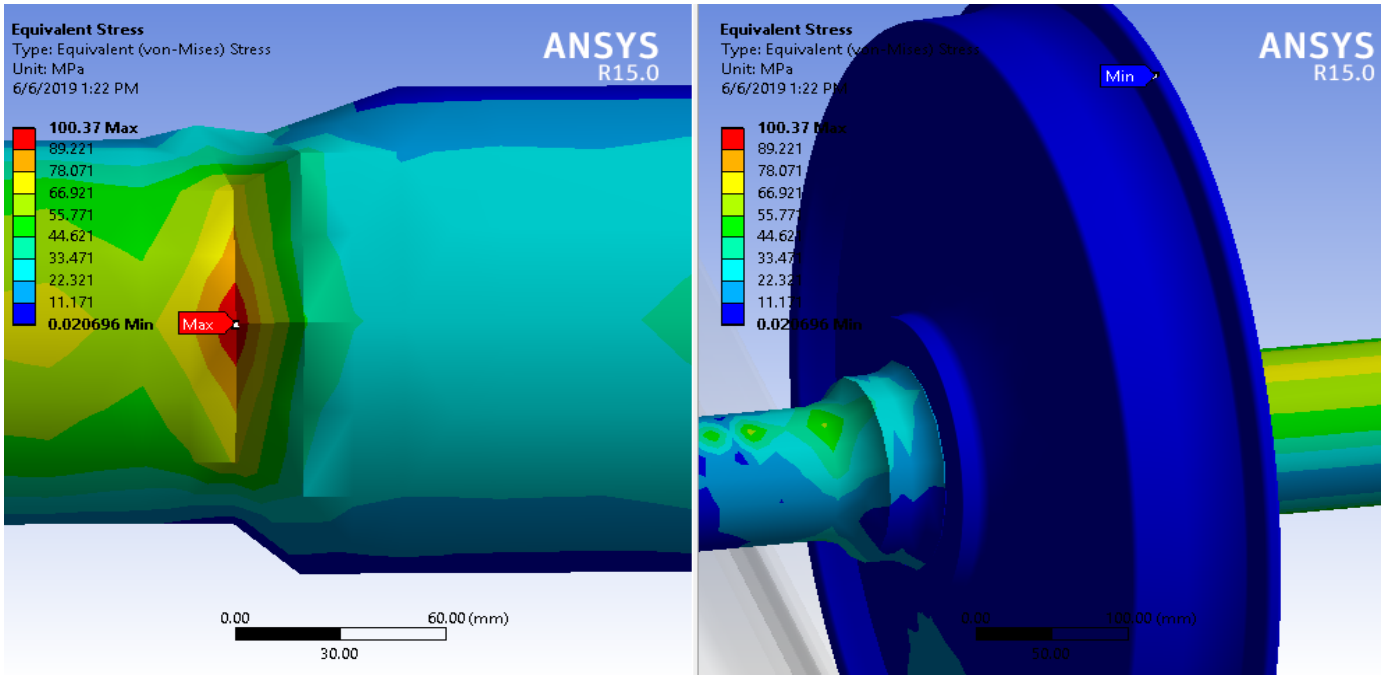

Fig 5.23 Contour plot of von Mises stress for traction condition II (40 km/hr.) .

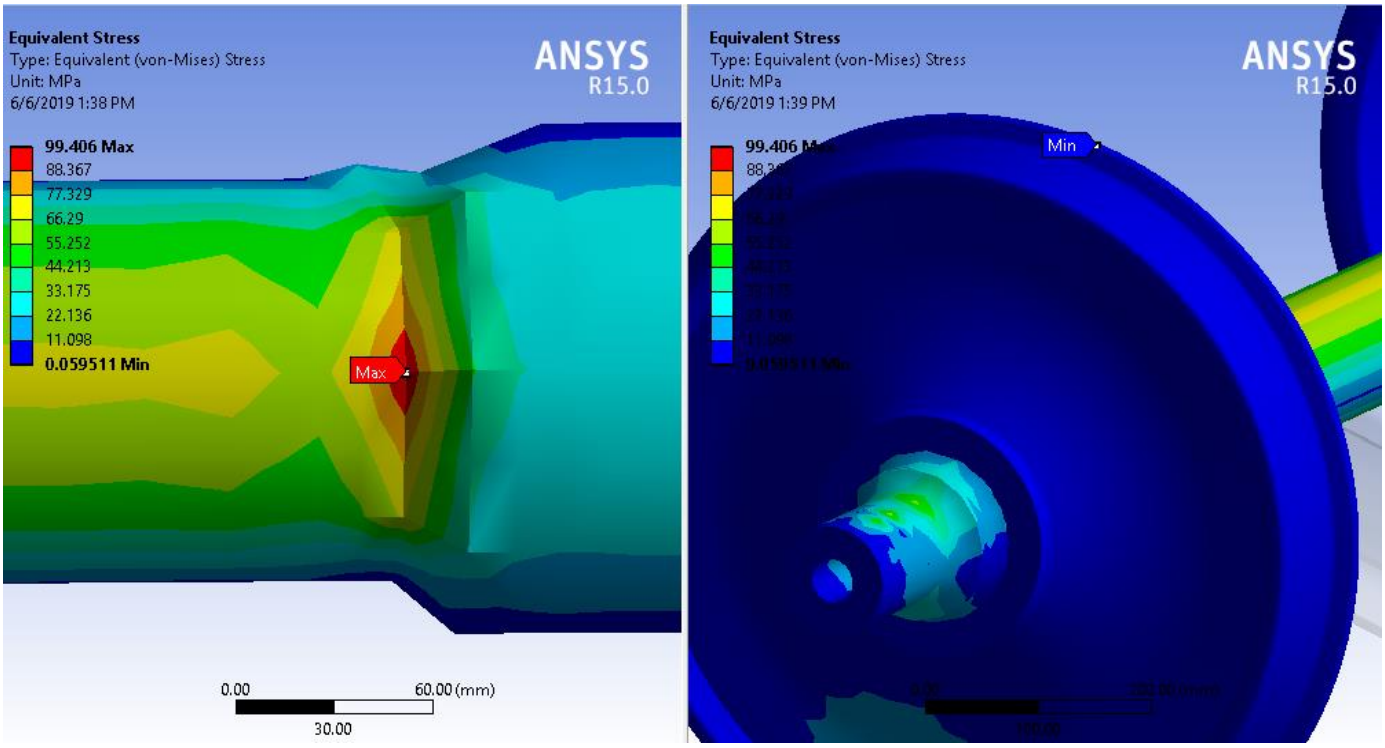

Fig 5.24 Contour plot of von Mises stress for traction condition III (70 km/hr.)

B. Fatigue life

Fatigue life is shown in Fig 5.25 for traction condition I (20 km/hr.) with maximum fatigue life is of 9997856.63 on the wheel and the minimum value is 2477461.7 cycles on the axle.

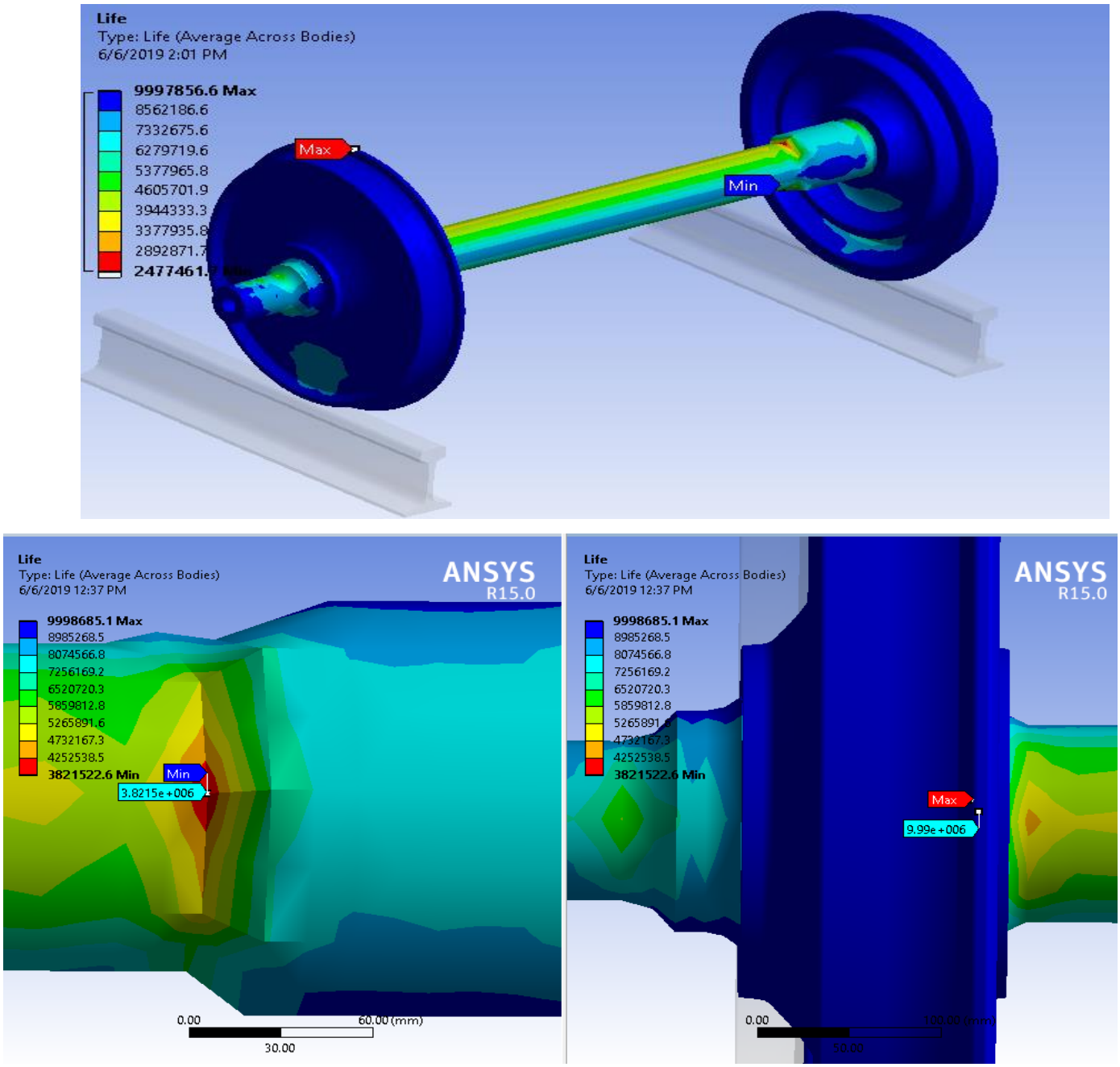

Fig 5.25 Contour plot of fatigue life for traction condition I (20 km/hr.) .

The next results in fig 5.26 & fig 5.2 show us the fatigue life of the wheelset for the second and third traction conditions respectively with passenger loading of 57307.88 N per wheel. From the result we can see that their minimum life available for traction condition II is 2552189.3 Cycles and for case III is 2562653.9 cycles before failure which Doesn't have a large variation as much as the speed difference.

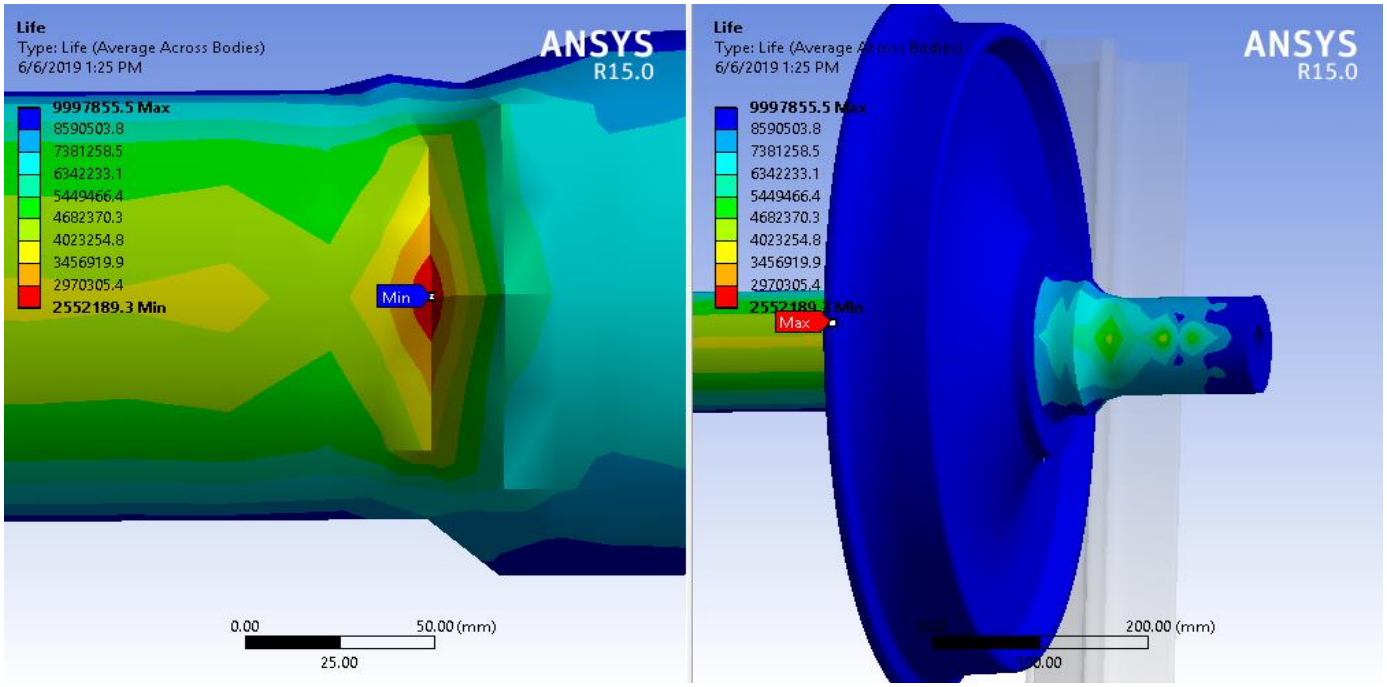

Fig 5.26 Contour plot of fatigue life for traction condition II (40 km/hr.).

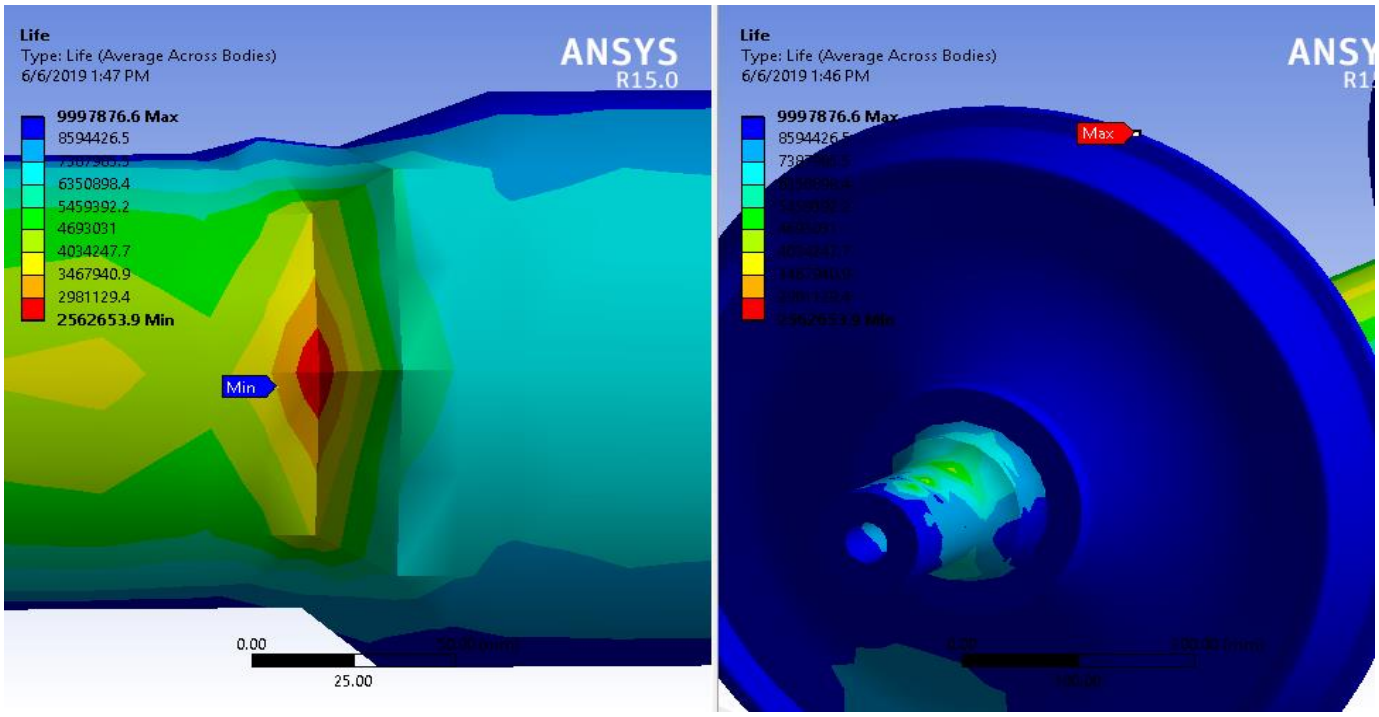

Fig 5.27 Contour plot of fatigue life for traction condition III (70 km/hr.).

C. Equivalent alternating stress

As we discussed before the equivalent alternating stress is used to query the fatigue SN curve. Here below we can see the decrease of equivalent alternation stress results with velocity increase. The maximum equivalent alternating stress is 52.23 MPa for traction case I and decreases to 51.12 Mpa on case II and to 50.97 Mpa on case III

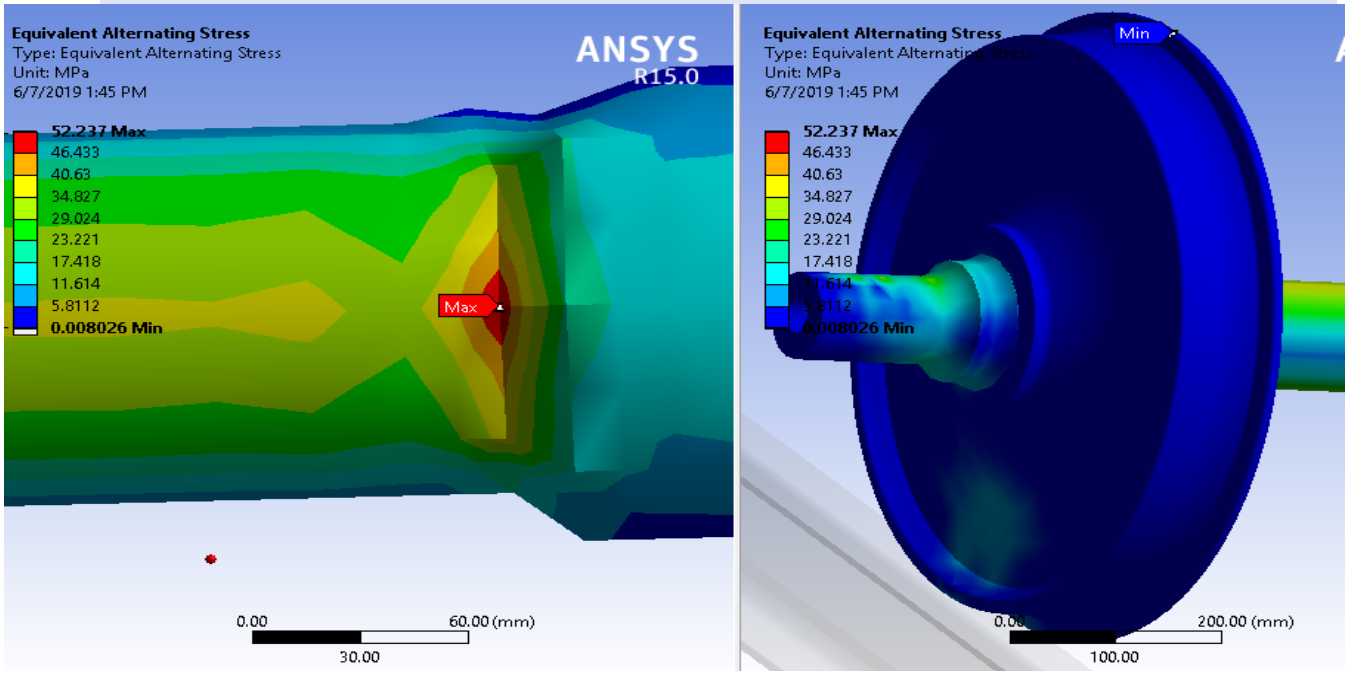

Fig 5.28 Contour plot of Equiv. alt. stress for traction condition I (20 km/hr.) .

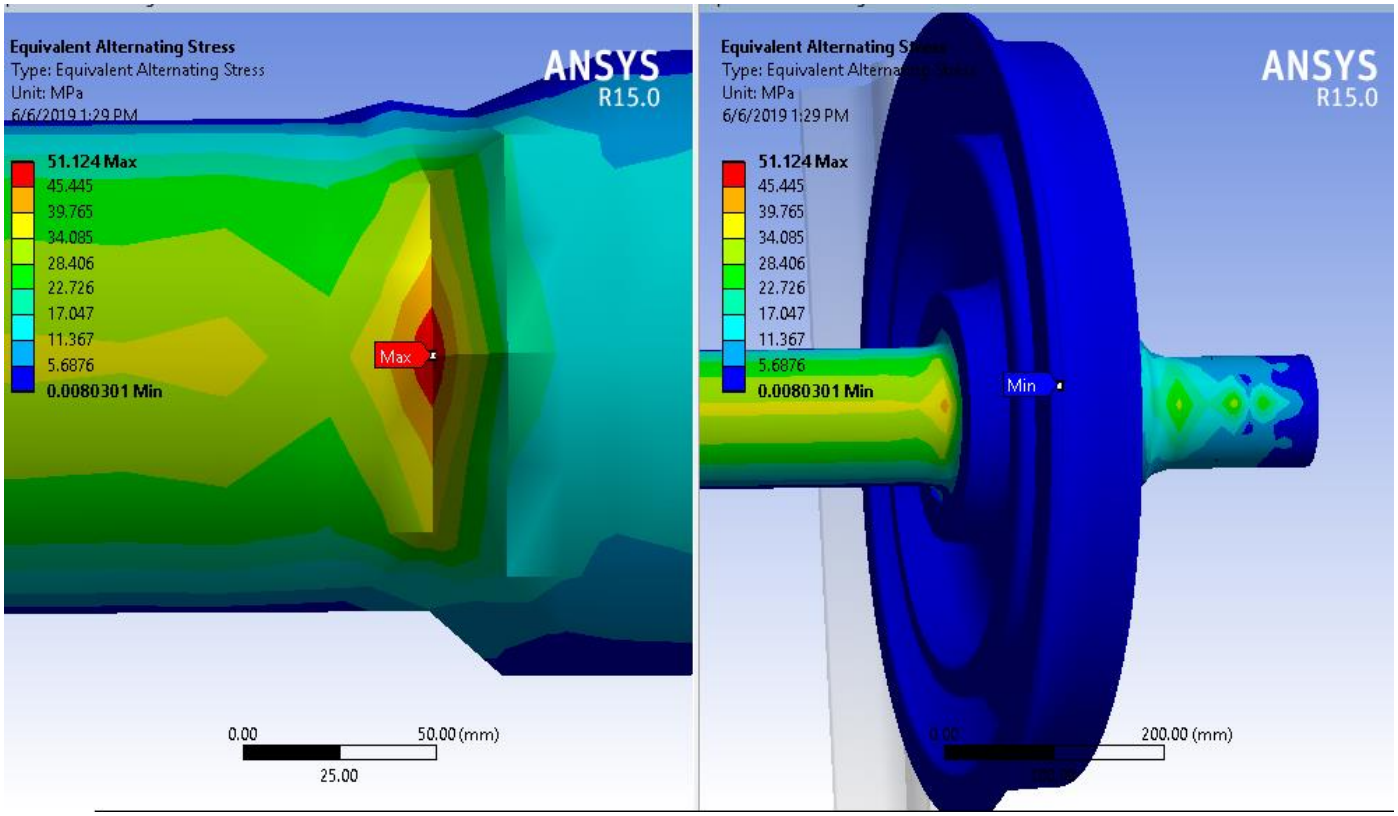

Fig 5.29 Contour plot of Equiv. alt. stress for traction condition II (40 km/hr.)

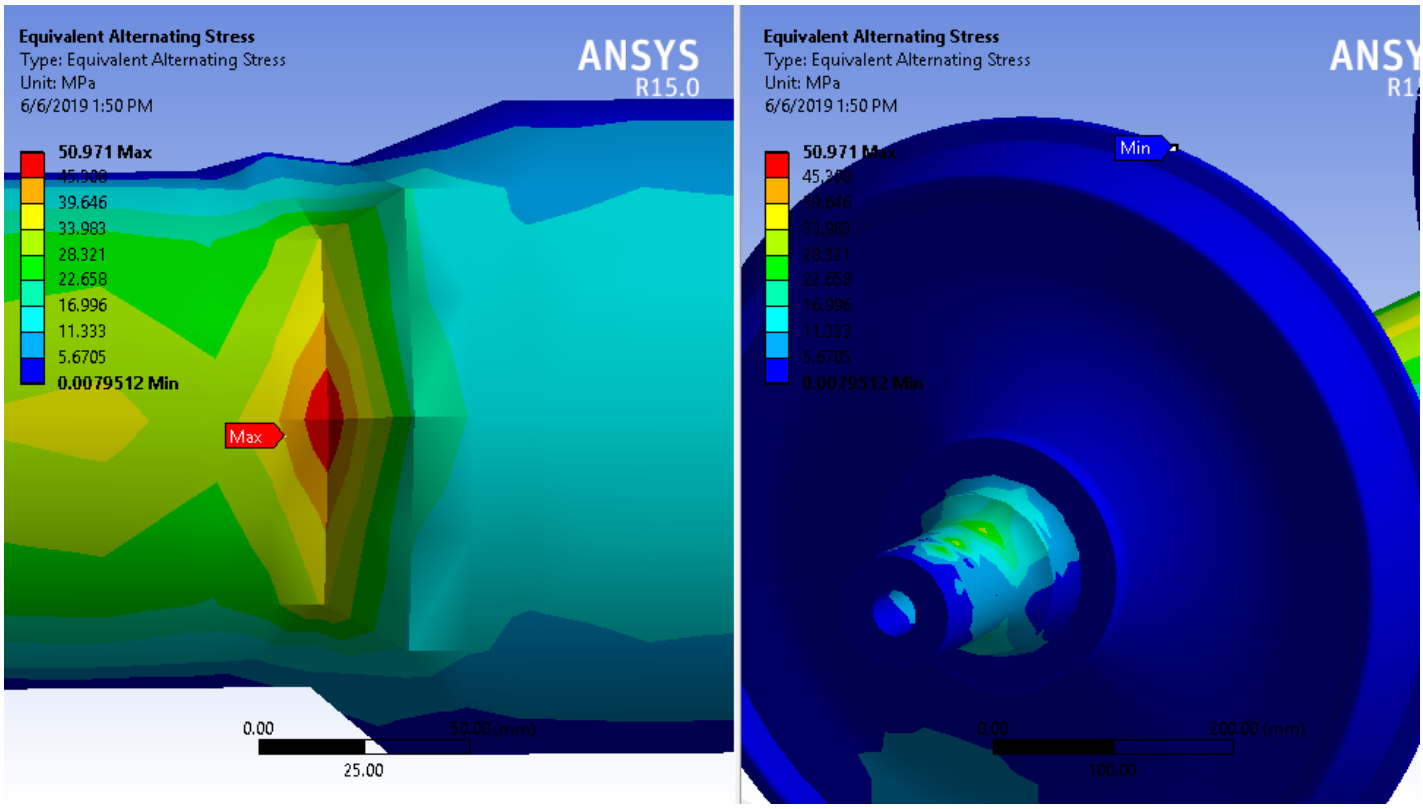

Fig 5.30 Contour plot of Equiv. alt. stress for traction condition III (70 km/hr.)

D. Factor of safety

Also the factor of safety increases with the increase in Velocity of the train. For traction condition I Factor of safety is 3.08 and increases to 3.18 and 3.21 for traction condition II & III respectively.

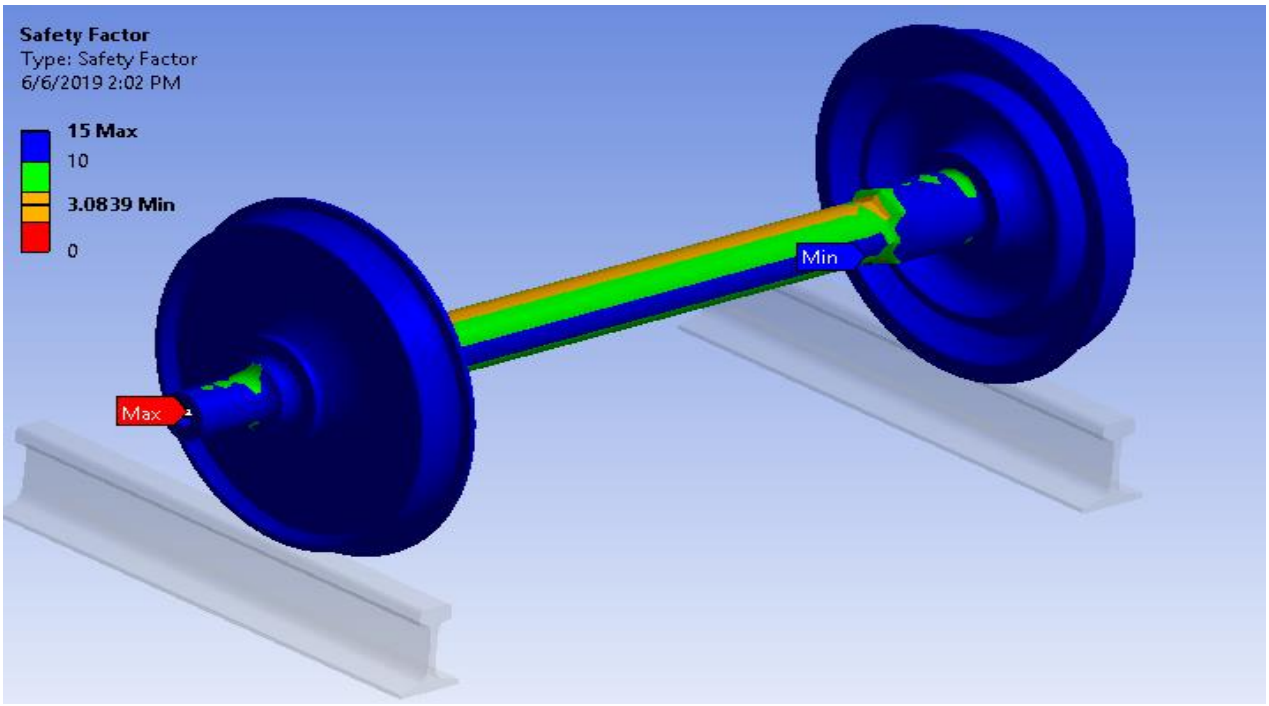

(a)

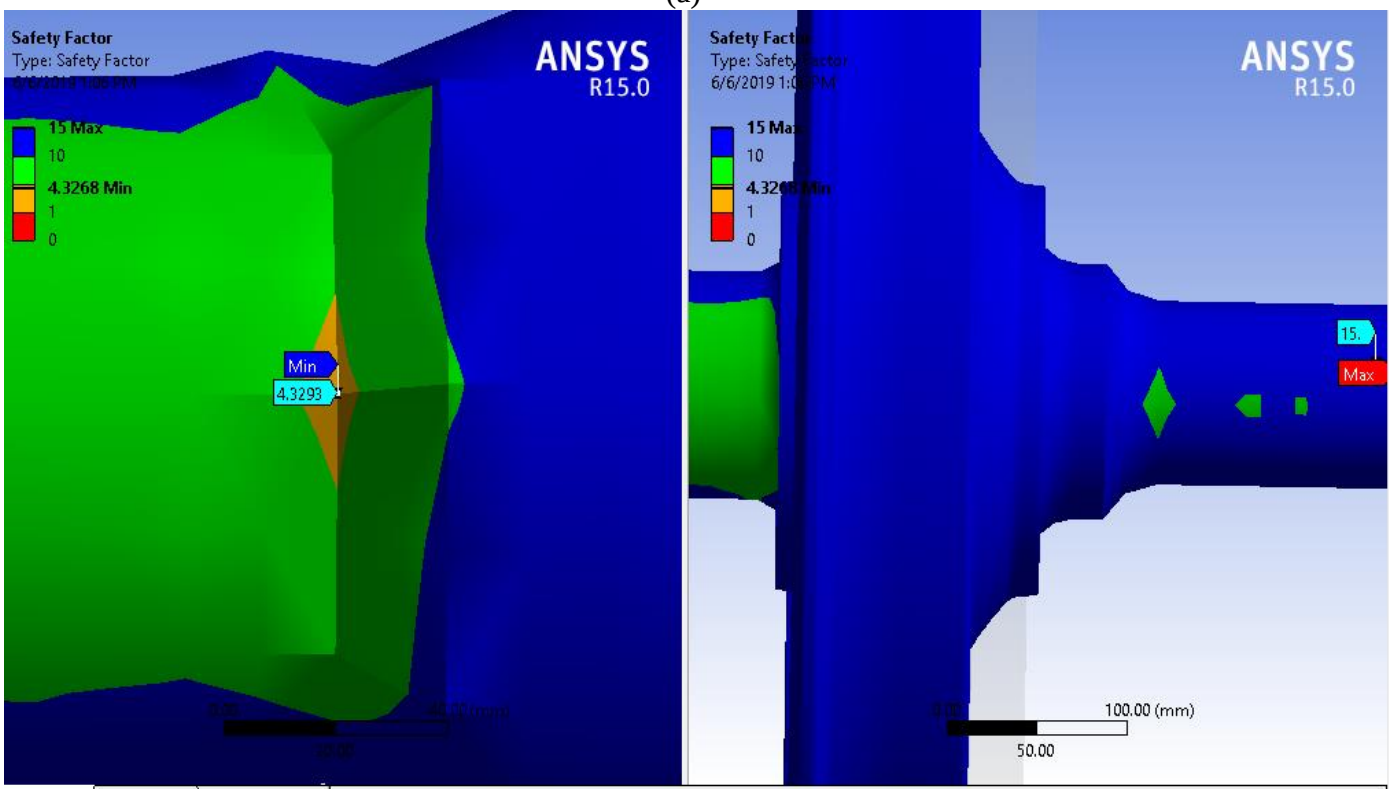

(b)

Fig 5.31 (a) and (b)Contour plot of safety factor for traction condition I (20 km/hr.) .

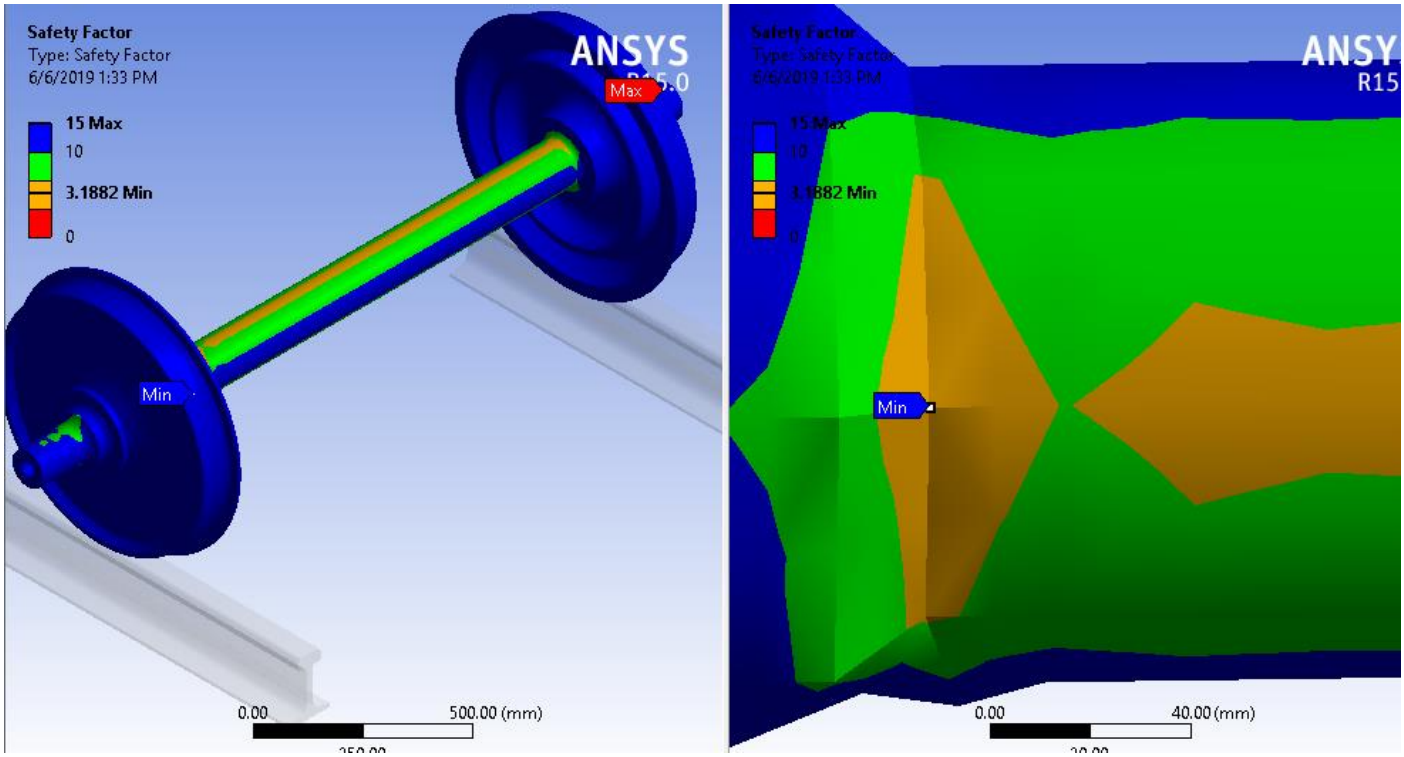

Fig 5.32 Contour plot of safety factor for traction condition II (40 km/hr.)

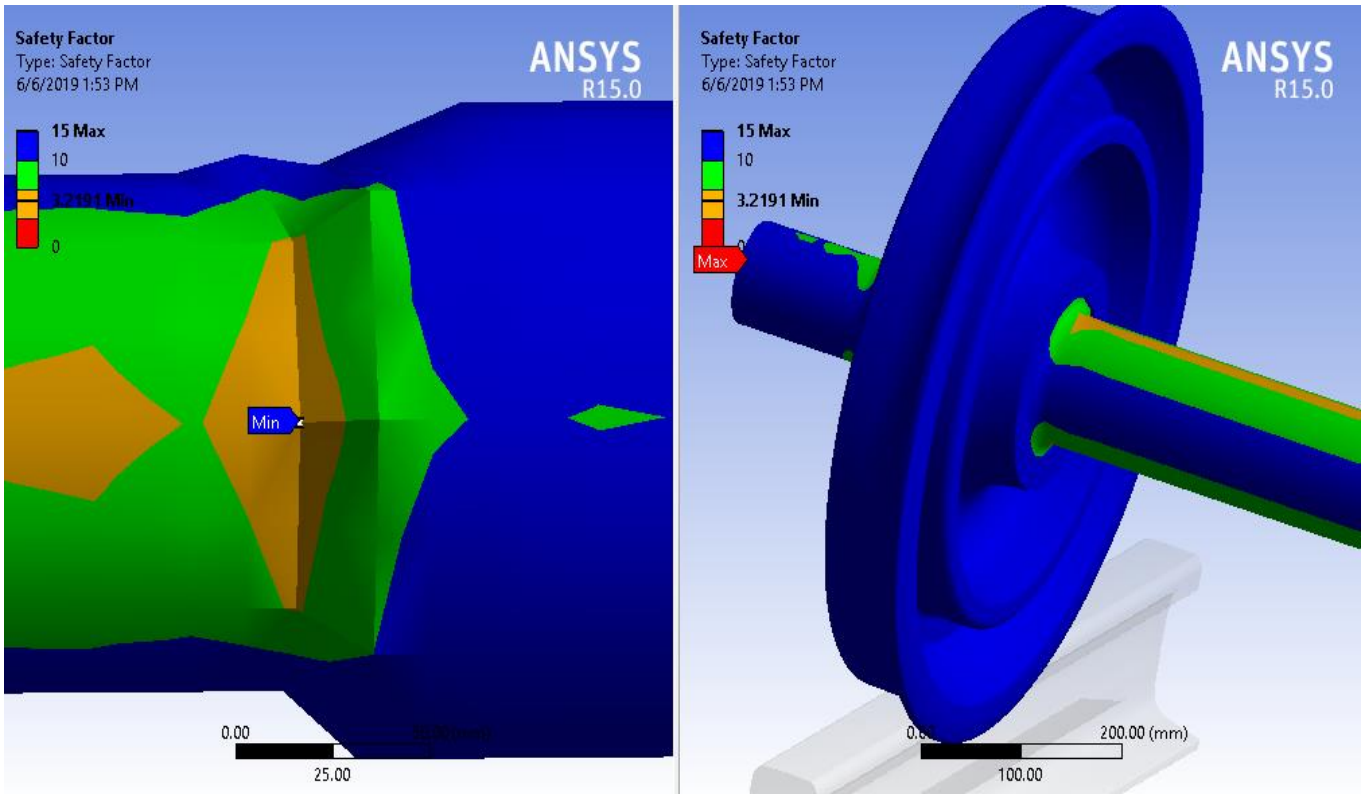

Fig 5.33 Contour plot of safety factor for traction condition III (70 km/hr.)

5.2 Discussions

In FEM analysis the geometry models are analyzed under the same non-proportional loading type, under the same material property and component of the railcar but using different loading and traction conditions.

5.2.1 Under Different Loading Condition

For our first discussion we use different loading conditions but same traction condition. As we can see clearly from the table 5.1 by taking different passenger loading conditions, case I (39134.25 N/Wheel), case II (51571.36 N/wheel) & case III (57307.88 N/wheel) and by keeping the traction condition constant (Rated torque and average velocity of 37.5 Km/hr.) for the analysis we can see that some changes on the behaviors and results of the wheelset.

Table 5.1 Summary of results of the different loading cases

Name	Results					
	Case 1		Case 2		Case 3	
	Min	Max	Min	Max	Min	Max
Von mises Stress (Mpa)	0.017	69.79	0.017	90.82	0.01	100.59
Fatigue life	3.989,826.3	9,998,511.6	2,945,128.5	9,998,060.3	2,548,694.6	9,997,852
Factor of Safety	4.58	15	3.52	15	3.18	15
Equivalent alternating(Mpa)	0.0055	34.39	0.0072634	45.765	0.008	51.175
Normal (Mpa)	-35.74	25.26	-47.077	33.27	-52.36	36.97
Shear(Mpa)	-16.88	16.3	-20.51	19.78	-22.19	21.39
Directional y(mm)	-0.91	0.95	-1.2	1.25E+00	-1.33	1.39
Directional z(mm)	-0.32	1.46	0.42	1.92	0.46	2.13

Some of the results like von mises stress, von mises strain, equivalent alternating stress normal and shear stress have directly proportional relation with of passenger loadings. Then passenger loading changes from case 1 (39134.25 N/Wheel) to case 2 (51571.36 N/wheel) & case 3 (57307.88 N/wheel) the above parameters of stresses and strain also

increases. This shows that increasing passenger loading on the railcar has negative effect on the stress induced on the wheel set.

In on other hand, the fatigue life and factor of safety of the wheel set under this different loading condition have inverse proportionality with the number of passengers and load supported by the wheel set. This means that when the loading on the axle and wheel increases it will shorten the life span of the wheel set and the safety factor also decreases means that the component is not safer with the increase in the loading.

Comparing the results which have been obtained using three different loads 57307.88 N, 51571.36 N and 39134.25 N.

Table 5.2 Evaluation of case I and case II

Name	Max/Min	Case I	Case II	Evaluation	
Max Von mises Stress(Mpa)	Max	69.79	90.82	23%	Increased
Min Fatigue life	Min	3,989,826.30	2,945,128.50	-35%	Decreased
Factor of Safety	Min	4.58	3.52	-30%	Decreased
Equivalent alternating(Mpa)	Max	34.39	45.765	25%	Increased
Normal (Mpa)	Max	25.26	33.27	24%	Increased
Shear(Mpa)	Max	16.3	19.78	18%	Increased
Directional y(mm)	Max	0.95	1.25	24%	Increased
Directional z(mm)	Max	1.46	1.92	24%	Increased
Bending stress on axle	Max	44.58	58.71	24%	Increased
Contact pressure (W/R Contact)	Max	1028	1106.17	7%	Increased

When looking the result of the Von mises stress at loading case I and Loading Case II it increases by 23 %. The Minimum available fatigue life and factor of safety decreases by 35 % and 30 % respectively. Also results like Equivalent alternating stress shows increments by 25 %, Normal and shear stresses by 24 % & 18 %. Also from analytical calculation the bending stress on the axle & the Wheel /rail contact pressure increased by 24% & 7 % respectively.

Table 5.3 Evaluation of case I to Case III

Name	Max/Min	Case I	Case III	Evaluation	
Von mises Stress(Mpa)	Max	69.79	100.59	31%	Increased
Fatigue life	Min	3989826	2548694.6	-57%	Decreased
Factor of Safety	Min	4.58	3.18	-44%	Decreased
Equivalent alternating(Mpa)	Max	34.39	51.17	33%	Increased
Normal (Mpa)	Max	25.26	36.97	32%	Increased
Shear(Mpa)	Max	16.3	21.39	24%	Increased
Directional y(mm)	Max	0.95	1.39	32%	Increased
Directional z(mm)	Max	1.46	2.13	31%	Increased
Bending stress on axle	Max	44.58	65.24	32 %	Increased
Contact pressure (W/R Contact)	Max	1028	1178.4	13%	Increased

Also when we compare results from case I and Case III we see that the Von mises stress is increases by 31 % and unfortunately Minimum available fatigue life of the wheel set is decreased by 57 % and the factor of safety also decreased by 44 %. Also Equivalent alternating stress, Normal and shear stresses results increased by 33 % ,32 % and 24 % respectively. Also from analytical calculation the bending stress on the axle & the Wheel /rail contact pressure increased by 32% & 13 %.

Table 5.4 Evaluation of case II Vs. case III

Name	Max/Min	Case II	Case III	Evaluation	
Von mises Stress(Mpa)	Max	90.82	100.59	10%	Increased
Fatigue life	Min	2945129	2548694.6	-16%	Decreased
Factor of Safety	Min	3.52	3.18	-11%	Decreased
Equivalent alternating(Mpa)	Max	45.765	51.17	11%	Increased
Normal (Mpa)	Max	33.27	36.97	10%	Increased
Shear(Mpa)	Max	19.78	21.39	8%	Increased

Directional y(mm)	Max	1.25	1.39	10%	Increased
Directional z(mm)	Max	1.92	2.13	10%	Increased
Bending stress on axle	Max	58.71	58.71	65.24	Increased
Contact pressure (W/R Contact)	Max	1106.17	1106.17	1178.4	Increased

Similarly, when we compare results from case II and case III we can see that the Von mises stress increased by 10 %, equivalent alternating stress by 11%, normal stress by 10 & shear stress by 8 % and minimum available life and factor of safety decreased by 16 % & 11 % respectively. Also bending stress on the axle & the Wheel /rail contact pressure increased by 10 %& 6 %.

5.2.2 Discussion under Different traction

For our next part we try to discuss the effect of different traction condition on the static and fatigue behavior of the Wheelset. For this part we use the same loading condition and we only alter the average traveling velocity of the rail car.

Based on the collected data and interviews of ERC employees they explain that AALRT rail car travel by approximately an average velocity of 20 km/hr. For the FEA analysis we use rotational velocity of the rail car instead of the linear velocity and also since the torque and the velocity are inversely proportional, we also change the amount of driving torque from the gearbox.

In the curve below we can see the how the driving torque changes with change in the travelling velocity of the rail car.

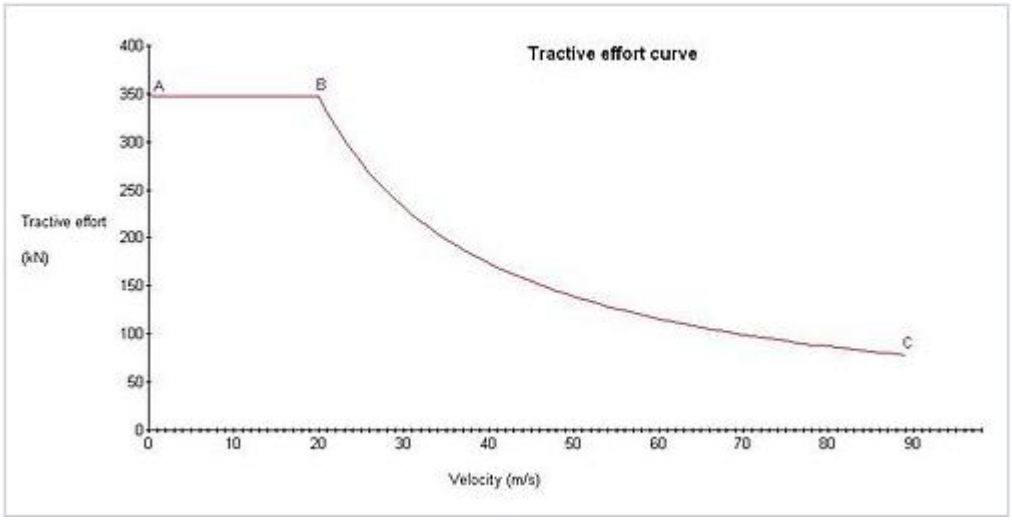

Fig 5.34 Diagram of tractive effort versus speed for a hypothetical locomotive with power at rail [27]

As we see from fig 5.34 the traction force needed for the of the railcar decreases when the speed of the train increases. This is due to the normal reaction between the object and the ground decreases.as the speed increase it tends to lose contact from the ground.

Fig 5.35 (a) shows us a typical relation between torque and speed; the curve shows use the reverse proportionality of torque and speed. When the rotational torque on a body increases since torque and torsional stress have a directly proportional relation the stress induced on the wheelset will be increases. Fig 5.35 (b) shows us the relation between stress induced and fatigue life cycle

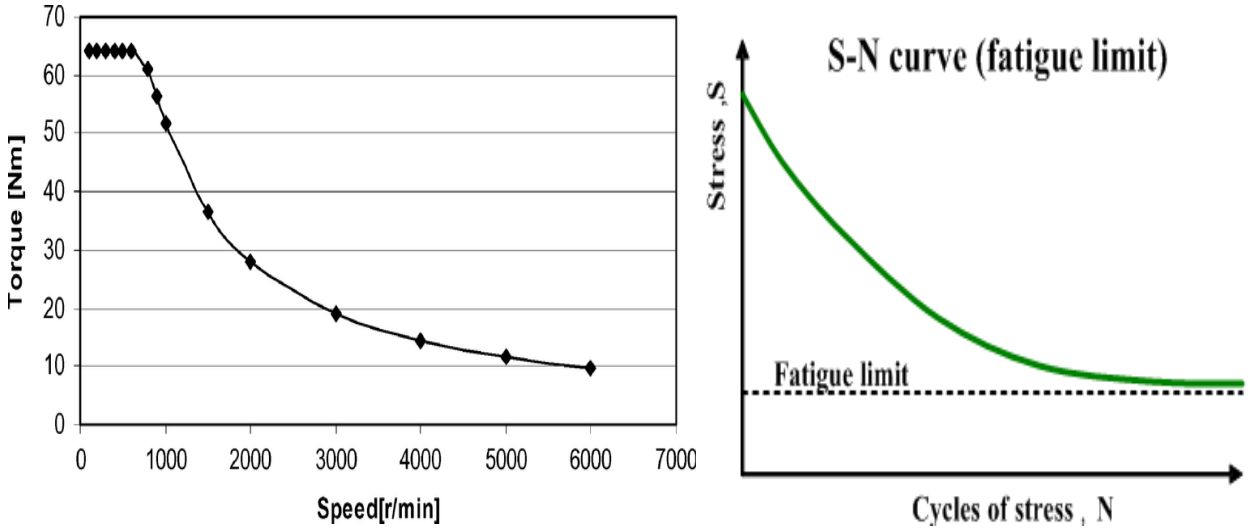

(a) typical torque vs. speed relation [28] (b) stress vs. fatigue No of cycle [29]

Fig 5.35 (a) & (b) torque speed and fatigue life relation

Therefore, we can say that increasing traction speed on the rail car will indirectly increase the fatigue life (No of cycles before failure happened) since it decrease the stress induced on the wheelset.

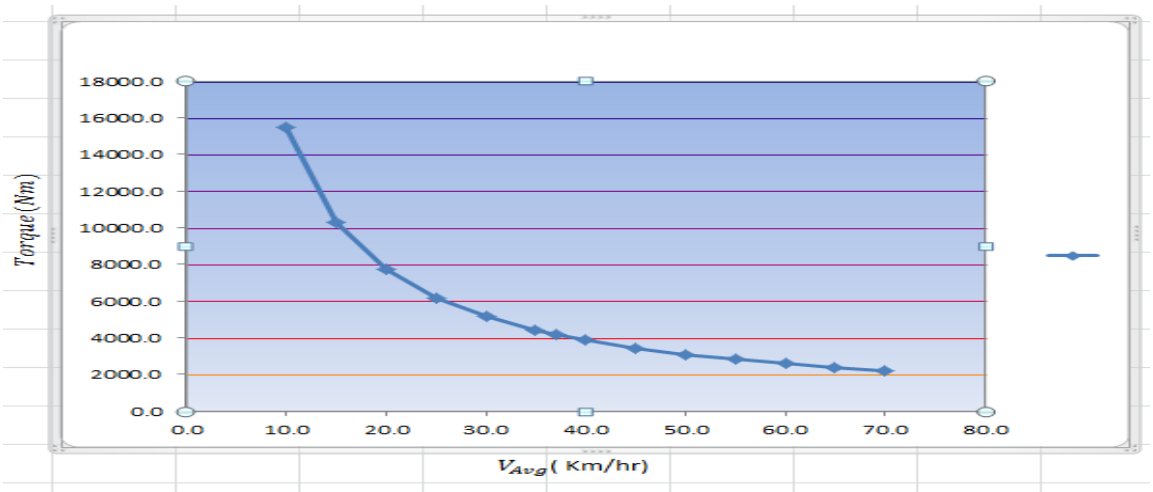

Fig 5.36 Torque vs. Velocity Curve in case of AALRT

Fig 5.36 is a typical figure that shows the torque and speed relation in the case of AALRT. As we can see torque and the speed have inversely proportional and have exponential relation. But also we can observe another relation of torque and velocity, since their relation is exponential other than linear the reduction in torque is not proportional, if we see the first with velocity profiles the decreasing in torque is in a large variation than the last velocity profiles. This relation between traveling velocity and driving torque also reflected on the fatigue life, stress induced and other results from the Ansys software.as we can see the table below, the results from like fatigue life, Von mises stress and factor of safety varies in a large value for low velocity profile results than for high velocity profiles.

	V(km/ hr)	T(Nm)	Loading Case I			Loading Case II			Loading Case III		
			Fatigue life(Cycles)	F.S	V. Stress (MPa)	Fatigue life(Cycles)	F.S	Von Stress (MPa)	Fatigue life(Cycles)	F.S	V. Stress (MPa)
1	10.0	15444.0	3169303	3.62	88.17	2454429	3.01	106.12	2,159,282.7	2.78	114.8
2	15.0	10296.0	363900.7	4.1	78	2744862	3.27	97.58	2,392,766.5	2.99	106.86
3	20.0	7722.0	3821523	4.32	73.95	2852536	3.39	94.24	2477461.7	3.08	103.76
4	25.0	6177.6	3908596	4.44	71.93	2901420	3.45	92.57	2515380.9	3.13	102.22
5	30.0	5148.0	3955071	4.52	70.76	2926758	3.49	91.61	2534804.3	3.15	101.33
6	35.0	4412.6	3982142	4.56	70.02	2841128	3.51	91	2545691.6	3.17	100.76
7	37.0	4172.7	3989826	4.58	69.79	2945129	3.52	90.82	2548694.6	3.18	100.59
8	40.0	3861.0	3998951	4.6	69.52	2949815	3.53	90.59	2552189.3	3.18	100.37
9	45.0	3432.0	4009899	4.62	69.16	2955312	3.54	90.29	2556241.9	3.19	100.09
10	50.0	3088.8	4017296	4.64	68.89	2958909	3.55	90.07	2558848.7	3.2	99.88
11	55.0	2808.0	4022439	4.65	68.69	2961320	3.55	89.9	2560559.6	3.2	99.7
12	60.0	2574.0	4026095	4.66	68.53	2962961	3.564	89.76	2561629.6	3.21	99.59
13	65.0	2376.0	4028738	4.67	68.4	2964089	3.569	89.65	2562262.5	3.21	99.49
14	70.0	2206.3	4030675	4.68	68.3	2964747	3.572	89.56	2562653.9	3.21	99.4

Table 5.5 summary of results of different traction conditions

As we can see from the table above the fatigue life decreases proportionally with the decreasing of the travelling speed and von mises stress increases. This behavior is because when the train speeds fast it needs small torque for driving and when it travels with low speed it will use high amount of torque from the motor for the driving and this torque results high amount of torsional stress on the Wheelset.

The chart below shows increasing in fatigue life of the wheel set directly proportional with the increase in average velocity of the railcar in all three loading cases.

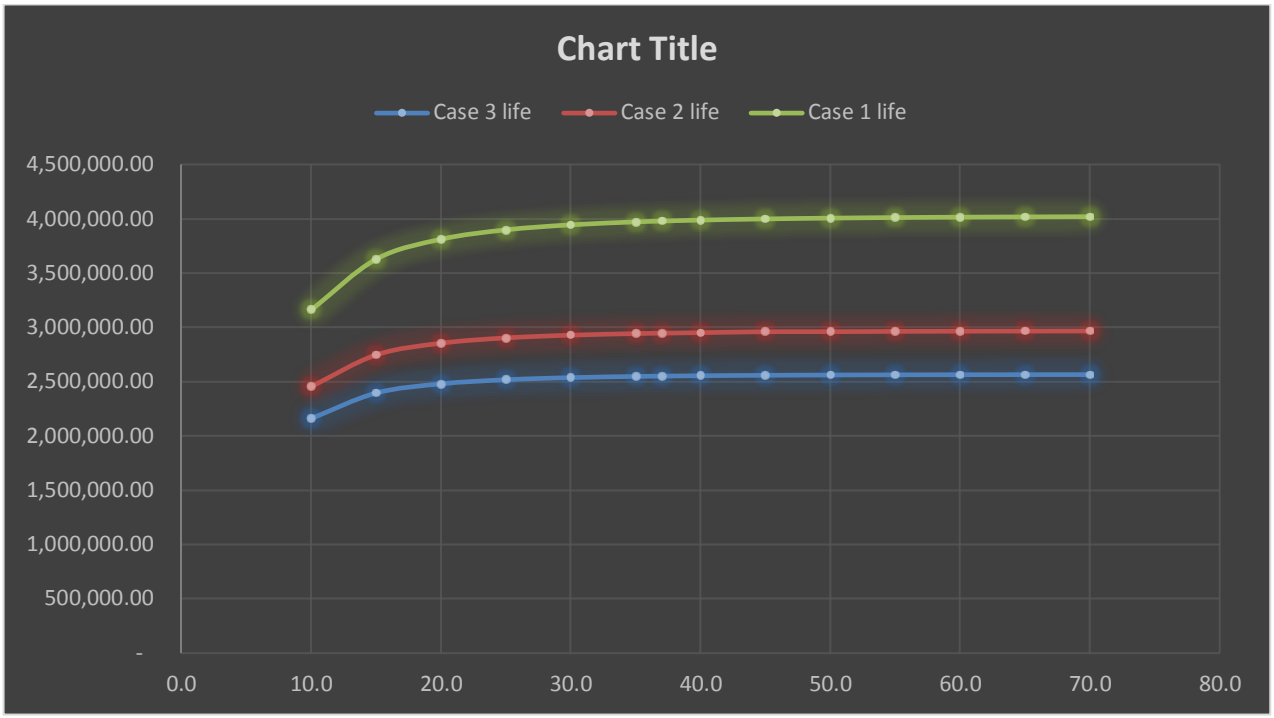

Fig 5.37 Velocity vs. Fatigue Life Curve

Table 5.6 Evaluating results of traction condition (20 Km/hr. & 40 Km/hr.)

	Traction condition		**Evaluation**	
	20 Km/hr	**40 Km/hr**		
Von mises Stress	103.76	100.37	-3.4%	Decreased
Fatigue life	2477461.7	2552189.3	3.1%	Increased
Safety Factor	3.08	3.18	3.1%	Increased

As we can see from table 5.6, the fatigue life of the wheel set can be increased by 3.1 % if the train travels by average speed of 40 Km/hr. rather than 20 Km/hr. Also von mises stress induced on the wheel set will be decreased by 3.4 %.

Table 5.7 Evaluating results of traction condition (20 Km/hr. & 70 Km/hr.)

	Traction condition		**Evaluation**	
	20 Km/hr	**70 Km/hr**		
Von mises Stress	103.76	99.4	-4.4%	Decreased
Fatigue life	2477461.7	2562653.9	3.3%	Increased
Safety Factor	3.08	3.21	4.0%	Increased

Also as we can see from the table above the fatigue life of the wheel set can be increased by 3.3 % if the train travels by average speed of 70 Km/hr. rather than 20 Km/hr. and Also von mises stress on the wheel set will be decreased by 4.4 % and the factor of safety improved by 4 %.

Table 5.8 Evaluating results of traction condition (40 Km/hr. & 70 Km/hr.)

	Traction condition		**Evaluation**	
	40 Km/hr	**70 Km/hr**		
Von mises Stress	100.37	99.4	-1.0%	Decreased
Fatigue life	2,552,189.30	2562653.9	0.4%	Increased
Safety Factor	3.18	3.21	0.9%	Increased

When we see results of 40 km/hr. and 70 km/hr. from the table above the variation in minimum and traction conditions after 40 km/hr. doesn't affect the fatigue life that much.

5.2.3 Fatigue Sensitivity

This fatigue sensitivity curve shows how the fatigue results change as a function of the loading at the critical location on the scoped region. Sensitivity may be found for life, damage, or factor of safety. It helps to see the sensitivity of the model's life if the FE load was 50% of the current load up to if the load 150% of the current load. A value of 100%

as shown in the figure 5.36 below the maximum fatigue sensitivity for Loading story of 150% of the current is 6.394 e +6 cycle and minimum fatigue sensitivity is 2.42 e +6 cycles.

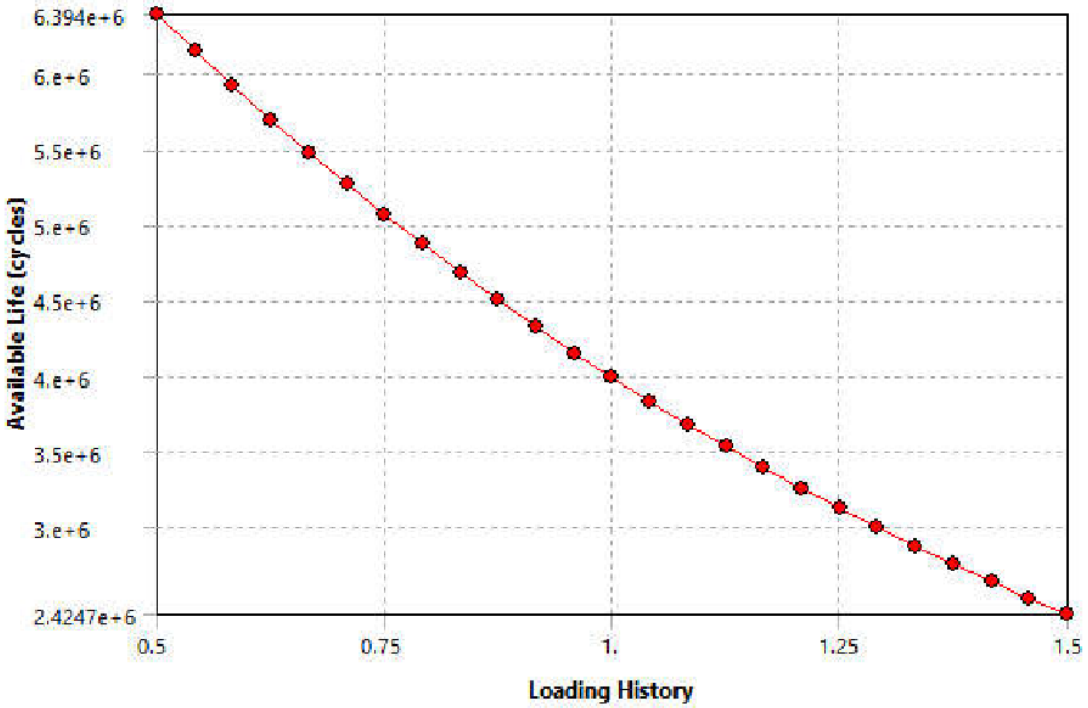

Fig 5.38 Fatigue sensitivity Case I

Also for loading case II the maximum fatigue life will be 5.54 e+6 and the minimum will be 1.49 e +6

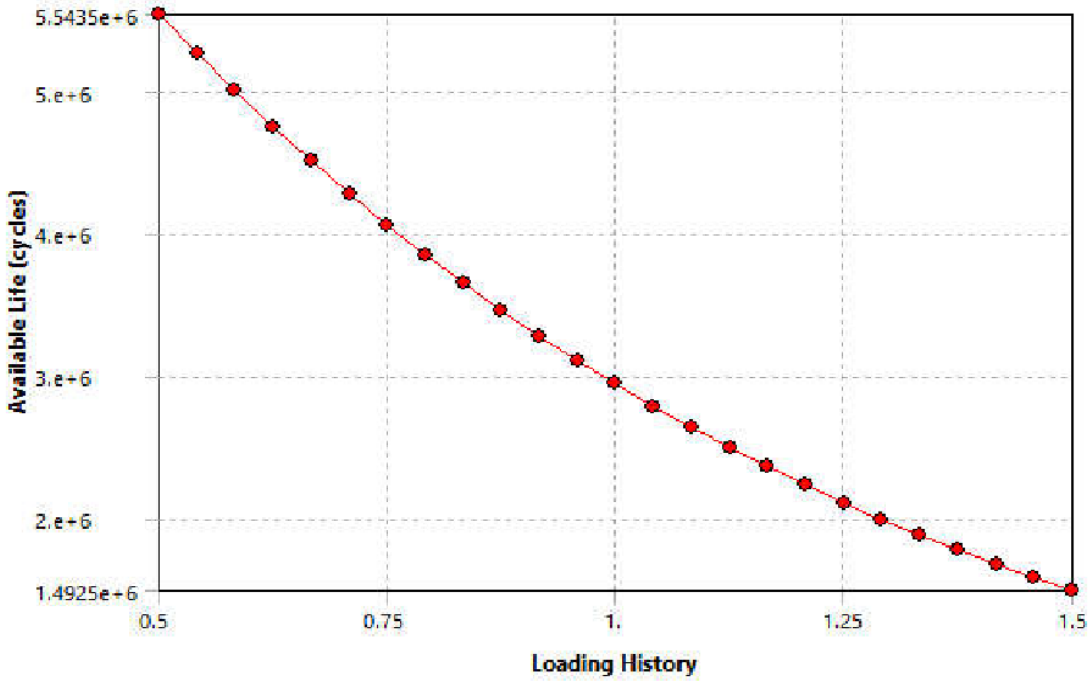

Fig 5.39 Fatigue sensitivity Case II

Also for Loading Case III the fatigue sensitivity curve will be reduced to 5.18 e +6 at maximum and 1.18 e +6 at minimum.

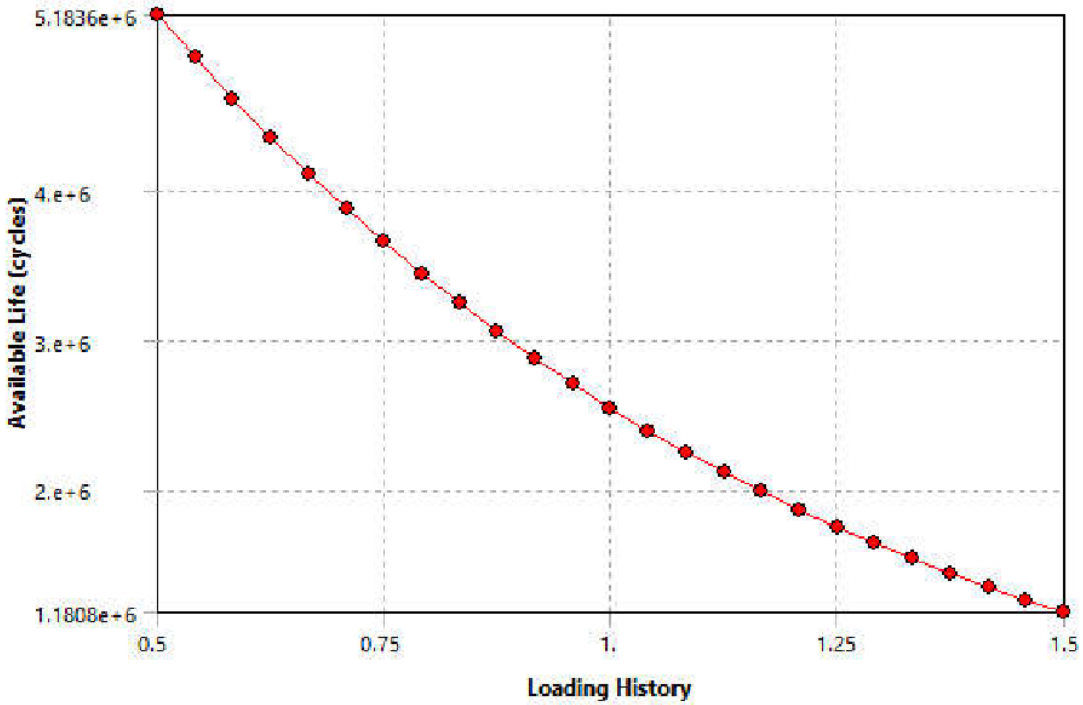

Fig 5.40 Fatigue sensitivity Case III.

CHAPTER 6
CONCLUSIONS AND RECOMMENDATIONS

6.1 Conclusion

The main purpose of the project is finding the static and fatigue behavior of the Wheelset under different loading (39158.25 N, 51571.36 N & 57307.88 N) and traction condition (V_{Avg} , $10\ Km/hr\ to\ 70\ Km/hr$) in case of AALRT. Then a FE model has been developed to analyze the Von mises stress, Maximum principal stress, Deformations, safety factors, fatigue life, fatigue sensitivity and equivalent alternating, on the wheelset. To analyze the above mentioned activities of the system, the wheel set has been modeled in solid works and imported to ANSYS work bench for analysis.

On the bases of this analysis and results the researcher forwards the following conclusions. From the first part of the analysis, using different loading condition and keeping the traction condition constant, we see that results like the fatigue life and factor of safety of the wheelset decreases inversely with the increasing of passenger Loadings while results like stresses induced on the wheelset increases.

When we see results from loading condition III (57307.88 N/wheel) the fatigue life which is (2,548,694.6 cycles) is decreased by 57 % relative to loading condition I & decreases 16 % with respect to loading condition II. On the other hand, normal stress (36.97 Mpa), shear stress (21.39 Mpa), and equivalent alternating stress (45.76 Mpa) induced on the wheel set increased by 10 %, 8 % ,10 % and 11 % with respect to loading condition II and 32%,24% ,31% & 33 % respectively relative to loading condition I. Also safety factor (3.18) of the wheelset decreases by 14 % and 44 % when we compare with loading case II and with loading case III. On the other hand, based on the analytical calculation (hertz theorem) the maximum contact pressure developed will be increased by 7 % and 13% relative to loading case II and loading case III. Therefore, from the above comparisons of different loading cases we can conclude that increasing passenger loading beyond the standard loading capacity of the train have a direct effect on the static and fatigue behavior and reduce lifespan of the wheelset.

Also for the second part of the analysis using different Traction conditions and keeping the loading condition constant, the researcher see change in static and fatigue behavior.

With the increase in traveling velocity of the railcar we can see the fatigue life of the wheelset increases exponentially. When we compare fatigue life of the wheelset travelling average velocity of 20 km/ hr. (2477461.7 Cycles) which is the current operating average velocity of AALRT considering overloaded loading condition (Case III) with average velocity of 40 km/hr. and the maximum operating velocity of the train 70 km/hr. with the same passenger loading condition the fatigue life increases by 3.1 % & 3.3 % respectively. Other results like von mises stress and the safety factor also improved. The von mises stress (103.76 Mpa) induced on the wheelset improved (decreased) by 3.4 % & 4.4 % if the train operates with average velocity of 40 km/hr. and 70 km/hr. respectively. Also safety factor increases by 3.1 % (40 km/hr.) & 4.0 % (70 km/hr.). On the other hand, when we see results of the two traction conditions, 40 km/hr. and 70 km/hr, the researcher observes the difference is minimum and can be negligible. On the other hand, it is expected that further increase in speed beyond 70 Km/hr will reduce the fatigue life as has been demonstrated by previous researchers.

Therefore, we can conclude that an optimum range of operating speed for improved fatigue life should not be too low and too high. This research focused wheelset fatigue due to twisting and bending moments. Because thermal effects, fretting effects, rolling contact effects on wheelset fatigue are out of scope of this research, we recommend to further investigate the relationship of traction conditions and wheelset fatigue due these effects in the case of AALT.

6.2 Recommendations

From the result found from both analytic approach and FEA simulation, this researcher would like to recommend that since the overloading of passenger beyond the train loading capacity affects the fatigue life of the wheelset, AALRT should to limit maximum Number of passengers per the train or as alternative solution if the train add additional trailer considering the motor power and efficiency, the concentration of load per axle will be reduced and life span of the wheelset might be improved.

On the other hand, since the travelling speed of the train is not on the recommended range and the fatigue life of the wheelset is affected by travelling speed of the train the researcher likes to recommend to operate the trains on the range of 35-45 km/hr. on average instead of 20 km/hr. When the researcher makes this recommendation, he considers the safety issue and problem rises with travelling with high speed and since this research doesn't consider the effect of increasing travelling speed on the material property and contact temperature of the wheelset which increase the wear rate on the wheelset the researcher recommends to further study on this issue.

Also additional factors such as environmental conditions, material, material microstructure and manufacturing process do have also an influence on the fatigue life of the railway wheelset. By research and implementing those additional factors, farther research could be made to select the best suitable and durable wheelset for the application of AALRT future demand.

Finally, the other thing the researcher like to recommend is that AALRT or ERC should have fatigue test laboratories and inspection equipment to detect the crack initiation and propagations on the wheel set before failure happens and to take proper actions and services to axle and wheel before it's too late.

Future Works

Since this research only deals with mechanical fatigue of the wheelset the researcher likes to recommend further study of thermal, fretting fatigue and rolling contact fatigue on the wheelset due to different loading and traction conditions in the case of AALRT.

Also the researcher would like to recommend further experimental studies on effect of low and medium speeds on fatigue of railway wheelset for the case of AALRT.

REFERENCES

[1]. Alem Behaylu, Parametric Studies on the Fatigue Life Improvement of Passenger Rail Vehicle Axlebox House,Addis Ababa University ,2015

[2]. S. Timoshenko, Strength of Material, ,2nd edition,D. Van Nostrand Company Inc. London,1940

[3]. P.J.E Forsyth,The physical basis of Metal fatigue,Blackie and son,London,1969

[4].Beza Takele, Analysis of Fatigue Failure on Motor Powered Train Axle of AALRT,Addis ababa University,2017

[5]. Solomon Kebebew, Analysis of Effect of Train Overload on Disc Brake of AALRT, Addis Ababa University,2015

[6]. Etaferahu Birhanu, Overloading effect on the life cycle of car body structures in case of AALRT, Addis Ababa University, 2015

[7]. R.S. Khurmi & J.K Gupta, A text of machine design, Eurasia publishing house LTD ,2005

[8]. Maintenance and Repair Manual of AALRT, Changchun railway vehicle.co. Ltd

[9]. S.Suresh, Fatigue of material ,2nd Edition, Cambridge University Press,2004

[10]. Meral Bayraktar, Necati Tahrali and Rahmi Guclu, Reliability and fatigue life evaluation of railway axles, Istanbul, Turkey

[11]. Australian Transport Safety Bureau, Australian Government, Rail safety Investigation Report, Derailment of XPT Passenger Train ST22, Harden, New South Wales, Australia Feb 9, 2006

[12]. C.Klinger, D.Bettge, R.Haccker, T.Heckel, D.Gohlke,D.Klingbei, Failure Analysis on A Broken ICE3 Railway Axle, Interdisciplinary Approach, , Germany, Oct 11,2010

[13]. Aurel Rădulă,Cosmin Locovei, Mircea Nicoară and Laurenliu Roland Cucuruz, The influences of residual stress on fatigue fracture of railway axle, Romania

[14]. G. Fischer, V. Grubisic and M. Grosse-Hovest, Methodology for Reliable Durability Validation of Wheelset-Axles Fraunhofer Institute for Structural durability and system Reliability, Darmstadt, Germany, 2011

[15]. Kidane Maryam G/Tsadik, predicting the analysis of fretting damage for addis ababa light rail train wheel set, Addis Ababa University,2014

[16]. Werku Leta, Analysis of Rolling Contact Fatigue Failures of Railway Wheels Due to Cyclic Load, Addis Ababa University,2017

[17]. Shoma Tadesse, Fatigue Failure On Railway Axle, Addis Ababa University ,2017

[18]. CAE Associated, Fatigue analysis in ANSYS,2011

[19]. Richard G. Budynas & K. Jeith Nisbett, Shigley's Mechanical engineering design,9th edition, Mc Graw-Hill,2011

[20]. Raymond Browell, Calculating and Displaying Fatigue Results, 2006

[21]. ANSYS Workbench User's Guide, Release 15.0, ANSYS, Inc., 2013

[22]. Ferdinand P. Beer,E. Russell Johnston Jr., John T. Dewolf ,David F. Mazurek, Mechanics of materials, 6th edition, McGraw−Hill , 2012

[23]. Robert L. Mott, Machine elements in mechanical design,4th edition, Pearson Prentice Hall,2004

[24] Hirakawa, K. & M. Kubotu, Fatigue design method of railway axle in high speed railways, Kyushu University,Japan. 2001

[25]. Dula Fikadu, Investigating the wheel wear of Addis Ababa Light Rail Transit (AALRT), Addis Ababa University, 2017

[25]. Prof.S.R Satish Kumar and Prof. A.R. Santha Kumar, Design of steel structure, Indian institute of technology

[26]. [https://en.wikipedia.org/wiki/Tractive_force]

[27]. Aymar M.Refaie,Thomas M, Analysis of surface permanent magnet machinewith fractional –slot Concentrated winding,2006

[28]. [www.substech.com]

APPENDIX

A- Summary Table of different traction condition results

	V (km/hr.)	V(m/s)	N(RPS)	N(RPM)	w(rad/sec)	T(Nm)	Case 1			Case 2			Case 3		
							Fatigue Life (Cycle)	F.S	Von mises Stress	Fatigue Life (Cycle)	F.S	Von mises Stress	Fatigue Life (Cycle)	F.S	Von mises Stress
1	10.0	2.8	1.3	80.4	8.4	15444.0	3169303	3.62	88.17	2454429	3.01	106.12	2,159,282.70	2.78	114.8
2	15.0	4.2	2.0	120.6	12.6	10296.0	3636900	4.1	78	2744862	3.27	97.58	2392766.9	2.99	106.86
3	20.0	5.6	2.7	160.8	16.8	7722.0	3821523	4.32	73.95	2852536	3.39	94.24	2477461.7	3.08	103.76
4	25.0	6.9	3.3	201.0	21.0	6177.6	3908596	4.44	71.93	2901420	3.45	92.57	2515380.9	3.13	102.22
5	30.0	8.3	4.0	241.1	25.3	5148.0	3955071	4.52	70.76	2926758	3.49	91.61	2534804.3	3.15	101.33
6	35.0	9.7	4.7	281.3	29.5	4412.6	3982142	4.56	70.02	2841128	3.51	91	2545691.6	3.17	100.76
7	37.0	10.3	5.0	297.5	31.2	4172.7	3989826	4.58	69.79	2945129	3.52	90.82	2548694.6	3.18	100.59
8	40.0	11.1	5.4	321.5	33.7	3861.0	3998951	4.6	69.52	2949815	3.53	90.59	2552189.3	3.18	100.37
9	45.0	12.5	6.0	361.7	37.9	3432.0	4009899	4.62	69.16	2955312	3.54	90.29	2556241.9	3.19	100.09
10	50.0	13.9	6.7	401.9	42.1	3088.8	4017296	4.64	68.89	2958909	3.55	90.07	2558848.7	3.2	99.88
11	55.0	15.3	7.4	442.1	46.3	2808.0	4022439	4.65	68.69	2961320	3.55	89.9	2560559.6	3.2	99.7

12	60.0	16.7	8.0	482.3	50.5	2574.0	4026095	4.66	68.53	2962961	3.564	89.76	2561629.6	3.21	99.59
13	65.0	18.1	8.7	522.5	54.7	2376.0	4028738	4.67	68.4	2964089	3.569	89.65	2562262.5	3.21	99.49
14	70.0	19.4	9.4	562.7	58.9	2206.3	4030675	4.68	68.3	2964747	3.5728	89.56	2562653.9	3.21	99.4

B. Comparison of analytical and FEA results

C. Material Property of wheel and Axle

- Material Property of wheel and Axle used in Ansys Work Bench as input for analysis are displayed Below. Table C -1 is for axle material and Table C – 2 is for wheel

Table C - 1

Structural Steel > Constants

Density	7.3e-006 kg mm^-3
Coefficient of Thermal Expansion	1.2e-005 C^-1
Specific Heat	4.34e+005 mJ kg^-1 C^-1
Thermal Conductivity	6.05e-002 W mm^-1 C^-1
Resistivity	1.7e-004 ohm mm

TABLE 56
Structural Steel > Compressive Ultimate Strength

Compressive Ultimate Strength MPa
650

TABLE 57
Structural Steel > Compressive Yield Strength

Compressive Yield Strength MPa
320

TABLE 58
Structural Steel > Tensile Yield Strength

Tensile Yield Strength MPa
320

TABLE 59
Structural Steel > Tensile Ultimate Strength

Tensile Ultimate Strength MPa
650

Table C - 2

Structural Steel 2 > Constants

Density	7.8e-006 kg mm^-3
Coefficient of Thermal Expansion	1.2e-005 C^-1
Specific Heat	4.34e+005 mJ kg^-1 C^-1
Thermal Conductivity	6.05e-002 W mm^-1 C^-1
Resistivity	1.7e-004 ohm mm

TABLE 66
Structural Steel 2 > Compressive Ultimate Strength

Compressive Ultimate Strength MPa
880

TABLE 67
Structural Steel 2 > Compressive Yield Strength

Compressive Yield Strength MPa
640

TABLE 68
Structural Steel 2 > Tensile Yield Strength

Tensile Yield Strength MPa
640

TABLE 69
Structural Steel 2 > Tensile Ultimate Strength

Tensile Ultimate Strength MPa
880

C - Types of loadings for Fatigue analysis

For the fatigue analysis since the type loadings act on the wheelset are different, bending load acts on the wheelset as a fully reversed type of load which means it changed from positive tensile to negative compressive in one cycle, and fluctuating loads due to torsion and lateral force from the rail on the wheel are zero based cyclic loads the researcher uses different environment for analysis to get more reliable fatigue results combine the solutions from each environment using solution combination module.

Here below we can see that different types of loadings we use on Ansys workbench for a typical Loading and traction condition.

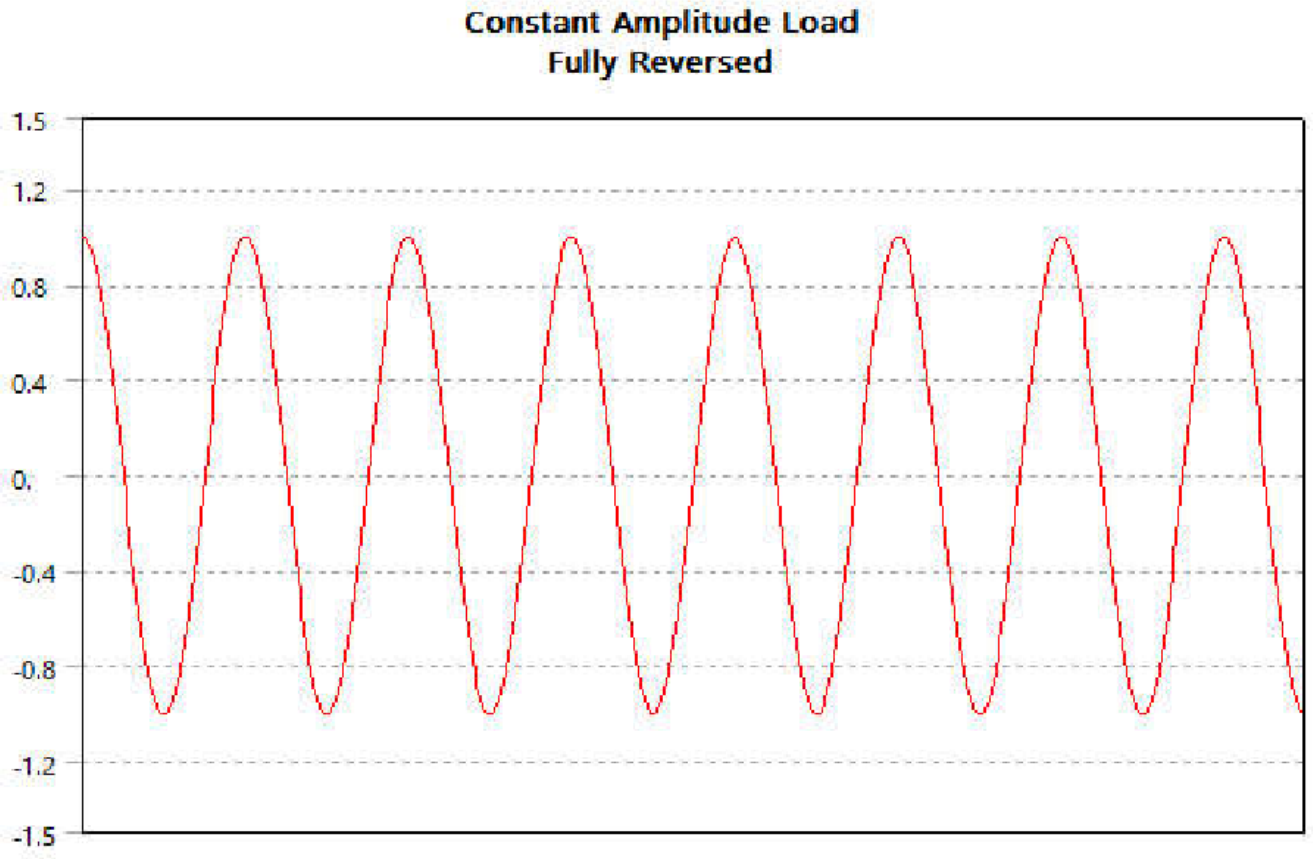

Fig. C – 1 fully reversed type of loading from Bending Environment

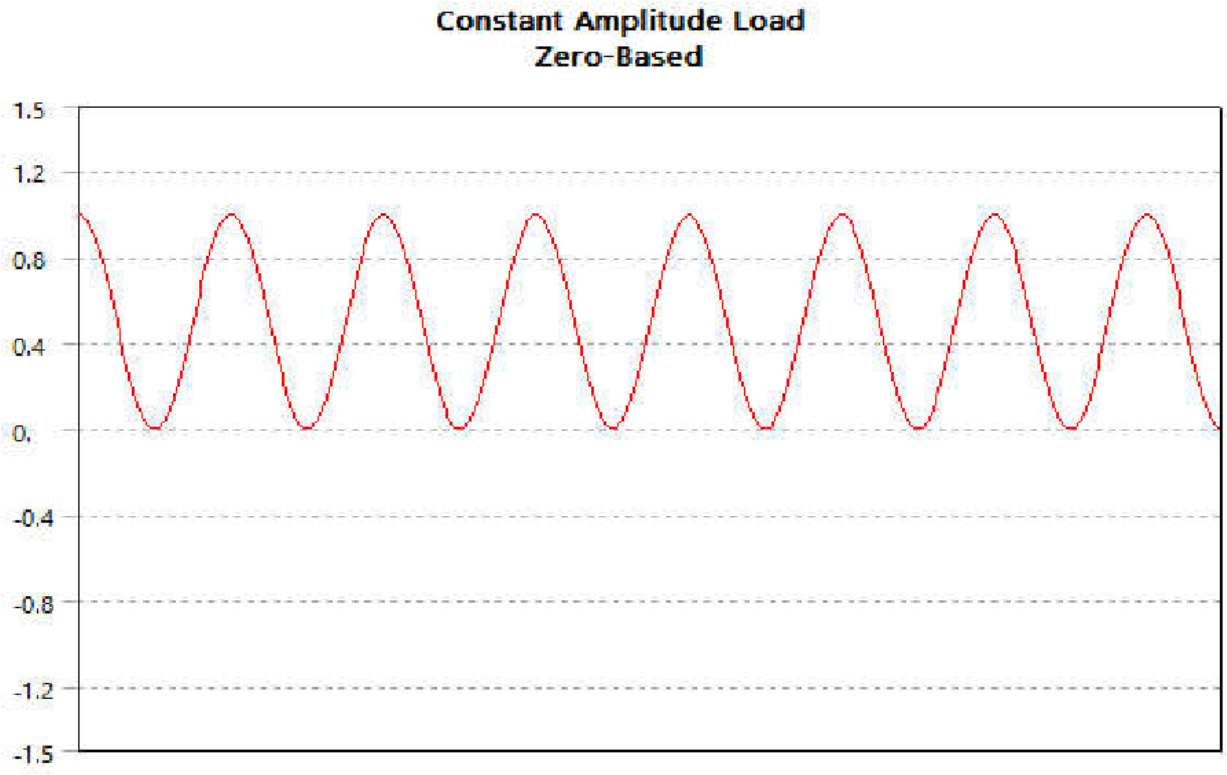

Fig C – 2 Zero - based Type of loading from Torsional and lateral load environment

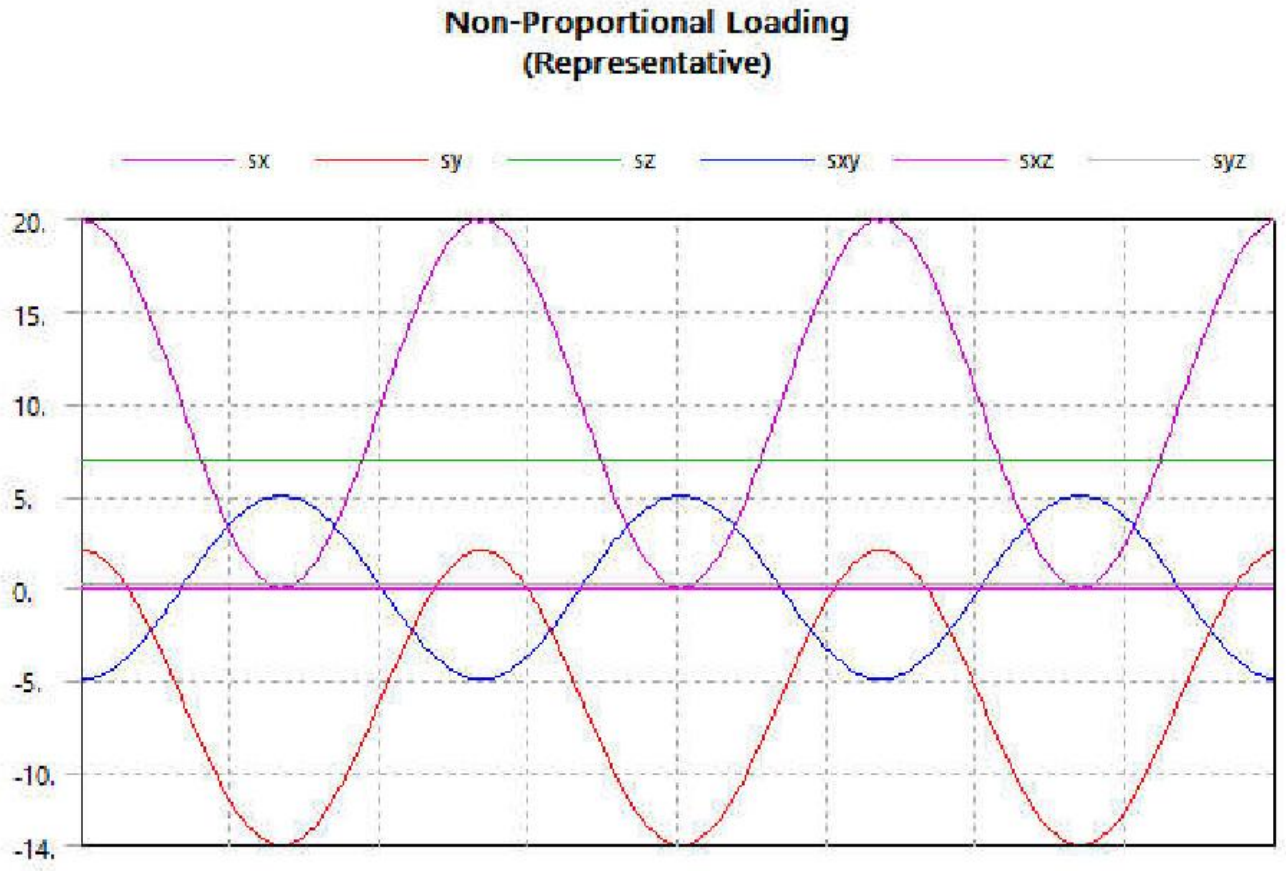

Fig C – 3 Non proportional Type of loadings from Combined environment